Automatic Structural Synthesis of Planar Mechanisms and Its Application to Creative Design

Von der Fakultät für Ingenieurwissenschaften

Abteilung Maschinenbau und Verfahrenstechnik der Universität Duisburg-Essen

zur Erlangung des akademischen Grades

eines

Doktors der Ingenieurwissenschaften

Dr.-Ing.

genehmigte Dissertation

von

Huafeng Ding

aus
Hebei

Gutachter: Prof. Dr.-Ing. Andrés Kecskeméthy
Prof. Dr.-Ing. Burkhard Corves, RWTH Aachen

Tag der mündlichen Prüfung: 18.02.2015

UNIVERSITÄT
DUISBURG
ESSEN

Automatic Structural Synthesis of Planar Mechanisms and Its Application to Creative Design

Doctor thesis

Written by

Huafeng Ding

Supervised by

Prof. Dr. Andrés Kecskeméthy

Fakultät für Ingenieurwissenschaften
Abteilung Maschinenbau
Institut für Mechanik und Robotik

Contents

1 Introduction

1.1 Purpose of the thesis

In the design of various mechanism-based products or systems, conceiving the kinematic structure of mechanisms with better performance has been a challenging yet pivotal issue for every specified design task [1-7]. For a long time, it has been researchers' experience and intuition that are mostly relied on in the conception of candidate structures and the selection of one of them for the task. Obviously, some of the feasible mechanisms satisfying the requirements of a specified design task can be conceived based on the researchers' experience with creative design methods [8-12]. But it is hard or impossible to conceive all the possible kinematic structures of mechanisms for each design task in this way and the best solution for a task can hardly be reached. The mechanism with the best performance for a specified design task can be selected only when all the feasible kinematic structures of mechanisms are obtained. For example, Figure 1(a) shows a road tractor [13]. The mechanism for the tractor has 11 links and two DOFs and its kinematic sketch is shown in Fig. 1(b). Now two important questions to ask are

(1) Is the mechanism in Fig. 1(b) the best for an 11-link 2-DOF road tractor?

(2) what are the alternatives for it?

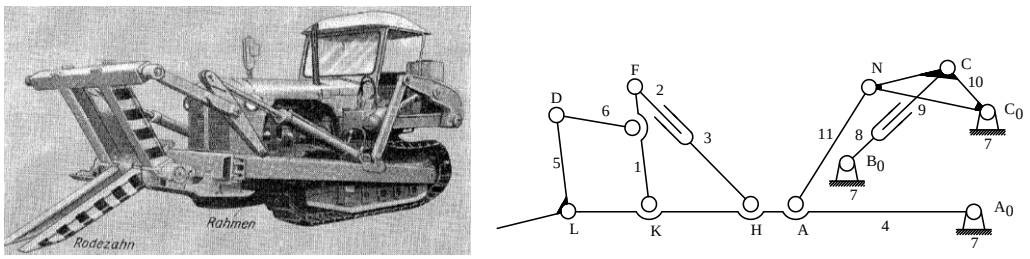

(a) (b)

Fig. 1 (a) A road tractor, (b) the kinematic sketch of the mechanism

Obviously, only when all feasible mechanisms that satisfy the design requirements are synthesized and evaluated against detailed design constraints it may be possible to obtain the best mechanism for the task. The structural synthesis of mechanisms which can generate a complete list of kinematic chains and mechanisms free from isomorphism and degenerate chains can provide the designers with all the independent candidate kinematic structures of mechanisms of choice [15-17]. From the reports in literature, the number of the topological structures of mechanisms is far more than the species of creatures in the nature [18-19]. Thus, in order to get the optimal result from structural synthesis, the synthesis method must have the following characteristics [20-22]:

(1) Effectiveness: The method must be abe to generate all valid topological structures, free from any degenerate structures (rigid sub-chains) and redundant structures (isomorphic

chains), and at once without omission of any independent structures (the charater of completeness).

(2) Automation: Synthesis must be carried out completely automatically in the computer.

(3) Designer-friendliness: Synthesis results should be displayed in intuitive forms instead of as algebraic representations so that designers can have a quick understanding of them.

Despite a great number of existing synthesis methods, no method so far meets the three requirements above [17]. This thesis attempts to develop a novel synthesis method which is at the same time effective, automatic and designer-friendly, and with which one can obtain at the one side all the valid topological structures of planar kinematic chains and mechanisms with simple or multiple joints, and on the other side develop the atlas database containing all the topological graphs for these kinematic chains and mechanisms with different numbers of links, classified by their structural characteristics. Based on the classified atlas database, a creative design method is also proposed to generate all the feasible mechanisms from the topological graphs for a specified task within specified design constraints.

1.2 Review of structural synthesis

Structure synthesis of planar mechanisms has attracted researchers for over a century and continues to do so. At its early time structure synthesis was mainly based on researchers' experience and intuition. Since the 1960s, many systematic approaches have been proposed for the synthesis of mechanism kinematic chains. The main synthesis methods reported in literature can be sorted into link-joint based methods, limb based methods, loop based methods, and some others.

1.2.1 Franke's notation methods

Davies and Crossley [23] proposed the structural synthesis method based on Franke's notation [24], with which 40 9-link 2-DOF kinematic chains and 230 10-link 3-DOF kinematic chains were synthesized in batch. Hass and Crossley [25] used Franke's notation to synthesize a class of four degrees of freedom kinematic chains. Soni [26] also employed Franke's notation to synthesize two general constraint kinematic chains.

1.2.2 Graph theory based methods

Freudenstein [27] and Crossley [28] employed the graphs in graph theory [29] to represent the topological structures of kinematic chains and developed a method to synthesize 16 8-link 1-DOF kinematic chains by hand. Woo [30] proposed an algebraic interchange method to synthesize contracted graphs and then add binary-link vertices to these contracted graphs to synthesize topological graphs. With this method he synthesized 230 10-link 1-DOF kinematic chains. Freudenstein and Woo [31-33] introduced Polya's theory to synthesize topological graphs by adding binary-link vertices to contracted graphs. Huang and Soni [34] further employed Polya's theory to synthesize 8-link 1-DOF kinematic chains with other types of joints. Kiper and Schian [35-36] employed the graph theory to synthesize 6856 12-link 1-DOF kinematic chains. Liu [37] presented a graph theory based approach to optimize type

synthesis of vehicle suspension mechanisms. Pucheta [38-39] used the graph representation to solve the number synthesis of a class of planar multiloop linkages. By adopting a Mckay-type algorithm [40], Sunkari and Schmidt [41] synthesized the graphs of planar kinematic chains using graph and group theoretic techniques. Lu [42-45] conducted the structural synthesis of some topological graphs of planar parallel mechanisms based on topology embryonic graphs and arrays. Based on the concept of the simplified unified graph, Yan [46] proposed a method for the configuration synthesis of mechanism with variable topologies. By constructing proper simplified graphs, Butcher and Hartman [47] listed the numbers of 12- and 14-bar planar single degree-of-freedom kinematic chains.

1.2.3 Assur group based methods

Assur [48] proposed the famous concept of Assur group to reveal the structure composition of planar mechanisms. The basis for the concept lies in the fact that additon of an Assur group to a link or links of an existing kinematic chain does not change the degrees of freedom of the chain. So kinematic chains of greater complexity (i.e. with greater number of links) could be built by the sequential addition of these Assur groups to simpler kinematic chains (i.e. with fewer number of links). Using the concept of Assur group, Manolescu [49-54] studied the structural synthesis of 1-DOF kinematic chains up to 10 links and 2-DOF kinematic chains up to 9 links. Chu and Cao [55-57] proposed a method for the synthesis of Assur groups with multiple joints by synthesizing the internal chains and external chains in turn. Tischler [58-59] developed a method to synthesize multi-tipped fingers of a robot hand on the basis of Assur groups. Based on Assur groups as the simplest basic blocks to build kinematic chains, Alexandre [60] proposed a method to synthesize hybrid robots as a whole structure. By integrating Assur groups as elements in the modified adjacency matrix, Li [61] proposed a method to synthesize planar mechanisms with both R and P joints.

1.2.4 Group theory based methods

Tuttle [62-65] proposed a method wherein the feasible patterns called the bases of connecting polygonal links are formed first and the desired kinematic chains are derived by distributing binary links among these bases. The theory of finite symmetry groups is used to eliminate isomorphic entities in the generation of bases as well as kinematic chains. Based on the theory of permutation groups, Yan and coworkers [66-68] proposed the method to synthesize kinematic chains and mechanisms. Based on modified permutation groups and Polya's theory, Yan and Hung [69-71] presented a systematic procedure to count the number of planar mechanisms subject to design constraints from the candidate kinematic chains. Hervé, Li and Lee [72-75] developed the group-based synthesis method to synthesize lower-mobility parallel mechanisms by using displacement subgroups to represent the motion of the moving platform and limb chains.

1.2.5 Transformation methods

By extending Manolescu’s work [76], Mruthyunjaya [77-82] proposed a method based on the transformation of binary chains to synthesize kinematic chains with positive, zero and

negative DOFs. The complete collection of 839 11-link 2-DOF kinematic chains was synthesized. Sohn and Freudenstein [83] represented a conventional graph with its dual graph in which the vertices represent the loops and the loops represent the vertices of the conventional graph and developed the dual graph based method to synthesize planar kinematic chains whose graphs are planar.

1.2.6 Additive methods

Yang [84-86] developed a method for structural synthesis of kinematic chains with planar and non-planar graphs on the basis of the single-opened chain technique. Rao [87-88] applied the Hamming number technique to the structural synthesis of kinematic chains by using F-DOF, (N-2)-link chains as the basic chains for the synthesis of F-DOF, N-link chains. Varadaraju [89] proposed a method to build simple joint kinematic chains by adding one link at a time in all possible ways to an existing structural pattern. Vijayananda [90] developed a synthesis method in which a desired chain is built by adding specially constructed assemblage of links called "link patterns" to a chain with fewer numbers of links called "parent kinematic chain".

1.2.7 Other methods

Hwang and Hwang [91] proposed a new matrix, the contracted link adjacency matrix, to represent kinematic chains, and used it as the representation matrix to synthesize kinematic chains. Yan and Hsu [92-94] proposed the graph representation of multiple joint kinematic chains using solid polygons to represent multiple joints, and based on the concept of contracted graphs developed a method for the structure synthesis of kinematic chains with simple and multiple joints. Also using solid polygons to represent multiple joints, Hsu and Hsu [95] proposed a systematic method to synthesize geared kinematic chains using acyclic graphs. Rao and Deshmukh [96] used the loop information of kinematic chains to synthesize planar kinematic chains obviating the test for isomorphism, and kinematic chains up to 230 10-link 1-DOF kinematic chains were synthesized successfully. Lan and Du [97] proposed a new adjacency matrix to represent the topological changes of metamorphic mechanisms [98]. Song [99-101] presented a combination method to synthesize planar multiple joint kinematic chain under 10-link. Li [102] used the linear equations to synthesize planar single-freedom, simple-joint kinematic chains with up to 12 links. Mitrouchev [103] proposed the notion of logical equations to synthesize planar kinematic chains.

1.3 Open problems in structural synthesis

Although structural synthesis methods proposed one after another resulted in successful synthesis of an enormous number of kinematic chains and mechanisms of various links and degrees of freedom, a general problem still unsolved in structural synthesis is the enumeration of a complete list of kinematic chains and mechanisms without isomorphism and without degenerate (or rigid-sub) chains [15,17].

1.3.1 No complete automation

Structure synthesis of mechanisms still lingers at a relatively low level in terms of automation. In practice, while there are abundant varieties of advanced CAD software for the benefit of other phases in mechanical design, software servicing structure synthesis is scarce. Low automation in structure synthesis seriously impedes the realization of complete CAD in mechanical design. For this reason, "the trend (in structural synthesis) in recent years has been on automating", as Mruthyunjaya [15] the prestigious mechanist has put it, and "a whole lot of concerted efforts, fresh insights and breakthroughs are needed to achieve the more important goal of enabling designers to make successful use of the wealth of information already generated". The new trend in structural synthesis has been on automation, as fully as possible, in the various steps involved in structural synthesis [15]. In this respect, development of reliable, efficient and automatic isomorphism identification [104-109] and rigid sub-chain detection [110-112] methods is undoubtedly an indispensable part for the realization of automatic structure synthesis of mechanisms. Ding and Huang proposed computer-aided algorithms to detected isomorphism [113-114] and rigid sub-chains [115] for simple joint kinematic chains on the basis of unique representation [116] and loop theory [117], which provided a good foundation towards further developing fully-automatic methods of structural synthesis of kinematic chains and mechanisms.

1.3.2 No classified atlas database

Most of the structure synthesis methods reported in literature output the synthesized structures in their algebraic representations [15]. It will, however, be desirable to display the kinematic structures in graphs to give the designer a direct visual impression of the link-joint interrelationship of the generated kinematic chains and an intuitive feel for the spatial relationships. It would help much if the algebraic representations can be transformed conveniently into corresponding kinematic structures in graphical forms, and vice versa.

To do so Olson[118], Belfiore and Pennestri[119], Mauskar and Krishnamurty [120] studied the automatic sketching of kinematic chains. Ding and Huang [116] proposed the unique representation for simple joint kinematic chains, which remains unchanged no matter how the drawing and labeling ways of the chain are changed. Hsieh [121] proposed an automatic algorithm to generate and sketch generalized kinematic chains based on the multiple link adjacency matrices. Pucheta [122] used the combined graph layout algorithms to sketch the planar simple joint kinematic chains of 8-link 1-DOF, 9-link 2-DOF and 10-link 3-DOF kinematic chains.

Even when the designers are presented with graphs instead of algebraic representations of kinematic chains, they are still faced with the great difficulty of selecting the best structure from perhaps hundreds of thousands of candidate topological graphs that meet the needs of the synthesis task. How to narrow down the choice and get the most appropriate kinematic chain from the massive output of automatic synthesis for a certain application task therefore is another fundamental subject that cannot be avoided in the study of synthesis automation. A

system that contains all the topological characteristics of the topological graphs produced from automatic synthesis and can classify, store and output these graphs by their topological characteristics might be a good solution to the problem.

1.3.3 No unified synthesis method

Besides simple joint kinematic chains, typical planar kinematic chains also include multiple joint chains, gear chains, etc. If we develop an individual synthesis theory for each kind of planar kinematic chains respectively, the overall issue of structure synthesis of planar mechanisms would become complex and confusing. Moreover, very likely a synthesis theory developed for a certain kind of mechanism in its isolated form cannot be applied to combined mechanisms directly and easily. So it would be more desirable both theoretically and practically to come up with a unified structure representation model and a unified structure synthesis theory applicable to all kinds of planar mechanisms. At present, researches on structure synthesis of simple joint chains are the most fruitful, but structure synthesis theories of other types of mechanisms are far from being fully developed. So it would save researchers much trouble if the unified model and the unified theory are closely related to those of simple joint kinematic chains, and the accomplishments on simple joint chains can service future researches into other types of planar mechanisms.

1.4 Contents of the thesis

Based on the discussed background this thesis aims to study a unified structure synthesis method of planar kinematic chains and mechanisms with simple and multiple joints characterized by effectiveness, automation and human-machine interaction, and to develop the atlas database containing all the topological graphs for these kinematic chains and mechanisms with different numbers of links, classified by their structural characteristics. Based on the classified atlas database, the creative design of several kinds of mechanisms is also conducted to verify the usefulness of the method. The overall structure of the thesis is as follows.

In chapter 2, the representation models of planar kinematic chains with simple joints, multiple joints and geared joints are proposed and the relationships between these models are also revealed.

In chapter 3, the relationships between the contracted graphs of planar non-fractionated kinematic chains are revealed first. Then a fully-automatic method is proposed to synthesize the whole family of contracted graphs for planar non-fractionated kinematic chains with all possible degrees of freedom.

In chapter 4, a general method is proposed to synthesize planar non-fractionated kinematic chains and mechanisms based on the contracted graphs obtained in chapter 3. The method is fully-automatic and designer-friendly, and planar non-fractionated kinematic chains and mechanisms with up to 19 links are synthesized. Moreover, the classified atlas databases for these kinematic chains and mechanisms are also established.

In chapter 5, based on the structure characteristics of fractionated kinematic chains, a general synthesis equation of planar fractionated kinematic chains is proposed first. Then an automatic method is proposed to synthesize planar fractionated kinematic chains by the combination of planar non-fractionated kinematic chains, and the whole family of planar fractionated kinematic chains up to seven basic loops is synthesized with the method.

In chapter 6, based on the new bicolor topological graph and its inter-convertible characteristics with that of simple joint kinematic chains, an automatic method is proposed to synthesize multiple joint kinematic chains from simple joint kinematic chains and their classified atlas databases. The whole family of multiple joint kinematic chains with up to 16 links is synthesized with the method and corresponding classified atlas databases are also established.

In chapter 7, based on the structural synthesis and classified atlas databases of kinematic chains with simple and multiple joints, a creative design method is proposed to obtain all the feasible mechanisms for a specified task from the topological graphs in the classified atlas databases subject to design constraints. Examples of the creative design of road tractors, hydraulic driven robots and forging manipulators are also conducted.

2 Graph based models of planar mechanisms

2.1 Foreword

The kinematic structure of a mechanism contains the essential information about which link is connected to which other link by what type of joint. In IFToMM, many different ways have been adopted to represent the kinematic structures of mechanisms, such as the functional schematic representation, structural representation, and so on. Graph theory, which is mathematically rigorous, visually intuitive, and easily adaptable to computation, is a powerful mathematical tool for the structural analysis and synthesis of various planar mechanisms. In the chapter, the graph based models of planar mechanisms or kinematic chains with simple joints, multiple joints and geared joints are presented.

2.2 Modeling of simple joint kinematic chains

In the process of structural synthesis and creative design of mechanisms, a mechanism is usually represented by its kinematic chain. The frame of the mechanism is represented by an appropriate link, and all joints are assumed to be revolute. Fig.2-1 (a) shows a heavy-load hydraulic excavator [123], and the upper carriage (arm) of the excavator can rotate 360° around its vertical axis. The upper carriage has four primary links: boom, stick, rocker, and shovel. These primary links perform a planar motion actuated by three pairs of hydraulic cylinders. The kinematic sketch for the mechanism of upper carriage is shown in Fig.2-1 (b). Fig.2-1 (c) shows the kinematic chain of the upper carriage.

The topological graph for the kinematic chain of the upper carriage can be obtained this way: the links of the chain are denoted by vertices and the joints are denoted by edges; the pair connection between links corresponds to the edge connection between vertices. Obviously, the topological graph and the topological structure of a kinematic chain are correspondent with each other. Thus, the research on the kinematic structure of a kinematic chain can be converted into the study of its topological graph. For example, Fig. 2-1 (d) shows the topological graph for the chain in Fig. 2-1 (c).

A topological graph can be represented by its adjacency matrix. The elements of the adjacency matrix are defined as follows:

$$A = \left[a_{ij} \right]_{n \times n} = \begin{cases} 1, \textit{ if vertices i and j are adjacent} \\ 0, \textit{ otherwise} \end{cases} \tag{2-1}$$

where n is the number of the vertices of the graph.

For the topological graph in Fig.2-1 (d), the corresponding adjacency matrix is

$$A=\begin{bmatrix}0&1&0&0&1&0&0&0&1&0&1&0\\1&0&1&0&0&0&0&0&0&0&0&1\\0&1&0&1&0&0&0&0&0&0&0&0\\0&0&1&0&1&0&0&0&0&0&0&0\\1&0&0&1&0&1&0&0&0&0&0&1\\0&0&0&0&1&0&1&0&0&0&0&0\\0&0&0&0&0&1&0&1&0&0&0&0\\0&0&0&0&0&0&1&0&1&0&0&0\\1&0&0&0&0&0&0&1&0&1&0&0\\0&0&0&0&0&0&0&0&1&0&1&0\\1&0&0&0&0&0&0&0&0&1&0&0\\0&1&0&0&1&0&0&0&0&0&0&0\end{bmatrix} \quad (2\text{-}2)$$

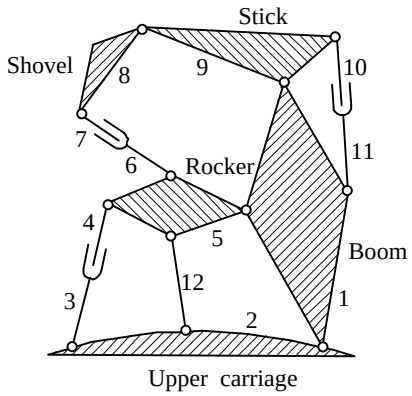

(a) A heavy-load hydraulic excavator (b) the kinematic sketch of its upper carriage

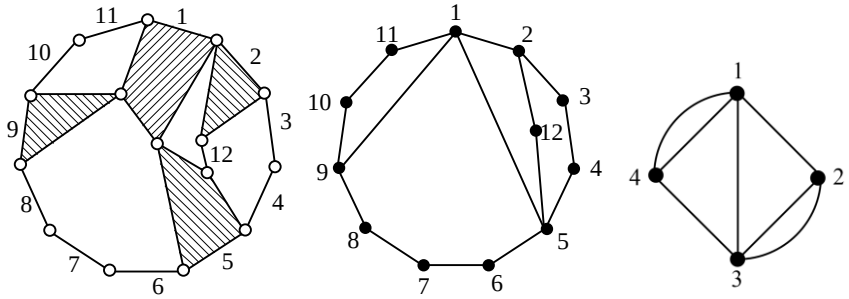

(c) the kinematic chain, (d) the topological graph, and (e) the contracted graph

Fig. 2-1 Mechanism and its representation graphs

The contracted graph can be obtained by replacing each alternating sequence of binary vertices and edges by an edge from its topological graph. For example, Fig.2-1 (e) is the contracted graph for the graph in Fig.2-1 (d).

A contracted graph can also be represented by its adjacency matrix. The elements of the adjacency matrix for a contracted graph are defined as follows:

$$A=\left[a_{ij}\right]_{N_m\times N_m}=\begin{cases}k, \text{if vertices } i \text{ and } j \text{ are adjacent } \textit{through } k \textit{ edges}\\ s, \text{if vertex } i \textit{ has } s \textit{ selfloops}\\ 0, \text{otherwise}\end{cases} \tag{2-3}$$

where N_m is the number of the vertices of the contracted graph. The adjacency matrix of the contracted graph in Fig.2-1(e) is

$$A=\begin{bmatrix}0 & 2 & 1 & 1\\ 2 & 0 & 1 & 0\\ 1 & 1 & 0 & 2\\ 1 & 0 & 2 & 0\end{bmatrix} \tag{2-4}$$

In a contracted graph, two vertices are said to have k-1 multiple-edges if they are connected directly through k (k>1) edges. The number of multiple-edges for a contracted graph is defined as the sum of the numbers of multiple-edges between every pair of vertices. For example, Fig.2-1(e) has two multiple-edges.

2.3 Non-fractionated and fractionated kinematic chains

If a kinematic chain can be separated into at least two independent kinematic chains at some link or joint, the chain is called a fractionated kinematic chain [11,124]. Fractionation can be divided into two basic types: link-fractionation (L-F) and joint-fractionation (J-F). Any fractionated kinematic chain is either one of them or their combination.

Figure 2-2 (a) shows a link-fractionated kinematic chain. At link 4 the kinematic chain can be separated into two independent kinematic chains, a 4-link kinematic chain and a 7-link kinematic chain.

The topological graph corresponding to a link-fractionated kinematic chain is called the vertex-fractionated topological graph, and the corresponding contracted graph is called the vertex-fractionated contracted graph. The topological graph and contracted graph for the link-fractionated kinematic chain are shown in Fig. 2-2 (b) and (c), respectively.

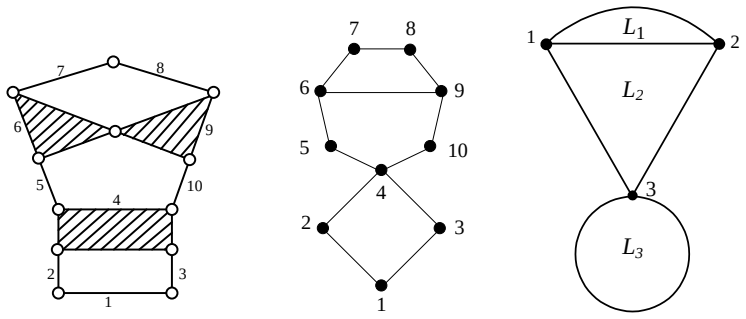

(a) A L-F kinematic chain, (b) its topological graph, (c) its contracted graph

Fig. 2-2 A L-F kinematic chain and its representation graphs

Figure 2-3 (a) shows a joint-fractionated kinematic chain. At joint *e* the kinematic chain can be separated into two independent kinematic chains, a 4-link kinematic chain and a 6-link kinematic chain.

The topological graph corresponding to a joint-fractionated kinematic chain is called the edge-fractionated topological graph, and the corresponding contracted graph is called the edge-fractionated contracted graph. The topological graph and contracted graph for the joint-fractionated kinematic chain are shown in Fig. 2-3 (b) and (c), respectively.

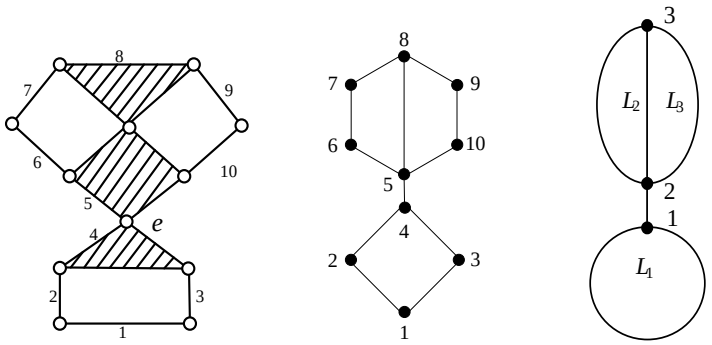

(a) A J-F kinematic chain, (b) its topological graph, (c) its contracted graph

Fig. 2-3 A J-F kinematic chain and its representation graphs

Obviously, fractionated kinematic chains can be synthesized through the combination of two or more independent non-fractionated kinematic chains.

2.4 Modeling of multiple joint kinematic chains

Many mechanisms contain multiple or compound joints for the sake of simplifying kinematic analysis and minimizing the space requirement. Studying simple joint kinematic chains using the above topological graph technique is very convenient. However, this technique cannot be applied directly to multiple joint kinematic chains because the resulting topological graphs contain polygons. Therefore, the topological structure of multiple joint kinematic chains is usually represented by a bicolor topological graph.

Conventional bicolor graphs are established as follows: solid ("●") and hollow ("○") vertices are used to represent links and joints, respectively, and the corresponding solid and hollow vertices are connected with an edge when a link is connected with a joint [86]. For example, Fig.2-4 (a) shows an eight-link multiple joint kinematic chain, and Fig.2-4 (b) shows its conventional bicolor topological graph.

A multiple joint kinematic chain and its conventional bicolor topological graph are also correspondent with each other. However, a conventional bicolor topological graph has too many vertices relative to its number of links (its number of vertices is equal to the sum of the numbers of links and joints of the chain). Therefore, more storage space is needed in the process of computerized structural synthesis. Moreover, conventional bicolor topological graphs fail to bridge the studies on simple joint chains and multiple joint chains. Thus, it is

hard to employ the studies on the structural analysis and synthesis theory of simple joint kinematic chains in the studies on kinematic chains with multiple joints.

Here, based on the topological graphs of simple joint kinematic chains, a new kind of bicolor topological graph is proposed to represent the topological structures of multiple joint kinematic chains. In the new graph, solid ("●") and hollow ("○") vertices denote the links of the chain and multiple joints, respectively. The two corresponding solid vertices are connected with an edge if the two links are connected directly by a simple joint, and the corresponding solid and hollow vertices are connected with an edge if a link is connected with a multiple joint. For example, Fig.2-4 (c) shows the new bicolor topological graph for the chain in Fig.2-4 (a). Obviously, a multiple joint kinematic chain and its new bicolor topological graph are also correspondent with each other.

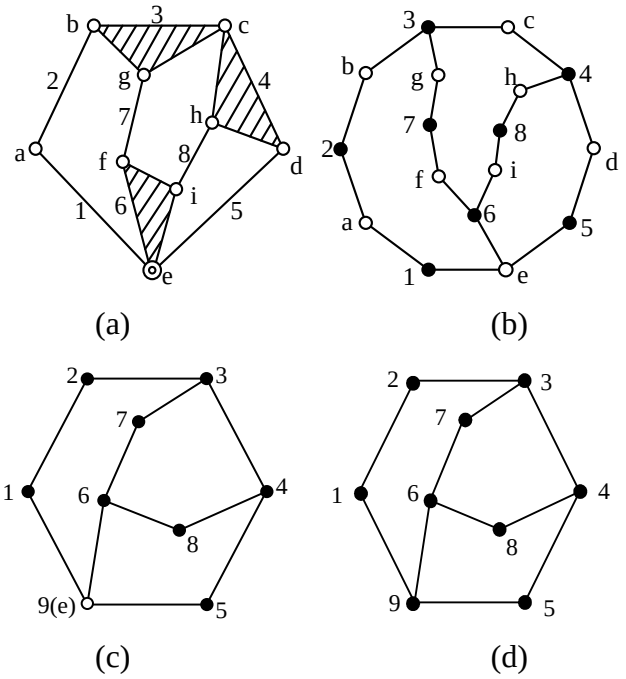

Fig.2-4 (a) A multiple joint kinematic chain, and its (b) conventional bicolor topological graph, (c) new bicolor topological graph, and (d) basic topological graph

The new bicolor topological graph can be represented by the adjacency matrix modified from that of the simple joint kinematic chain. The elements of the adjacency matrix are

$$A=\left[a_{ij}\right]_{n\times n}=\begin{cases}1, \textit{if vertices i and j are adjacent}\\ -d, \textit{if } i=j \textit{ and } i\,(\textit{or } j\,) \textit{is the label of a hollow vertex}\\ 0, \textit{otherwise}\end{cases} \tag{2-5}$$

where n is the number of the vertices of the graph, and d is the pseudo-degree of the hollow vertices (The pseudo-degree of a hollow vertex is equal to the number of edges connected with the hollow vertex).

The adjacency matrix of the topological graph in Fig.2-4 (c) is

$$A=\begin{bmatrix} 0 & 1 & 0 & 0 & 0 & 0 & 0 & 0 & 1 \\ 1 & 0 & 1 & 0 & 0 & 0 & 0 & 0 & 0 \\ 0 & 1 & 0 & 1 & 0 & 0 & 1 & 0 & 0 \\ 0 & 0 & 1 & 0 & 1 & 0 & 0 & 1 & 0 \\ 0 & 0 & 0 & 1 & 0 & 0 & 0 & 0 & 1 \\ 0 & 0 & 0 & 0 & 0 & 0 & 1 & 1 & 1 \\ 0 & 0 & 1 & 0 & 0 & 1 & 0 & 0 & 0 \\ 0 & 0 & 0 & 1 & 0 & 1 & 0 & 0 & 0 \\ 1 & 0 & 0 & 0 & 1 & 1 & 0 & 0 & -3 \end{bmatrix} \tag{2-6}$$

The characteristics of the new bicolor topological graph for a multiple joint kinematic chain are as follows.

(1) In a new bicolor topological graph, the number of vertices is equal to the sum of the numbers of links and multiple joints. This number is reduced noticeably compared with that of the conventional graph.

(2) The degree of any solid vertex is equal to the number of joints connected with the corresponding link. The pseudo-degree of a hollow vertex is greater than two, and is one more than the factors of the multiple joint. The factors of a multiple joint are the number of the kinematic pairs presented by the joint.

(3) For a multiple joint kinematic chain of N links and M kinematic pairs encompassing J multiple joints, the number of vertices and edges of its new bicolor topological graph are $(N+J)$ and $(M+J)$, respectively. Both numbers are thus increased by J compared with the number of links and kinematic pairs of its structural diagram.

For example, Fig.2-4 (c) is the new bicolor topological graph of the eight-link kinematic chain with one multiple joint in Fig.2-4 (a). Only one multiple joint exists in this kinematic chain; thus, the numbers of vertices and edges of its new bicolor topological graph [Fig.2-4(c)] are 9 and 11, respectively.

If the difference between the solid vertex and the hollow vertex is ignored, then the new bicolor topological graph is converted to the topological graph of simple joint kinematic chains, which is termed the basic topological graph of the multiple joint kinematic chain. For example, Fig.2-4 (d) is the basic topological graph of the multiple joint kinematic chain in Fig.2-4 (a).

2.5 Modeling of geared kinematic chains

A geared mechanism is a complex mechanical system including simple joints, multiple joints, and geared pairs. This system is obtained by adding a series of meshing gears to a basic kinematic chain of planar or spatial linkages.

Generally, the topological structure of the geared kinematic chain is represented by a tricolor topological graph. In conventional tricolor topological graphs [86], solid vertices (“●”) represent links, hollow vertices (“○”) represent joints, bicyclic vertices (“◎”) represent

geared pairs, and vertices are connected with edges according to the relationship of the corresponding parts in the geared chain.

Fig.2-5 (a) shows a six-link geared chain with two multiple joints and two gear pairs, obtained by adding two pairs of meshing gears to a four-link linkage. Fig. 2-5 (b) shows the conventional tricolor topological graph of Fig. 2-5 (a).

The conventional tricolor topological graph is correspondent with its geared kinematic chain, but it is too complex because the number of its vertices is equal to the sum of the numbers of links, joints (simple and multiple joints), and geared pairs. Moreover, the conventional tricolor topological graph is hard to associate with the above two kinds of kinematic chains.

Here, based on the topological graph of simple joint kinematic chains and the new bicolor topological graph of multiple joint kinematic chains, the new topological graph of geared kinematic chains is proposed.

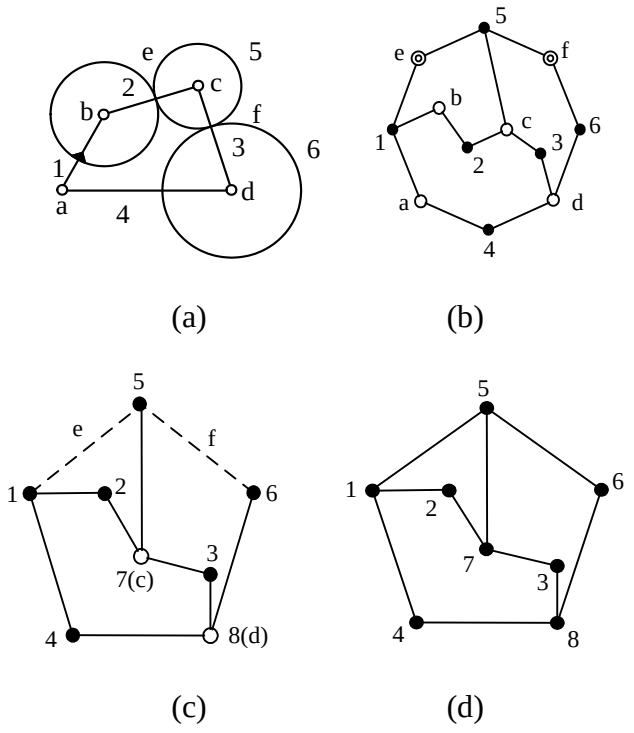

Fig.2-5 (a) A geared kinematic chain and its (b) conventional tricolor topological graph, (c) new topological graph, and (d) basic topological graph

(1) Solid vertices ("●") are used to denote links of the chain, and hollow vertices ("○") are used to denote multiple joints.

(2) Dashed lines ("--") are used to denote geared or cam pairs, and solid lines ("—") are used to denote other joints of the chain.

For example, Fig. 2-5 (c) shows the new topological graph of the geared chain in Fig. 2-5 (a). Obviously, a geared chain and its new topological graph are also correspondent.

The new topological graph of the geared kinematic chain can also be represented by the adjacency matrix modified from that of the simple/multiple joint kinematic chain. The elements of the adjacency matrix are

$$A=\left[a_{ij}\right]_{n\times n}=\begin{cases}1, \textit{if vertices } i \textit{ and } j \textit{ are connected by a solid line}\\ -1, \textit{if vertices } i \textit{ and } j \textit{ are connected by a dashed line}\\ -d, \textit{if } i=j \textit{ and } i(\textit{or } j) \textit{is the label of a hollow vertex}\\ 0, \textit{otherwise}\end{cases} \tag{2-7}$$

where n is the number of vertices of the graph, and d is the pseudo-degree of the hollow vertices.

For the topological graph in Fig. 2-5 (c), its adjacency matrix is

$$\mathrm{A}=\begin{bmatrix}0&1&0&1&-1&0&0&0\\1&0&0&0&0&0&1&0\\0&0&0&0&0&0&1&1\\1&0&0&0&0&0&0&1\\-1&0&0&0&0&-1&1&0\\0&0&0&0&-1&0&0&1\\0&1&1&0&1&0&-3&0\\0&0&1&1&0&1&0&-3\end{bmatrix} \tag{2-8}$$

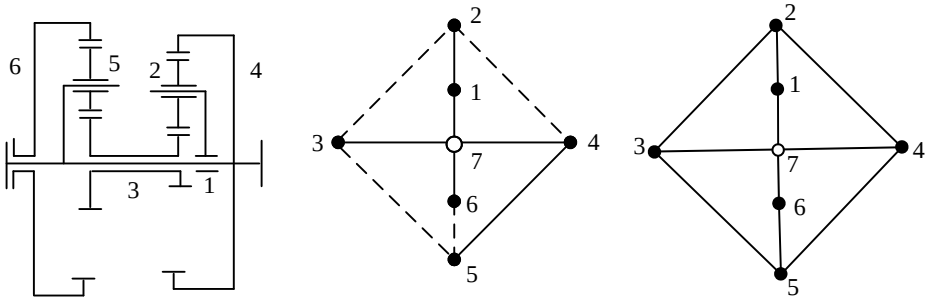

(a) A geared kinematic chain (b) the new topological graph (c) the basic topological graph

Fig.2-6 A geared kinematic chain and its representation graph

Another geared kinematic chain is shown in Fig. 2-6 (a), and Fig.2-6 (b) is its new topological graph. The adjacency matrix of the new topological graph is

$$A = \begin{bmatrix} 0 & 1 & 0 & 0 & 0 & 0 & 1 \\ 1 & 0 & -1 & -1 & 0 & 0 & 0 \\ 0 & -1 & 0 & 0 & -1 & 0 & 1 \\ 0 & -1 & 0 & 0 & 1 & 0 & 1 \\ 0 & 0 & -1 & 1 & 0 & -1 & 0 \\ 0 & 0 & 0 & 0 & -1 & 0 & 1 \\ 1 & 0 & 1 & 1 & 0 & 1 & -4 \end{bmatrix} \tag{2-9}$$

The characteristics of the new topological graph of the geared chain are:

(1) The number of vertices of the new topological graph is equal to the sum number of links and multiple joints. This number is reduced remarkably compared with the number of vertices in the conventional tricolor graph.

(2) The degree of any solid vertex is equal to the number of joints connected with the corresponding link. The pseudo-degree of every hollow vertex is greater than two, and is one more than the number of the corresponding kinematic pair.

(3) For a geared kinematic chain with *J* multiple joints and *P* geared (or cam) pairs, both the numbers of vertices and edges of its new topological graph increase by *J* compared with the numbers of links and kinematic pairs of its structural diagram.

For example, the kinematic chain shown in Fig. 2-5 (a) has two multiple joints and two geared pairs. Its new topological graph has 8 and 10 vertices and edges, respectively. Both increase by two compared with the numbers of links and kinematic pairs of its structural diagram.

If the difference between the solid vertices and hollow vertices as well as that between dash lines and solid lines is ignored, then the new topological graph representing the geared kinematic chain is converted into the topological graph of the simple joint kinematic chain, which is termed the basic topological graph of the geared kinematic chain. For example, Fig.2-6 (c) is the basic topological graph of the geared kinematic chain in Fig. 2-6(a).

2.6 Summary

This chapter introduces some basic concepts of the graph theory essential for the representation of the kinematic structures of planar kinematic chains or mechanisms with simple joints, multiple joints and geared joints. To facilitate the development of a unified and automated structural synthesis methodology, the representation models of various planar mechanisms have close relationships with each other and these relationships are also revealed.

3 Structural synthesis of non-fractionated contracted graphs

3.1 Foreword

The contracted graph of a kinematic chain shows its primary (or abstract) topological structure. So the synthesis of contracted graphs is the foundation for the construction of the kinematic structures of kinematic chains and mechanisms. This chapter attempts to develop a fully-automatic method to synthesize the whole family of contracted graphs for planar non-fractionated kinematic chains with all possible degrees of freedom. First the relationships of non-fractionated contracted graphs for different types of kinematic chains are revealed based on the parameter 4-bit group and link assortment array. Then a general algorithm for the generation of the adjacency matrices of contracted graphs from the synthesis equation set is presented. Efficient methods to detect fractionated structures and isomorphism are also addressed. Finally, a human-machine interactive synthesis program is developed, and the complete lists of contracted graphs and valid contracted graphs for planar non-fractionated kinematic chains with up to 19 links and all possible degrees of freedom are provided.

3.2 4-parameter index of a kinematic family

In the structural analysis and synthesis of kinematic chains, four parameters, namely N (number of links), F (degrees of freedom), M (number of kinematic pairs), and L (number of indepentent loops), are the most important and we define the four parameters [N, F, L, M] as the 4-parameter index of a kinematic family.

According to the Grübler equation and Euler's formula for graphs, we have

$$F = 3(N-1) - 2M \tag{3-1}$$

$$L = M - N + 1 \tag{3-2}$$

From Eqs. (3-1) and (3-2), we get

$$L = (N - F - 1)/2 \tag{3-3}$$

$$M = L + N - 1 \tag{3-4}$$

If any two of the four parameters are given, the other two can be determined. For example, the 4- parameter index for 10-link 1-DOF kinematic chain is [10, 1, 4, 13].

3.3 Link assortment array

The type of links and their number that are necessary to form a kinematic chain with specified number of links and degrees of freedom are defined as the link assortment. The link assortment array of a kinematic chain is represented by

$$[N_2, N_3, \ldots, N_p] \tag{3-5}$$

where N_2, N_3, N_4, … are the numbers of binary, ternary, quaternary links, etc, in order. If the number is greater than 9, alphabetic letters are used instead in order to avoid multi-digital numbers: A represents 10, B represents 11, C represents 12, and so on. For example, the link

assortment array [4, A, 0, 0, 0, 0] denotes that the number of ternary links (N_3) is 10. The highest connectivity p is determined by the following two equations

(1)if $F \le 1$， then $p = (N - F + 1)/2$；

(2)if $F \ge 2$， then $p = \min\{(N - F - 1),\quad (N + F - 1)/2\}$.

For a kinematic chain for which N_m and M_c are the numbers of vertices and edges, respectively, of its contracted graph, we have

$$N_m = \sum_{d=3}^{p} N_d \tag{3-6}$$

and

$$L = M - N + 1 = M_c - N_m + 1 \tag{3-7}$$

Based on graph theory, we have

$$\sum_{d=3}^{p} d \cdot N_d = 2M_c \tag{3-8}$$

From Eqs. (3-6), (3-7) and (3-8), we have

$$2(L-1) = \sum_{d=3}^{p} (d-2) N_d \tag{3-9}$$

From Eqs. (3-1) and (3-2), we have

$$N = 2L + F + 1 \tag{3-10}$$

The number of links in a kinematic chain satisfies

$$N = N_2 + N_3 + \cdots + N_p \tag{3-11}$$

From Eqs. (3-9) and (3-10), we have

$$N_2 = F + 3 + \sum_{d=4}^{p} (d-3) N_d \tag{3-12}$$

The link assortment equation for N-link F-DOF kinematic chains can thus be written as

$$\begin{cases} N_2 = F + 3 + \sum_{d=4}^{p} (d-3) N_d \\ N = N_2 + N_3 + \cdots + N_p \end{cases} \tag{3-13}$$

From Eq. (3-13), the link assortment arrays of kinematic chains with specified number of links and DOFs can be solved easily.

As the 4-parameter index for 10-link 1-DOF kinematic chains is [10, 1, 4, 13] and the highest connectivity is p＝5, from Eq. (3-13) seven link assortment arrays are obtained, that is [4,6,0,0], [5,4,1,0], [6,2,2,0], [7,0,3,0], [6,3,0,1], [7,1,1,1] and [8,0,0,2].

3.4 Relationship of link assortment arrays

Based on Eq. (3-13), N-link 1-DOF kinematic chains and (N+i)-link (i+1)-DOF (i = 1,2,3, …) kinematic chains have the same number of basic loops (L). The relationships of link assortment arrays for kinematic chains with the same number of basic loops (L) are as follows.

Theorem 3-1: If [N_2, N_3, …, N_p] is a link assortment array for N-link 1-DOF kinematic chains, then [(N_2+1), N_3, …, N_p, 0] must be a link assortment array for (N+1)-link 2-DOF kinematic chains, [(N_2+2), N_3, …, N_p, 0, 0] must be a link assortment array for (N+2)-link 3-DOF kinematic chains, [(N_2+3), N_3, …, N_p, 0, 0, 0] must be a link assortment array for (N+3)-link 4-DOF kinematic chains, etc.

Proof:

Let [N_2, N_3, …, N_p, N_{p+1}] be a link assortment array for (N+1)-link 2-DOF kinematic chains, according to link assortment equation (3-13), we have

$$N+1=N_2+N_3+\cdots+N_p+N_{p+1} \tag{3-14}$$

and

$$N_2=(1+1)+3+\sum_{d=4}^{P}(d-3)N_d+(p-2)N_{p+1} \tag{3-15}$$

Rewriting Eqs. (3-14) and (3-15), we get

$$N=(N_2-1)+N_3+\cdots+N_p+N_{p+1} \tag{3-16}$$

and

$$(N_2-1)=1+3+\sum_{d=4}^{P}(d-3)N_d+(p-2)N_{p+1} \tag{3-17}$$

Obviously, if $N_{p+1}=0$, then [N_2-1, N_3, ..., N_p] is a link assortment array for N-link 1-DOF kinematic chains. So we have proven also that if [N_2, N_3, …, N_p] is a link assortment array for N-link 1-DOF kinematic chains, then [(N_2+1), N_3, …, N_p, 0] is a link assortment array for (N+1)-link 2-DOF kinematic chains.

Tab. 3-1 Link assortment arrays of 10-link 1-DOF, 11-link 2-DOF and 12-link 3-DOF kinematic chains

No	10-link 1-DOF KCs	11-link 2-DOF KCs	12-link 3-DOF KCs
1	[4,6,0,0]	[5,6,0,0,0]	[6,6,0,0,0,0]
2	[5,4,1,0]	[6,4,1,0,0]	[7,4,1,0,0,0]
3	[6,2,2,0]	[7,2,2,0,0]	[8,2,2,0,0,0]
4	[7,0,3,0]	[8,0,3,0,0]	[9,0,3,0,0,0]
5	[6,3,0,1]	[7,3,0,1,0]	[8,3,0,1,0,0]
6	[7,1,1,1]	[8,1,1,1,0]	[9,1,1,1,0,0]
7	[8,0,0,2]	[9,0,0,2,0]	[A,0,0,2,0,0]
8		[8,2,0,0,1]	[9,2,0,0,1,0]
9		[9,0,1,0,1]	[A,0,1,0,1,0]
10			[A,1,0,0,0,1]

(In link assortment array, A=10, B=11, C=12, etc.)

Similarly, we can also prove that if [N_2, N_3, …, N_p] is a link assortment array for N-link 1-DOF kinematic chains, then [(N_2+2), N_3, …, N_p, 0, 0] is a link assortment array for (N+2)-link

3-DOF kinematic chains, [(N_2+3), N_3, …, N_p, 0, 0, 0] is a link assortment array for (N+3)-link 4-DOF kinematic chains, etc.

As an example to verify Theorem 3-1, link assortment arrays of 10-link 1-DOF, 11-link 2-DOF and 12-link 3-DOF kinematic chains are given in Table 3-1. Here, "[4,6,0,0]" is a link assortment array for 10-link 1-DOF kinematic chains, [(4+1),6,0,0,0] is a link assortment array for 11-link 2-DOF kinematic chains, and [(4+2),6,0,0,0,0] is a link assortment array for 12-link 3-DOF kinematic chains, etc.

If from a link assortment array at least one non-fractionated contracted graph can be obtained, the assortment array is defined as a *non-fractionated link assortment array*; otherwise, it is a fractionated link assortment array.

Theorem 3-2: The number of non-fractionated link assortment arrays for N-link 1-DOF kinematic chains and (N+i)-link (i +1)-DOF (i = 1, 2, 3, …) kinematic chains are the same.

Proof:

If [N_2, N_3, …, N_p, N_{p+1}] is a link assortment array for (N+1)-link 2-DOF kinematic chains, according to link assortment equation (3-13) we have

$$N_2 = (1+1) + 3 + \sum_{d=4}^{p-1}(d-3)N_d + (p-3)N_p + (p-2)N_{p+1} \tag{3-18}$$

Obviously, if N_{p+1}=1, then N_p=0. Assume that N_{p+1}=1, and $N_p \neq 0$, thus based on Eq. (3-18), we have

$$N_2 = N + \sum_{d=4}^{p-1}(d-3)N_d + (p-3)(N_p - 1) \tag{3-19}$$

and from Eq. (3-19) it would follow $N_2 \geq N$.

Assume now that one has a link assortment array [N_2, N_3, …, $N_{p\text{-}1}$, 0, 1] (0= N_p and 1= N_{p+1}) for (N+1)-link 2-DOF kinematic chains, according to link assortment equation (3-18), we can conclude that [(N_2-3), N_3, …, ($N_{p\text{-}1}$+1)] is a link assortment array for (N-2)-link 1-DOF kinematic chains. The contracted graphs corresponding to [N_2, N_3, …, $N_{p\text{-}1}$, 0, 1] can be obtained through the combination of the contracted graphs corresponding to [(N_2-3), N_3, …, ($N_{p\text{-}1}$+1)] and a self-loop. Thus all contracted graphs corresponding to [N_2, N_3, …, $N_{p\text{-}1}$, 0, 1] are fractionated contracted graphs, containing the same subgraphs as the contracted graphs corresponding to [(N_2-3), N_3, …, ($N_{p\text{-}1}$+1)].

Moreover, if for any link assortment array [N_2, N_3, …, N_p, N_{p+1}] of (N+1)-link 2-DOF kinematic chain it holds N_{p+1}=0, then [N_2-1, N_3, …, N_p] is a link assortment array of N-link 1-DOF kinematic chains.

So we can conclude that the number of non-fractionated link assortment arrays for N-link 1-DOF kinematic chains and (N+1)-link 2-DOF kinematic chains are the same.

Similarly, we can also prove that the number of non-fractionated link assortment arrays for N-link 1-DOF kinematic chains and any (N+i)-link (i +1)-DOF (i = 1, 2, 3, …) kinematic chains are the same.

For example, in Tab. 3-1, 10-link 1-DOF, 11-link 2-DOF and 12-link 3-DOF kinematic chains have the same number of non-fractionated link assortment arrays. The last two link assortment arrays, "[8,2,0,0,1]" and "[9,0,1,0,1]", for 11-link 2-DOF kinematic chains are fractionated link assortment arrays. The contracted graphs corresponding to "[8,2,0,0,1]" can be obtained through the combination of the contracted graphs corresponding to link assortment array [5,2,1] of 8-link 1-DOF kinematic chains and a self-loop. The last three link assortment arrays for 12-link 3-DOF kinematic chains are also fractionated link assortment arrays.

3.5 Synthesis equation set of contracted graphs

For a link assortment array [N_2, N_3, …, N_p] of N-link F-DOF kinematic chains, if $N_q \neq 0$ ($3 \le q \le p$), then there are N_q vertices whose degrees are all equal to q in the corresponding contracted graphs. For all $N_q \neq 0\,(3 \le q \le p)$ in the link assortment array, the degrees of all vertices are represented by a degree-array

$$[d_1, d_2, \ldots, d_{N_m}] \tag{3-20}$$

where, N_m is the total number of vertices and $d_i \ge d_{i+1}$ (i=1, 2, …, (N_m-1)).

For example, [7, 3, 1, 1, 0] is a link assortment array for 12-link 1-DOF kinematic chains. Here N_3=3 ≠ 0, so there are 3 vertices whose degrees are equal to 3; N_4=1 ≠ 0, so there is 1 vertex whose degree is equal to 4; N_5=1 ≠ 0, so there is 1 vertex whose degree is equal to 5. The corresponding degree-array is [5, 4, 3, 3, 3].

It is clear that the sum of all elements (x_{ij}) in a row in an adjacent matrix is equal to the degree of corresponding vertex. Based on the adjacency matrices of contracted graphs and the degree-arrays of link assortment arrays, we have

$$\begin{cases} x_{12} + x_{13} + x_{14} + \ldots + x_{1N_m} = d_1 \\ x_{12} + x_{23} + x_{24} + \ldots + x_{2N_m} = d_2 \\ x_{13} + x_{23} + x_{34} + \ldots + x_{3N_m} = d_3 \\ \ldots \\ x_{1N_m} + x_{2N_m} + x_{3N_m} + \ldots + x_{(N_m-1)N_m} = d_{N_m} \end{cases} \tag{3-21}$$

Equation set (3-21) is defined as the synthesis equation set of contracted graphs.

Theorem 3-3: The non-fractionated contracted graphs for N-link 1-DOF kinematic chains and (N+i)-link (i +1)-DOF (i = 1, 2, 3, …) kinematic chains are the same.

Proof:

As the degree-array of the link assortment array [N_2, N_3, …, N_p] for N-link 1-DOF kinematic chains is the same as that of [(N_2+1), N_3, …, N_p, 0] for (N+1)-link 2-DOF kinematic chains, the non-fractionated contracted graphs for the two types of kinematic chains are the same. According to Theorem 3-2, the numbers of non-fractionated link assortment arrays for the two types of kinematic chains are the same. So the non-fractionated contracted graphs for N-link 1-DOF kinematic chains and (N+1)-link 2-DOF kinematic chains are the same.

Similarly, we can prove that the non-fractionated contracted graphs for N-link 1-DOF kinematic chains are the same as those for any (N+i)-link (i +1)-DOF (i = 1, 2, 3, …)

kinematic chains.

For the link assortment array [7, 3, 1, 1, 0] of 12-link 1-DOF kinematic chains, the corresponding degree-array is [5, 4, 3, 3, 3]. The synthesis equation set of contracted graphs for the link assortment array is

$$\begin{cases} x_{12}+x_{13}+x_{14}+x_{15}=5 \\ x_{12}+x_{23}+x_{24}+x_{25}=4 \\ x_{13}+x_{23}+x_{34}+x_{35}=3 \\ x_{14}+x_{24}+x_{34}+x_{45}=3 \\ x_{15}+x_{25}+x_{35}+x_{45}=3 \end{cases} \tag{3-22}$$

Obviously, Eq.(5-22) is the synthesis equation set of contracted graphs for any link assortment arrays with the degree-array [5, 4, 3, 3, 3] for (12+i)-link (i +1)-DOF (i = 0, 1, 2, 3, …) kinematic chains.

3.6 Generation of contracted graph matrices

A general progress to solve the synthesis equation set is given as follows.

Step 1: Determine the connection relationships between vertex 1 and the others by solving the first equation of the synthesis equation set

$$x_{12}+x_{13}+x_{14}+...+x_{1N_m}=d_1 \tag{3-23}$$

As only non-fractionated contracted graphs are considered, at least two variables in Eq.(3-23) are greater than zero and each variable in Eq.(3-23) satisfies

$$0\le x_{1j}<d_j\ (2\le j\le N_m) \tag{3-24}$$

Based on the degrees of vertices, vertices 2~ N_m are divided into symmetry sets ($\boldsymbol{SS_1}$) where the vertices in each symmetry set have the same degrees. Without loss of generality, if vertices i and j (i>j) are in the same symmetry set, we have

$$x_{1i}\le x_{1j} \tag{3-25}$$

According to Eqs.(3-24) and (3-25), the values of all variables x_{12}, x_{13}, …, x_{1N_m} in Eq.(3-23) can be determined. For example, according to Eq.(3-24), the variables in the first equation of equation set (3-22) satisfy

$$0\le x_{12}\le 3,\ 0\le x_{1i}\le 2\ (i=3,\ 4,\ 5) \tag{3-26}$$

The degrees of vertices 2~5 are 4, 3, 3 and 3, respectively, so vertices 2~5 are divided into two symmetry sets: {2} and {3, 4, 5}. In the symmetry set {3, 4, 5}, according to Eq.(3-25), we have

$$x_{15}\le x_{14}\le x_{13} \tag{3-27}$$

Based on Eqs.(3-26) and (3-27), the seven solutions for the first equation of equation set (3-22) are shown in Tab. 3-2.

After determining all solutions x_{12}, x_{13}, …, x_{1N_m} in Eq.(3-23), these solutions can be inserted in the remaining part of Eq.(3-21), giving the reduced set of equations.

$$\begin{cases} x_{23}+x_{24}+\ldots+x_{2N_m}=d_2-x_{12} \\ x_{23}+x_{34}+\ldots+x_{3N_m}=d_3-x_{13} \\ \ldots \\ x_{2N_m}+x_{3N_m}+\ldots+x_{(N_m-1)N_m}=d_{N_m}-x_{1N_m} \end{cases} \tag{3-28}$$

Tab. 3-2 The seven solutions for the first equation of equation set (3-22)

No	x_{12}	x_{13}	x_{14}	x_{15}
1	3	2	0	0
2		1	1	0
3	2	2	1	0
4		1	1	1
5	1	2	2	0
6		2	1	1
7	0	2	2	1

Step 2: Determine the connection relationships between vertex 2 and the others by solving the first equation of equation set (3-28)

$$x_{23}+x_{24}+\ldots+x_{2N_m}=d_2-x_{12} \tag{3-29}$$

Each variable in Eq.(3-29) satisfies

$$0\le x_{2i}\le \min(d_2-x_{12}, d_i-x_{1i})(3\le i\le N_m) \tag{3-30}$$

Based on the values of $x_{13}, \ldots, x_{1N_m}$, vertices 3~ N_m are further divided into new symmetry sets (***SS*₂**). Two vertices *m* and *n* are in the same new symmetry set (***SS*₂**) if and only if they belong to the same symmetry set (***SS*₁**) in Step 1 and they have the same values of x_{1m} and x_{1n}. Without loss of generality, if vertices *i* and *j* (*i*>*j*) are in the same new symmetry set, we have

$$x_{2i}\le x_{2j} \tag{3-31}$$

According to Eqs.(3-30) and (3-31), the values of all variables $x_{23}, x_{24}, \ldots, x_{2N_m}$ in Eq.(3-29) can be determined. For example, for the first solution in Tab.3-2, equation set (3-22) is converted into

$$\begin{cases} x_{23}+x_{24}+x_{25}=1 \\ x_{23}+x_{34}+x_{35}=1 \\ x_{24}+x_{34}+x_{45}=3 \\ x_{25}+x_{35}+x_{45}=3 \end{cases} \tag{3-32}$$

For the first equation of equation set (3-32), according to Eq.(3-30), we have

$$0\le x_{2i}\le 1 \ (i=3, 4, 5) \tag{3-33}$$

As $x_{15}=x_{14}\ne x_{13}$, vertices 3, 4 and 5 are divided into two new symmetry sets: {3} and {4, 5}. According to Eq.(3-31), we have

$$x_{25}\le x_{24} \tag{3-34}$$

The two solutions for the first equation in equation set (3-32) are thus: $x_{23}=1$, $x_{24}=0$, $x_{25}=0$ or $x_{23}=0$, $x_{24}=1$, $x_{25}=0$.

After determining all solutions x_{23}, x_{24}, …, x_{2N_m} in Eq.(3-29), these solutions can be inserted in the remaining part of Eq.(3-28), giving the reduced set of equations.

$$\begin{cases} x_{34}+x_{35}+\ldots+x_{3N_m}=d_3-x_{13}-x_{23} \\ x_{34}+x_{45}+\ldots+x_{4N_m}=d_4-x_{14}-x_{24} \\ \ldots \\ x_{3N_m}+x_{4N_m}+\ldots+x_{(N_m-1)N_m}=d_{N_m}-x_{1N_m}-x_{2N_m} \end{cases} \tag{3-35}$$

Step *n* for $\mathbf{3 \le n \le N_m\text{-}3}$: Determine the connection relationships between vertex *n* and the others by solving the first equation in Eq. (3-36)

$$\begin{cases} x_{n(n+1)}+x_{n(n+2)}+\ldots+x_{nN_m}=d_n-\sum_{i=1}^{n-1}x_{in} \\ x_{n(n+1)}+x_{(n+1)(n+2)}+\ldots+x_{(n+1)N_m}=d_{(n+1)}-\sum_{i=1}^{n-1}x_{i(n+1)} \\ \ldots \\ x_{nN_m}+x_{(n+1)N_m}+\ldots+x_{(N_m-1)N_m}=d_{N_m}-\sum_{i=1}^{n-1}x_{iN_m} \end{cases} \tag{3-36}$$

Each variable of the first equation satisfies

$$0 \le x_{nj} \le \min\left(d_n-\sum_{i=1}^{n-1}x_{in},\ d_j-\sum_{i=1}^{n-1}x_{ij}\right)\ ((n+1) \le j \le b) \tag{3-37}$$

Based on the values of $x_{(n-1)(n+1)}$, …, $x_{(n-1)N_m}$, vertices $(n+1)$~ N_m are divided into new symmetry sets ($\boldsymbol{SS_n}$). Two vertices *p* and *q* are in the same new symmetry set ($\boldsymbol{SS_n}$) if and only if they belong to the same symmetry set ($\boldsymbol{SS_{n-1}}$) in Step $(n-1)$ and they have the same values of $x_{(n-1)p}$ and $x_{(n-1)q}$. Without loss of generality, if vertices *i* and *j* ($i>j$) are in the same symmetry set $\boldsymbol{SS_n}$, we have

$$x_{ni} \le x_{nj} \tag{3-38}$$

According to Eqs.(3-37) and (3-38), the values of all variables $x_{n(n+1)}$, $x_{n(n+2)}$, …, x_{nN_m} in the first equation of Eq. (3-36) can be determined.

Step ($\boldsymbol{N_m}$-2) [final step]: The synthesis equation set is converted into the following form at the last step.

$$\begin{cases} x_{(N_m-2)(N_m-1)}+x_{(N_m-2)N_m}=d_{(N_m-2)}-\sum_{i=1}^{N_m-3}x_{i(N_m-2)} \\ x_{(N_m-2)(N_m-1)}+x_{(N_m-1)N_m}=d_{(N_m-1)}-\sum_{i=1}^{N_m-3}x_{i(N_m-1)} \\ x_{(N_m-2)N_m}+x_{(N_m-1)N_m}=d_{N_m}-\sum_{i=1}^{N_m-3}x_{iN_m} \end{cases} \tag{3-39}$$

If Eq. (3-39) has a solution, then it is a contracted graph matrix; otherwise, there is no contracted graph corresponding to the link assortment array. In order to obtain all the contracted graphs without fractionated and isomorphic structures, the detection of fractionated structure and isomorphism is necessary.

3.7 Identification of fractionated structures

Fractionated mechanisms or kinematic chains can be synthesized through combination of several mechanisms or kinematic chains of non-fractionated structures, so only the contracted graphs of non-fractionated structures are considered in the synthesis process. Below the loop based method is proposed to detect both isomorphic and fractionated structures.

Among all the loops of a graph, a loop comprising the largest number of vertices or edges is defined as its *maximum loop*. For a maximum loop, one can define the set of degree sequences of the loop as the sequences of degrees of contiguous vertices either in clockwise or in counter-clockwise direction, starting at any vertex. Thus there will be $2k$ degree sequences for a loop with k vertices. Each degree sequence can be viewed as a number. The largest number of a degree sequence corresponding to a maximum loop is defined as the *canonical perimeter degree-sequence* and the corresponding loops are defined as the perimeter loops (one or several) .

If the following conditions (1) and (2) are satisfied, then the graph contains a vertex-fractionated structure:

(1) There exists a loop with only one shared vertex with any one of the perimeter loops.

(2) The other vertices in the loop are not adjacent with the vertices on the perimeter loop.

If the following (1) and (2) are both satisfied, then the graph contains an edge-fractionated structure:

(1) There exists a loop which has no shared vertex with any one of the perimeter loops.

(2) Only one vertex in the loop is adjacent with the vertices on the perimeter loop.

For all the synthesized connected graphs, after those with vertex-fractionated or edge-fractionated structures are deleted, the rest are those with non-fractionated contracted graphs.

3.8 Unique representation of contracted graphs[114]

The problem of isomorphism identification is one of the most difficult problems in structural synthesis. Based on the loops of kinematic chains, the technique of unique representation of graphs was developed to detect isomorphism between graphs of kinematic chains[114]. Here, we briefly summarise our previous work of unique representation of graphs [114] for better understanding in the present context.

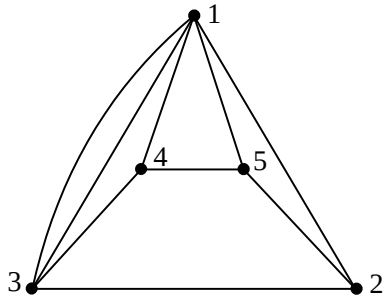

Fig. 3-1 A contracted graph

Step 1: Obtain the perimeter loops of a contracted graph.

In a contracted graph, the loops with the most vertices or edges are defined as its *maximum loops*. For example, the contracted graph in Fig. 3-1 has two maximum loops: the first is constituted by vertices 1,3,2,5,4 and the second is by vertices 1,3,4,5,2.

The degree-sequence of a maximum loop is the degree permutation of vertices sequenced one by one from a starting vertex along the loop clockwise or counterclockwise. In Fig. 3-1 the degree-sequence for the first maximum loop is 54333, and the degree-sequence for the second is also 54333.

A degree-sequence can be viewed as a number. For a contracted graph, the largest of the degree-sequences of the maximum loops is defined as the *canonical perimeter degree-sequence* and the corresponding loop is defined as the perimeter loop. Obviously, both maximum loops are perimeter loops in Fig. 3-1.

Step 2: Obtain the perimeter graph.

The perimeter graph of a contracted graph is drawn as follows.

(1) Draw the perimeter loop as the outmost loop in the form of an equilateral polygon.

(2) Put the remaining vertices of the graph inside the perimeter loop.

For example, the two perimeter graphs corresponding to the two perimeter loops in Fig. 3-1 are shown in Fig. 3-2.

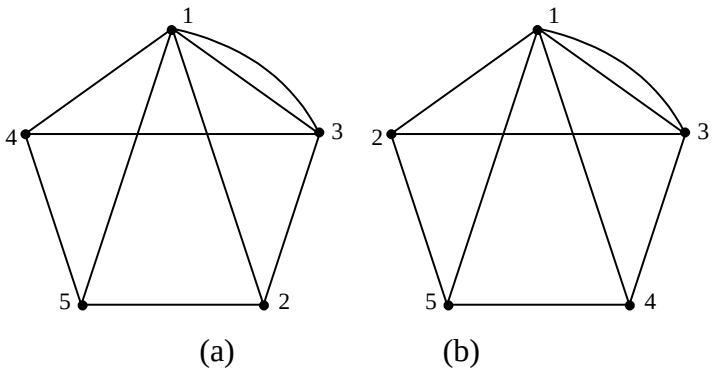

(a) (b)

Fig. 3-2 The two perimeter graphs for Fig. 3-1

Step 3: Obtain the canonical perimeter graphs and canonical adjacency matrices.

(1)Assign natural numbers 1~*t* in turn to each vertex as its label on the perimeter loop according to the canonical perimeter degree-sequence.

(2) In a perimeter loop, if the canonical perimeter degree-sequence can be obtained by counting from different starting vertices, any vertex connected to the inner sub-chain with the most vertices is selected as the starting vertex.

(3) Relabel the vertices on inner sub-chains according to their degrees: the vertices with the bigger degrees are relabeled first.

The perimeter graph labeled in the above way is defined as the *canonical perimeter graph*. The corresponding adjacency matrix is defined as the *canonical adjacency matrix*. The

canonical perimeter graphs for Figs. 3-2(a) and (b) are the same, and their shared canonical perimeter graph is shown in Fig. 3-3.

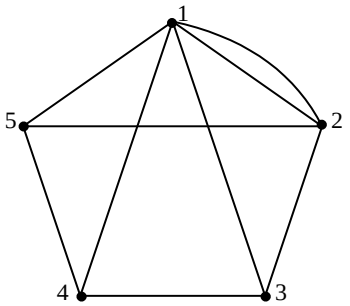

Fig. 3-3 The shared canonical perimeter graph for the two graphs in Fig. 3-2

Step 4: Obtain characteristic number string.

From a contracted graph, the matrix with the largest value of the number string concatenated by the upper-right triangle of the matrix among the canonical adjacency matrices is defined as the *characteristic adjacency matrix (CAM)*, and the corresponding canonical perimeter graph is defined as the *characteristic perimeter contracted graph(CPCG).*

Obviously, the characteristic adjacency matrix of a contracted graph is unique. The number string concatenated by the upper-right triangle of the characteristic adjacency matrix is defined as the *characteristic number string* (*CNS*), which is used to identify isomorphism in the synthesis process.

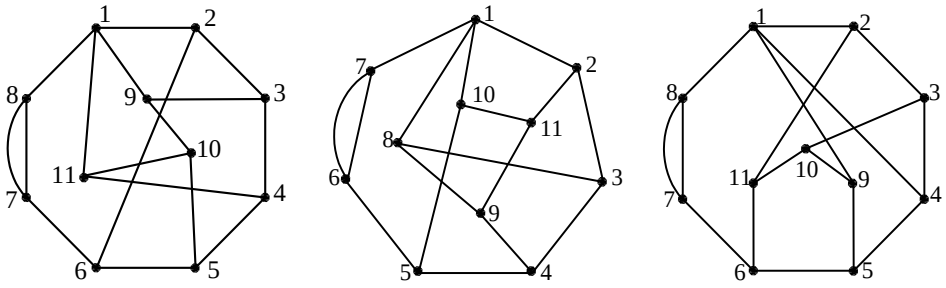

Fig. 3-4 Three contracted graphs

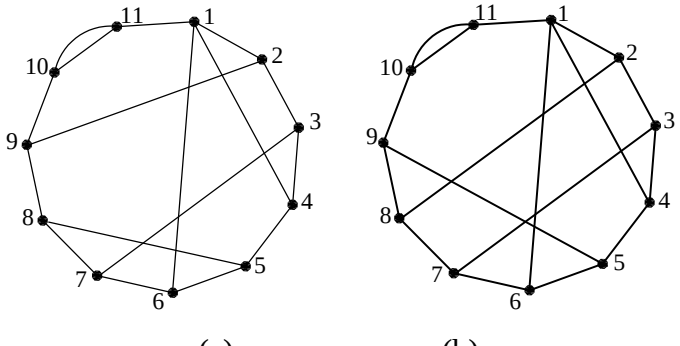

Fig. 3-5 (a) The shared *CPCG* of Fig. 3-4 (a) and (b), (b) the *CPCG* of Fig. 3-4 (c)

As only one canonical perimeter graph exists for the contracted graph in Fig. 3-1, the canonical perimeter graph is also the characteristic perimeter contracted graph. The characteristic adjacency matrix and characteristic number string of the contracted graph in Fig. 3-1 are

$$CAM = \begin{bmatrix} 0 & 2 & 1 & 1 & 1 \\ 2 & 0 & 1 & 0 & 1 \\ 1 & 1 & 0 & 1 & 0 \\ 1 & 0 & 1 & 0 & 1 \\ 1 & 1 & 0 & 1 & 0 \end{bmatrix} \tag{3-53}$$

$$CNS = 2111101101 \tag{3-54}$$

Three contracted graphs are shown in Fig. 3-4. The characteristic number strings for these contracted graphs are as follows.

$$\begin{aligned} &CNS \text{ (a)} = 10101000011000001001001000010000001010001000010001000102 \\ &CNS \text{ (b)} = 10101000011000001001001000010000001010001000010001000102 \\ &CNS \text{ (c)} = 10101000011000010001001000010000001001001000010001000102 \end{aligned} \tag{3-55}$$

As CNS (a) = CNS (b) $\neq$ CNS (c), it is clear that the contracted graphs in Figs. 3-4(a) and (b) are isomorphic, and Fig. 3-4(c) is a different contracted graph. The shared characteristic perimeter contracted graph for Figs. 3-4(a) and (b) are shown in Fig. 3-5 (a), and Fig. 3-5(b) is the characteristic perimeter contracted graph for Fig. 3-4 (c).

3.9 Synthesis results

Based on the above method, a synthesis program has been developed in Visual C++6.0. With the program, the one contracted graph for 6-link 1-DOF kinematic chains, all the four contracted graphs for 8-link 1-DOF kinematic chains, all the 17 contracted graphs for 10-link 1-DOF kinematic chains, all the 118 contracted graphs for 12-link 1-DOF kinematic chains, all the 1198 contracted graphs for 14-link 1-DOF kinematic chains, all the 17072 contracted graphs for 16-link 1-DOF kinematic chains, and all the 309147 contracted graphs for 18-link 1-DOF kinematic chains are synthesized.

Tab. 3-3 Synthesis results for the contracted graphs of 1-DOF kinematic chains

No. of links	No. of basic loops	No. of synthesized contracted graphs	Computation time
6	2	1	-
8	3	4	-
10	4	17	-
12	5	118	48(ms)
14	6	1198	1.657(s)
16	7	17072	57.846(s)
18	8	309147	1h37m

The efficiency of the synthesis method is demonstrated by the time taken in the synthesis process: less than 2 seconds to synthesize all the 1198 contracted graphs of 14-link 1-DOF kinematic chains, less than 1 minute to synthesize all the 17072 contracted graphs of 16-link 1-DOF kinematic chains, and about one hour and a half to synthesize all the 309147 contracted graphs of 18-link 1-DOF kinematic chains on a standard personal computer (CPU2.91GHZ, RAM2.0G). The synthesis results and corresponding computation time are shown in Tab. 3-3.

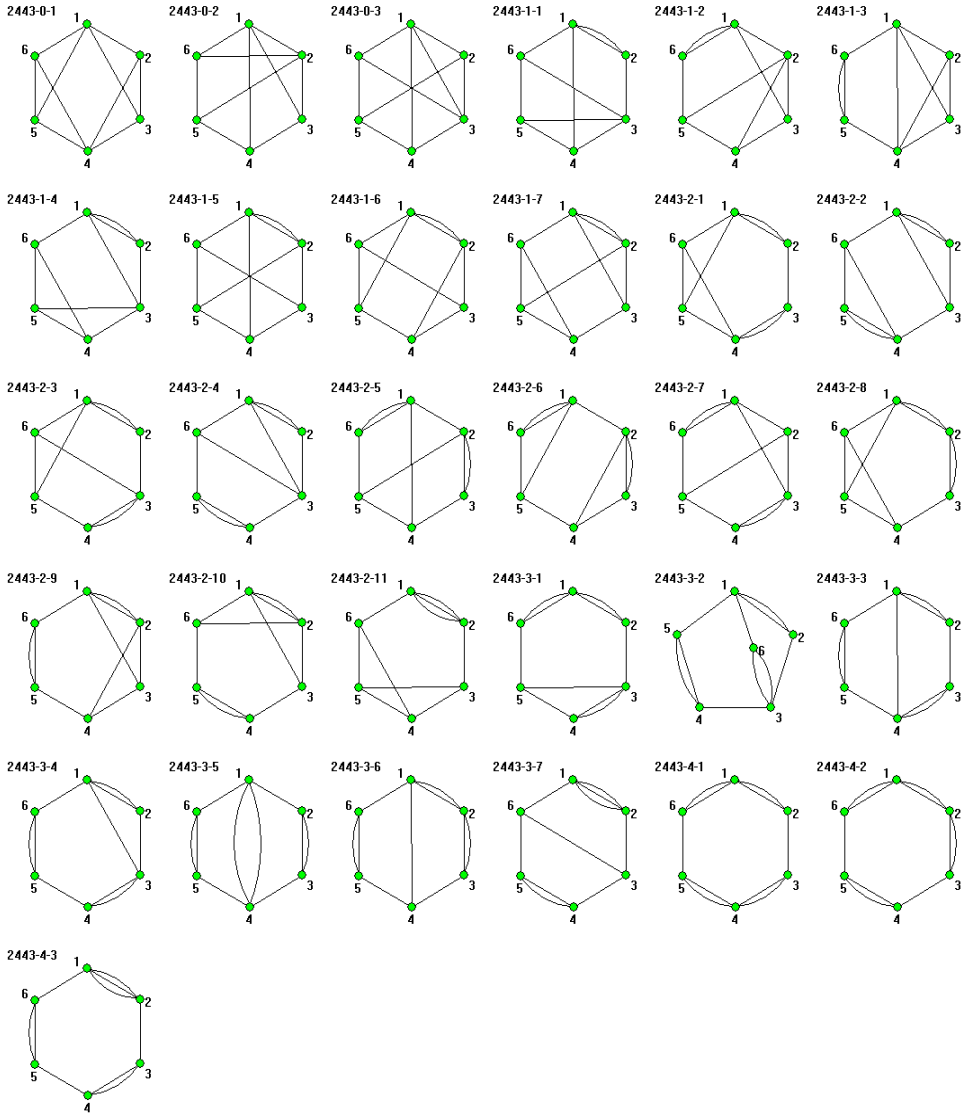

Fig. 3-6 All 31 contracted graphs for link assortment "[6,4,2,0,0]" of 12-link 1-DOF kinematic chains

For 12-link 1-DOF kinematic chains, the numbers of contracted graphs corresponding to every link assortment are shown in Tab. 3-4. Here, we use A, B, C etc. to represent digits greater or equal to ten in the link assortment, i.e. A=10, B=11, C=12, etc. Altogether 16 contracted graphs correspond to the link assortment "[4,8,0,0,0]", 23 contracted graphs correspond to the link assortment "[5,6,1,0,0]", and 31 contracted graphs correspond to the

link assortment "[6,4,2,0,0]", etc. For example, the 31 contracted graphs corresponding to link assortment "[6,4,2,0,0]" are shown in Fig. 3-6. Reading in Fig. 3-6 from left to right and from top to bottom, the first three contracted graphs have no multiple edges; the 4th to the 10th contracted graphs have one multiple edge; the 11th to the 21st contracted graphs have two multiple edges; the 22nd to the 28th contracted graphs have 3 multiple edges; and the last three contracted graphs have four multiple edges.

If from a contracted graph no valid kinematic chains can be synthesized, the contracted graph is termed a *rigid contracted graph* (*RCG*); otherwise, the contracted graph is termed a *valid contracted graph* (*VCG*). For example in the synthesis of 1-DOF kinematic chains from the contracted graphs in Fig. 3-6, because N_2=6 in the link assortment [6,4,2,0,0] and only six binary vertices (N_2) can be inserted into these contracted graphs, the contracted graphs having more than three multiple edges between any two vertices (in Fig. 3-6 the contracted graphs 2443-4-1, 2443-4-2 and 2443-4-3) are rigid contracted graphs. Besides, the contracted graphs 2443-3-1 and 2443-3-4 are also rigid contracted graphs.

Tab. 3-4 Classification of contracted graphs for 12-link 1-DOF kinematic chains

No	Link Assortment	No. of CGs	No	Link Assortment	No. of CGs
1	[4,8,0,0,0]	16	9	[8,2,0,2,0]	4
2	[5,6,1,0,0]	23	10	[9,0,1,2,0]	1
3	[6,4,2,0,0]	31	11	[7,4,0,0,1]	2
4	[7,2,3,0,0]	11	12	[8,2,1,0,1]	2
5	[8,0,4,0,0]	3	13	[9,0,2,0,1]	1
6	[6,5,0,1,0]	7	14	[9,1,0,1,1]	1
7	[7,3,1,1,0]	11	15	[A,0,0,0,2]	1
8	[8,1,2,1,0]	4			

In the link assortment, A=10, B=11, C=12, etc.

For 14-link 1-DOF kinematic chains, all 50 contracted graphs for link assortment "[8,2,4,0,0,0]" are shown in Fig. 3-7. Reading in Fig. 3-7 from left to right and from top to bottom, the first two have no multiple edges; the 3rd to the 7th graph have one multiple edge; the 8th to the 21st graph have two multiple edges; the 22nd to the 37th graph have three multiple edges; the 38th to the 47th graph have four multiple edges; the last three have five multiple edges. The last three and the 38th, 39th, and 40th contracted graphs are rigid contracted graphs. The rest 44 are valid contracted graphs.

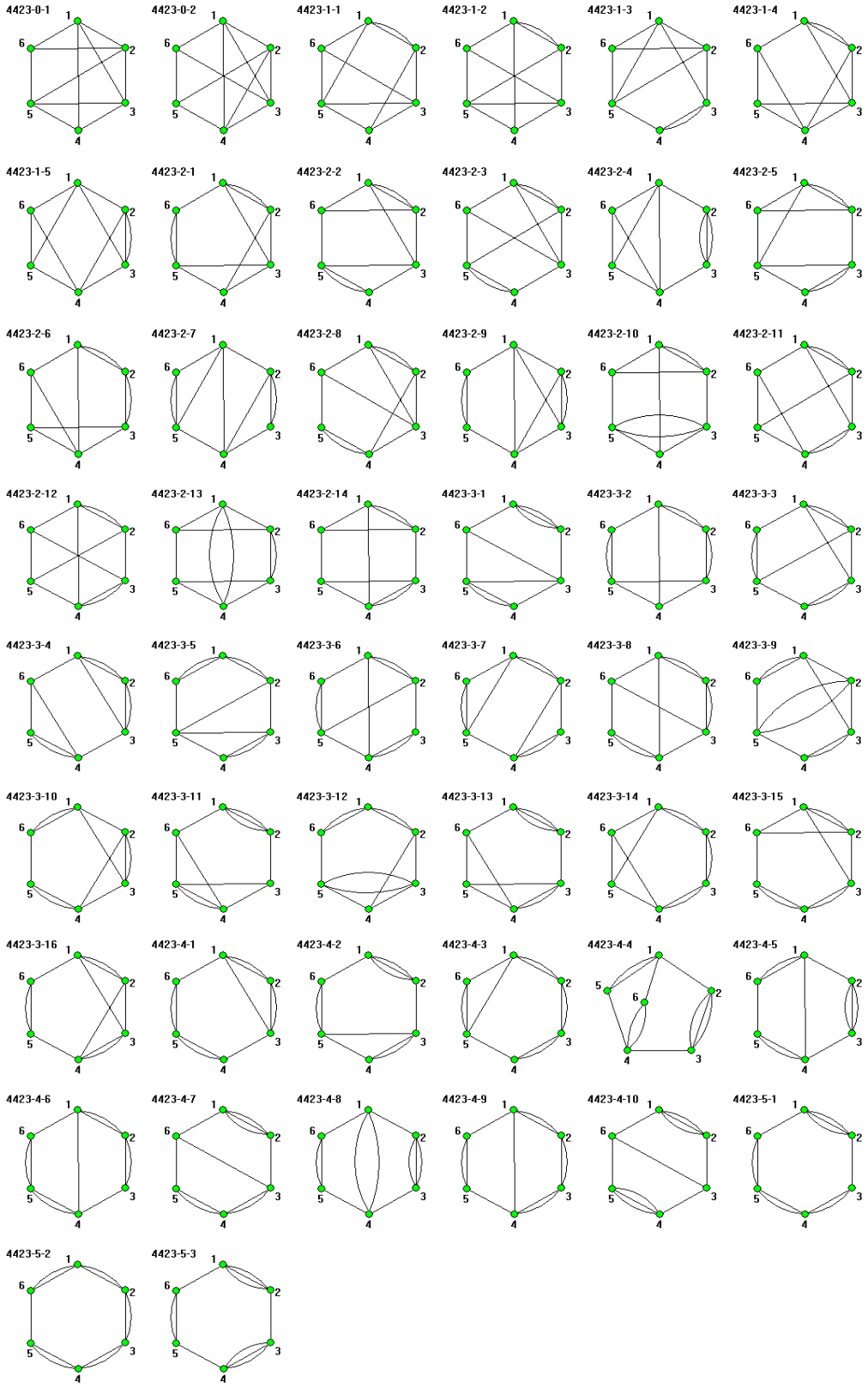

Fig. 3-7 All 50 contracted graphs for link assortment "[8,2,4,0,0,0]" of 14-link 1-DOF kinematic chains

Table 3-4 presents the numbers of link assortment arrays, non-fractionated link assortment arrays, contracted graphs and valid contracted graphs for planar non-fractionated kinematic

chains with N ($6 \le N \le 19$) links and F ($1 \le F \le 14$) degrees of freedom. Because the topological structures of some kinematic chains, such as 4-link 1-DOF, 5-link 2-DOF, 6-link 3-DOF, 7-link 4-DOF, are too simple (only a loop), these kinematic chains are not included. The correctness of theorems 1, 2 and 3 is also verified by the synthesis results in Tab.3-4. The valid contracted graphs, from which at least one proper kinematic chain can be synthesized, are also included in the last column of Tab.3-4. So a complete list of contracted graphs and valid contracted graphs for planar non-fractionated kinematic chains up to 19 links and all possible degrees of freedom are obtained.

Tab. 3-4 Numbers of contracted graphs and valid contracted graph of non-fractionated kinematic chains

N	F	No. of link assortment arrays	No. of non-fractionated link assortment arrays	No. of contracted graphs	No. of valid contracted graphs
6	1	1	1	1	1
7	2	2	1	1	1
8	1	3	3	4	4
	3	2	1	1	1
9	2	4	3	4	4
	4	2	1	1	1
10	1	7	7	17	15
	3	5	3	4	4
	5	2	1	1	1
11	2	9	7	17	16
	4	5	3	4	4
	6	2	1	1	1
12	1	15	15	118	97
	3	10	7	17	17
	5	5	3	4	4
	7	2	1	1	1
13	2	18	15	118	109
	4	11	7	17	17
	6	5	3	4	4
	8	2	1	1	1
14	1	30	30	1198	923
	3	20	15	118	116
	5	11	7	17	17
	7	5	3	4	4
	9	2	1	1	1
15	2	75	30	1198	1090

	4	21	15	118	117
	6	11	7	17	17
	8	5	3	4	4
	10	2	1	1	1
16	1	58	58	17072	12612
	3	38	30	1198	1169
	5	22	15	118	118
	7	11	7	17	17
	9	5	3	4	4
	11	2	1	1	1
17	2	65	58	17072	15154
	4	40	30	1198	1188
	6	22	15	118	118
	8	11	7	17	17
	10	5	3	4	4
	12	2	1	1	1
18	1	105	105	309147	224771
	3	70	58	17072	16470
	5	41	30	1198	1196
	7	22	15	118	118
	9	11	7	17	17
	11	5	3	4	4
	13	2	1	1	1
19	2	116	105	309147	271153
	4	73	58	17072	16879
	6	42	30	1198	1197
	8	22	15	118	118
	10	11	7	17	17
	12	5	3	4	4
	14	2	1	1	1

3.10 Summary

This chapter first reveals the relationships of link assortment arrays and non-fractionated contracted graphs for N-link 1-DOF kinematic chains and any (N+i)-link (i+1)-DOF (i = 1, 2, 3, …) kinematic chains. Then a general method is proposed to synthesize the contracted graphs of planar non-fractionated kinematic chains with simple joints. The method has two main advantages: on the one hand, with it contracted graphs, even those with complex topological structures can be synthesized, and on the other hand, the synthesis task can be realized automatically on a computer.

For the automatic synthesis, a human-machine interactive synthesis program is developed, in which just the number of links and degrees of freedom are input, and all the corresponding link assortment arrays and contracted graphs are synthesized automatically. Contracted graphs for planar non-fractionated kinematic chains with N ($4 \le N \le 19$) links and F ($1 \le F \le 14$) degrees of freedom are synthesized with the method.

4 Structural synthesis of non-fractionated kinematic chains and mechanisms

4.1 Foreword

The contracted graph of a kinematic chain is obtained by replacing every binary path with an edge in the topological graph of the chain. Vice versa, from a contracted graph the corresponding topological graph of a kinematic chain can be obtained by inserting appropriate number of binary vertices into the edges of the contracted graph. Although the concept of the contracted graph in the graph theory had been adopted by many researchers to synthesize kinematic chains, only those chains consisting of up to 12 links have been previously reported in literature [5]. This chapter attempts to develop a new fully-automatic method to synthesize non-fractionated kinematic chains with more complex structures based on the synthesis of contracted graphs in chapter 3.

4.2 Synthesis requirements

The main aim of structural synthesis of kinematic chains is to serve the conceptual design of mechanisms by providing the designers with all the candidate kinematic structures of mechanisms for choice. From the reports in literature, there are more topological structures of various types as there are species of creatures in the nature. So in order to reach the aim of structural synthesis, an ideal synthesis method must have the following three characteristics:

(1) Effectiveness. The method generates all the valid topological structures, free from any wrong structures (no rigid sub-chains) and reduplicate or missing structures (no isomorphic chains).

(2) Automation. Synthesis can be carried out fully in the computers.

(3) Designer-friendliness. Synthesized topological structures are output in the form of graphs rather than in the single form of algebraic representations.

Despite the great number of existing synthesis methods, hardly any method meets all the three requirements above. As pointed out by Al-Dweiri et al in 2010 in MMT [17], “It should be noted here that, regardless of the method used, a general problem still unsolved in structural synthesis is the enumeration of a complete list of kinematic chains and mechanisms without isomorphism and without degenerate chains.” In the following of the chapter, we introduce an effective, fully-automatic and designer-friendly method for the synthesis of non-fractionated kinematic chains.

4.3 Synthesis progress

In general, there are many different ways for inserting binary vertices to the edges of a contracted graph, especially for those with complex structures. Some insertion ways may lead to resulting kinematic chains containing rigid sub-chains, and some others may lead to resulting kinematic chains having reduplicate structures. For a given contracted graph, the

main steps for generating a complete list of valid kinematic chains (after deleting the wrong and the reduplicate structures) with specified number of links (N) and degrees of freedom (F) are given as follows (see Fig. 4-1).

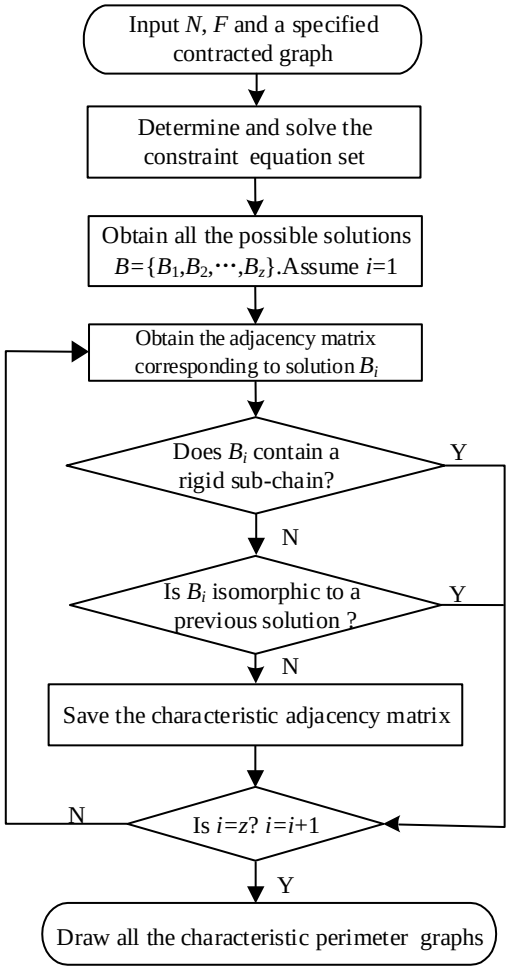

Fig. 4-1 The flow chart for the synthesis of non-fractionated kinematic chains

Step 1: Determine the constraint equation set by determining the constraint equations for the number of binary vertices, the symmetry of edges, and the vertices on loops, respectively.

Step 2: Solve the constraint equation set and obtain all the possible solutions $B=\{B_1, B_2, \ldots, B_z\}$. Assume $i=1$.

Step 3: Obtain the adjacency matrix corresponding to solution B_i.

Step 4: Determine whether the topological graph corresponding to solution B_i containing rigid sub-chain. If it does, delete it; otherwise, go to the next step.

Step 5: Isomorphism identification. Obtain the characteristic adjacency matrix corresponding to solution B_i. If the matrix is different from the former ones, save it; otherwise, delete the solution B_i.

Step 6: Determine whether i=z. If i=z, then all the characteristic adjacency matrices corresponding to the specified N-link F-DOF kinematic chains are obtained; go to step 7. Otherwise i=i+1, and return to step 3.

Step 7: Draw all the characteristic perimeter graphs corresponding to the obtained characteristic adjacency matrices. So a whole set of all the required kinematic chains is obtained.

The flow chart for the structural synthesis of kinematic chains for a specified contracted graph is shown in Fig.4-1.

4.4 Synthesis equation set

From a contracted graph, all the corresponding topological graphs of kinematic chains can be obtained through the addition of N_2 binary vertices by some rules. In order to improve the computational efficiency, three constraint conditions are presented when x_i binary vertices are to be inserted into an edge e_i.

Rule 4-1: constraint condition for the scope of binary vertices

Theorem 1: For a topological graph of non-fractionated F-DOF kinematic chains with more than one loop, the number of binary vertices on any binary path is less than or equal to F +1.

Proof: Kinematic chains with only one loop, such as 4-link 1-DOF kinematic chains, 5-link 2-DOF kinematic chains, etc., need not to be considered here. For a topological graph of non-fractionated kinematic chains, the sub-graph obtained by deleting any binary path is also a valid topological graph with DOF $\geq$ 1. If in a topological graph of non-fractionated kinematic chains there exists a binary path with F+2 or more binary vertices on it, the removal of the binary path will reduce the DOFs of the topological graph by at least F. This would lead to a DOF of the remaining sub-graph of less than one. Thus, it is impossible that any binary path in a topological graph of non-fractionated F-DOF kinematic chains has F+2 or more binary vertices.

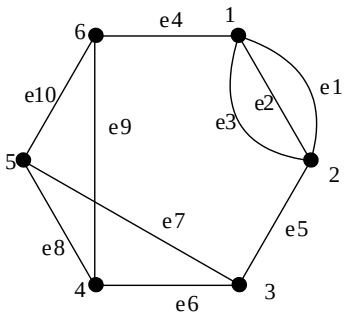

Fig. 4-2 A contracted graph

So the scope of x_i and the sum of x_i satisfies

$$\begin{cases} \sum_{i=1}^{t} x_i = N_2 \\ 0 \le x_i \le F+1 \end{cases} \tag{4-1}$$

where t is the total number of the edges of the contracted graph.

For example, if the contracted graph in Fig. 4-2 is used to synthesize 12-link 1-DOF kinematic chains, based on rule 4-1, we have

$$\begin{cases} \sum_{i=1}^{10} x_i = 6 \\ 0 \le x_i \le 2 \end{cases} \tag{4-2}$$

Rule 4-2: Constraint condition for the symmetry of edges

For k parallel edges e_i, e_{i+1}, ..., e_{i+k-1} connecting directly one single pair of vertices (V_p and V_q), without loss of generality, assume $x_i \le x_{i+1} \le \cdots \le x_{i+k-1}$.

(1)If vertices V_p and V_q are connected with two different vertices in the contracted graph, the number of binary vertices to be inserted into these parallel edges satisfies

$$\begin{cases} x_i \le x_{i+1} \le \cdots \le x_{i+k-1} \\ x_i + x_{i+1} \ge 2 \\ x_{i+2} \ge 2 \\ x_i + x_{i+1} + \cdots + x_{i+k-1} \le F + 2k - 3 \end{cases} \tag{4-3}$$

(2)If there is a vertex connected with the two vertices V_p and V_q, the number of binary vertices to be inserted into these parallel edges satisfies

$$\begin{cases} x_i \le x_{i+1} \le \cdots \le x_{i+k-1} \\ x_i + x_{i+1} \ge 2 \\ x_{i+2} \ge 2 \\ x_i + x_{i+1} + \cdots + x_{i+k-1} \le F + 2k - 2 \end{cases} \tag{4-4}$$

For example, in Fig. 4-2, edges e_1, e_2 and e_3 are parallel edges. According to rule 4-2, the numbers of binary vertices to be inserted into these edges satisfy

$$\begin{cases} x_1 \le x_2 \le x_3 \\ x_1 + x_2 \ge 2 \\ x_3 \ge 2 \\ x_1 + x_2 + x_3 \le 4 \end{cases} \tag{4-5}$$

Rule 4-3: Constraint condition for vertices on loops

In order to reduce the number of topological graphs containing rigid sub-chains, at least (4-T_j) binary vertices must be inserted for each loop j with T_j<4 vertices except for the loops constituted by parallel edges, i.e.

$$\sum_{i \in SL(j)} x_i \ge 4 - T_j \tag{4-6}$$

where *SL(j)* is the set of edges of a loop j for which the number of vertices is smaller than 4.

According to rule 4-3, for the contracted graph in Fig. 4-2, one can obtain

$$\begin{cases} x_6 + x_7 + x_8 \geq 1 \\ x_8 + x_9 + x_{10} \geq 1 \end{cases} \tag{4-7}$$

The synthesis equation set for the contracted graph of Fig. 4-2 is thus

$$\begin{cases} \sum_{i=1}^{10} x_i = 6 \\ 0 \leq x_i \leq 3 \\ x_1 \leq x_2 \leq x_3 \\ x_3 \geq 2 \\ x_1 + x_2 \geq 2 \\ x_1 + x_2 + x_3 \leq 4 \\ x_6 + x_7 + x_8 \geq 1 \\ x_8 + x_9 + x_{10} \geq 1 \end{cases} \tag{4-8}$$

Eq.(4-8) can be reduced to

$$\begin{cases} \sum_{i=1}^{10} x_i = 6 \\ 0 \leq x_i \leq 3 \\ x_1 \leq x_2 \leq x_3 \\ x_3 = 2 \\ x_1 + x_2 = 2 \\ x_6 + x_7 + x_8 \geq 1 \\ x_8 + x_9 + x_{10} \geq 1 \end{cases} \tag{4-9}$$

If the contracted graph in Fig. 4-2 is used to synthesize 13-link 2-DOF kinematic chains, based on rules 4-1, 4-2 and 4-3, we have

$$\begin{cases} \sum_{i=1}^{10} x_i = 7 \\ 0 \leq x_i \leq 3 \\ x_1 \leq x_2 \leq x_3 \\ x_3 \geq 2 \\ x_1 + x_2 \geq 2 \\ x_1 + x_2 + x_3 \leq 5 \\ x_6 + x_7 + x_8 \geq 1 \\ x_8 + x_9 + x_{10} \geq 1 \end{cases} \tag{4-10}$$

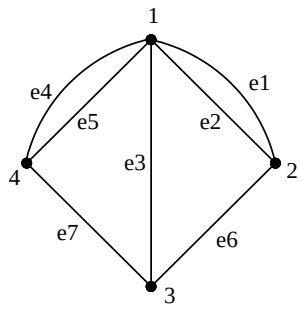

Fig. 4-3 A contracted graph

If the contracted graph in Fig. 4-3 is used to synthesize 12-link 3-DOF kinematic chains, according to rule 4-1, we have

$$\begin{cases} \sum_{i=1}^{7} x_i = 8 \\ 0 \le x_i \le 4 \end{cases} \tag{4-11}$$

In Fig. 4-2, edges e_1 and e_2 as well as edges e_4 and e_5, respectively, are parallel edges. According to rule 4-2, the numbers of binary vertices to be inserted into these edges satisfy

$$\begin{cases} x_1 \le x_2 \\ x_4 \le x_5 \\ 2 \le x_1 + x_2 \le 5 \\ 2 \le x_4 + x_5 \le 5 \end{cases} \tag{4-12}$$

According to rule 4-3, one can obtain

$$\begin{cases} x_1 + x_3 + x_6 \ge 1 \\ x_3 + x_4 + x_7 \ge 1 \end{cases} \tag{4-13}$$

So the synthesis equation set for the contracted graph of Fig. 4-3 is thus

$$\begin{cases} \sum_{i=1}^{7} x_i = 8 \\ 0 \le x_i \le 4 \\ x_1 \le x_2 \\ x_4 \le x_5 \\ 2 \le x_1 + x_2 \le 5 \\ 2 \le x_4 + x_5 \le 5 \\ x_1 + x_3 + x_6 \ge 1 \\ x_3 + x_4 + x_7 \ge 1 \end{cases} \tag{4-14}$$

If the contracted graph in Fig. 4-3 is used to synthesize 13-link 4-DOF kinematic chains, based on rules 4-1, 4-2 and 4-3, we have

$$\begin{cases} \sum_{i=1}^{7} x_i = 9 \\ 0 \le x_i \le 5 \\ x_1 \le x_2 \\ x_4 \le x_5 \\ 2 \le x_1 + x_2 \le 6 \\ 2 \le x_4 + x_5 \le 6 \\ x_1 + x_3 + x_6 \ge 1 \\ x_3 + x_4 + x_7 \ge 1 \end{cases} \tag{4-15}$$

For a synthesis equation set, one can obtain easily all its solutions by a simple program. For example, the 22 solutions for the synthesis equation set of Eq.(4-9) are given in Tab.4-1.

Tab. 4-1 The 22 solutions for the synthesis equation set of Eq.(4-9)

No.	x_1	x_2	x_3	x_4	x_5	x_6	x_7	x_8	x_9	x_{10}
1	1	1	2	0	0	0	0	2	0	0
2				1	0	0	0	1	0	0
3				0	1	0	0	1	0	0
4				0	0	1	0	1	0	0
5				0	0	0	1	1	0	0
6				0	0	0	0	1	1	0
7				0	0	0	0	1	0	1
8				0	0	1	0	0	1	0
9				0	0	1	0	0	0	1
10				0	0	0	1	0	1	0
11				0	0	0	1	0	0	1
12	0	2		0	0	0	0	2	0	0
13				1	0	0	0	1	0	0
14				0	1	0	0	1	0	0
15				0	0	1	0	1	0	0
16				0	0	0	1	1	0	0
17				0	0	0	0	1	1	0
18				0	0	0	0	1	0	1
19				0	0	1	0	0	1	0
20				0	0	1	0	0	0	1
21				0	0	0	1	0	1	0
22				0	0	0	1	0	0	1

From a solution, a corresponding topological graph can be obtained. In order to avoid the wrong structures and reduplicate structures and generate all the valid topological structures, methods to detect isomorphism and rigid sub-chains are necessary.

4.5 Unique representation of graphs[114]

In order to eliminate isomorphism and to sketch topological graphs, the unique representation of topological graphs is required. Here, we briefly summarise our previous work of unique representation of graphs [114] for better understanding in the present context.

Step 1: Obtain all the perimeter loops and the corresponding perimeter graphs.

In a topological graph, define the degree sequence of a loop as the sequence of degrees of its vertices starting from any vertex and proceeding once around the loop in clockwise or in counter clockwise direction. For a graph, the degree sequences with the largest number of vertices are termed the canonical perimeter degree-sequences and the corresponding loops are termed the perimeter loops.

The perimeter graphs are obtained by drawing each perimeter loop as a uniform polygon and filling in the rest of the connections as inner sub-chains. There will be thus one perimeter graph for each perimeter loop.

Step 2: Obtain for each perimeter graph the corresponding canonical perimeter graphs by relabeling the vertices as follows:

(1) Re-label each vertex of the perimeter loop by the numbering i=1,2,3... in the order of the canonical perimeter degree-sequence.

(2) If several canonical perimeter degree-sequences can be obtained, start the numbering at the vertex connected to the inner sub-chain with the largest number of vertices.

(3) Re-label the vertices on inner sub-chains by continuing the numbering of the perimeter loop according to their degrees, re-labeling the vertices with the larger degree first.

The perimeter graph labeled in this way is termed the *canonical perimeter graph*. The corresponding adjacency matrix is defined as the *canonical adjacency matrix*.

Step 3: Obtain the characteristic perimeter graph and the corresponding characteristic number string.

Among the canonical adjacency matrices for a graph, the matrix with the largest value of the number string obtained by concatenating as digits the values of the elements in the upper-right triangle from the first row to the last row is defined as the characteristic adjacency matrix, and the corresponding canonical perimeter graph is defined as the *characteristic perimeter graph*.

For example, one solution for Eq.(4-9) is x_1=1, x_2=1, x_3=2, x_4=0, x_5=0, x_6=1, x_7=0, x_8=0, x_9=1, x_{10}=0. The topological graph for this solution is shown in Fig. 4-4(a) and its characteristic perimeter graph is shown in Fig. 4-4(b).

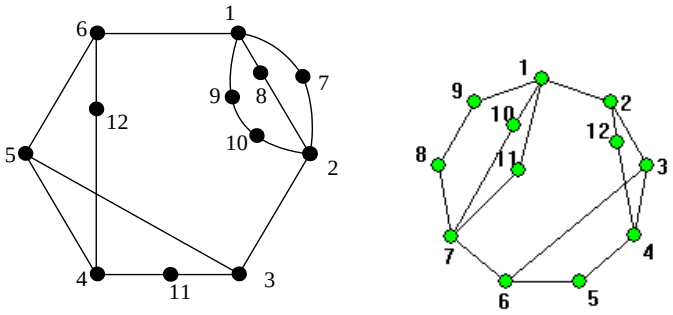

a. A synthesized topological graph b. Its characteristic perimeter graph

Fig. 4-4 A topological graph and its characteristic perimeter graph

4.6 Detection of rigid sub-chains[115]

Not all the solutions correspond to proper topological graphs of kinematic chains. Some solutions may correspond to kinematic chains containing rigid sub-chains. Here, we briefly summarise our previous work of the detection of rigid sub-chain[115] for better understanding in the present context.

Among the loops of a generated topological graph, if any three loops $L(i)$, $L(j)$ and $L(k)$ (i, j, k=1, 2, … v) in a loop set $S\{L(1),L(2),\dots L(v)\}$($v$ is the number of its basic loops) satisfy

$$L(i) \oplus L(j) \neq L(k) \tag{4-16}$$

the loop set $S\{L(1),L(2),\dots L(v)\}$ is a basic loop set. After the basic loop set is determined, all the other loops of the topological graph can be obtained through the "$\oplus$" operation of loops in the basic loop set. Obviously, the basic loop set is not unique for a topological graph. Based on the basic loop set, here is an efficient method to detect rigid sub-chains..

Step 1: Select the first basic loop $L(1)$ and determine its mobility factor w_1

Here a loop with the smallest sub-dimension is selected as the first basic loop $L(1)$. For the loop $L(1)$, if its sub-dimension is q, then its mobility factor is q-3. the mobility factor w_1 of the loop $L(1)$ is

$$w_1 = N[L(1)]-3 \tag{4-17}$$

If Q=w_1-1<0, then the topological graph contains rigid sub-chains. Delete it. Otherwise, go to step 2.

Step 2: Select the second basic loop $L(2)$ and determine the mobility factor w_2

A loop $L(i)$ which satisfies the following two conditions in sequence is selected as the loop $L(2)$

(1) Of all the loops of the topological graph, $N\{L(i)\,\Theta\,L(1)\}$ is the smallest one. Here, $L(a)\,\Theta\,L(b)$ denotes the path consisting of those vertices that are on loop L(a) but not on loop L(b).

(2) Of the loops satisfying the above condition, loop $L(i)$ is the one with the smallest sub-dimension.

The mobility factor w_2 of the remainling path is

$$w_2 = N[P(2)]-2, \text{ and } P(2)= L(2)\,\Theta\,L(1) \tag{4-18}$$

If Q=w_1+w_2-2<0, then the topological graph contains rigid sub-chains. Delete it. Otherwise, go to step 3.

… …

Step *n*: Select the n^{th} basic loop $L(n)$ and determine the mobility factor w_n

A loop $L(i)$ satisfying the following two conditions in sequence is selected as the loop $L(n)$

(1) Of all the loops of the topological graph, $N\{L(i)\Theta P(n\text{-}1)\ \Theta \ldots \Theta P_1(2)\Theta L(1)\}$ is the smallest one.

(2) Of the loops satisfying the above condition, loop $L(i)$ is the one with the smallest sub-dimension.

The mobility factor of path w_n is

$$w_n = N[P(n)]\text{-}2, \text{ and } P(n)=L(i)\Theta P(n\text{-}1)\Theta \ldots \Theta P_1(2)\Theta L(1) \qquad (4\text{-}67)$$

If $Q=\sum_{i=1}^{n} w_i - n < 0$, then the topological graph contains rigid sub-chains. Delete it. Otherwise, go to step (n +1).

… …

Step *v*: Follow the steps above until step v (step v included), and the last basic loop $L(v)$ and the mobility factor w_v are obtained. If $Q=\sum_{i=1}^{v} w_i - v < 0$, then the topological graph contains rigid sub-chains. Delete it. Otherwise, the topological graph corresponds to a kinematic chain with proper structure. Store it.

For example, one solution for Eq.(4-9) is x_1=1, x_2=1, x_3=1, x_4=1, x_5=1, x_6=0, x_7=0, x_8=1, x_9=0, x_{10}=0. The mobility-factor array is w=[1, 0, …]. Hence, the solution contains a rigid sub-chain and is thus an improper topological structure.

After deleting isomorphic and rigid structures, the valid structures can be obtained. For example, eight valid 1-DOF topological graph can be obtained from the contracted graph in Fig. 4-2, shown in Fig. 4-5.

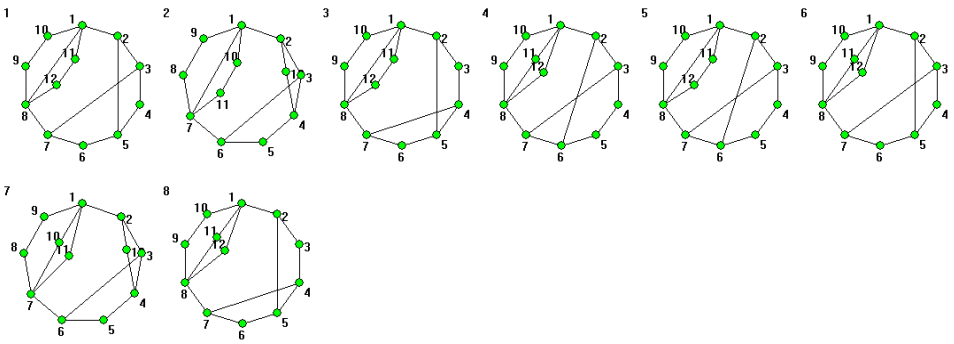

Fig. 4-5 Eight non-degenerated 1-DOF topological graphs for Fig. 4-2

40 valid 2-DOF topological graph can be obtained from the contracted graph in Fig. 4-2, shown in Fig. 4-6.

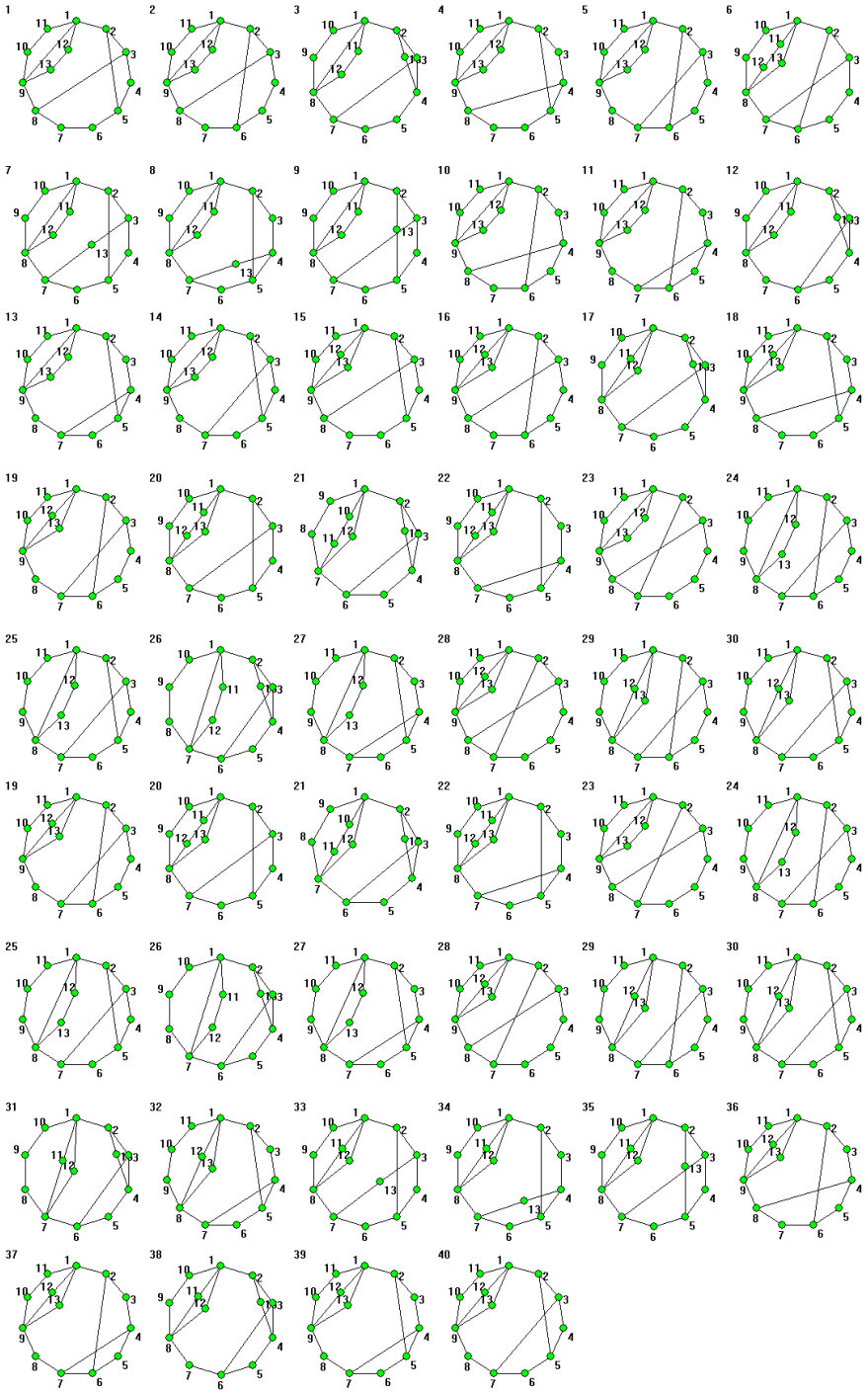

Fig. 4-6 40 non-degenerated 2-DOF topological graphs for Fig. 4-2

4.7 Atlas database of kinematic chains and mechanisms

For each contracted graph, all the valid topological graphs can be synthesized after isomorphism identification and rigid sub-chain detection. The topological graphs are represented by their characteristic perimeter graphs. In this way, the complete set of planar non-fractionated kinematic chains can be synthesized. Based on the synthesis method, a fully-automatic synthesis program has been developed, and the complete atlas databases containing all topological graphs classified has been established.

Fig. 4-7 shows for example an excerpt of the complete atlas database for planar 12-link 1-DOF kinematic chains. The user simply inputs the number of links and degrees of freedom, and all the link assortments are obtained automatically, shown in the left window. All the topological graphs corresponding to each link assortment can be synthesized automatically and are displayed in the right window. Displayed in Fig. 4-7 is an excerpt of all 2339 topological graphs corresponding to the link assortment "[6,4,2,0,0]".

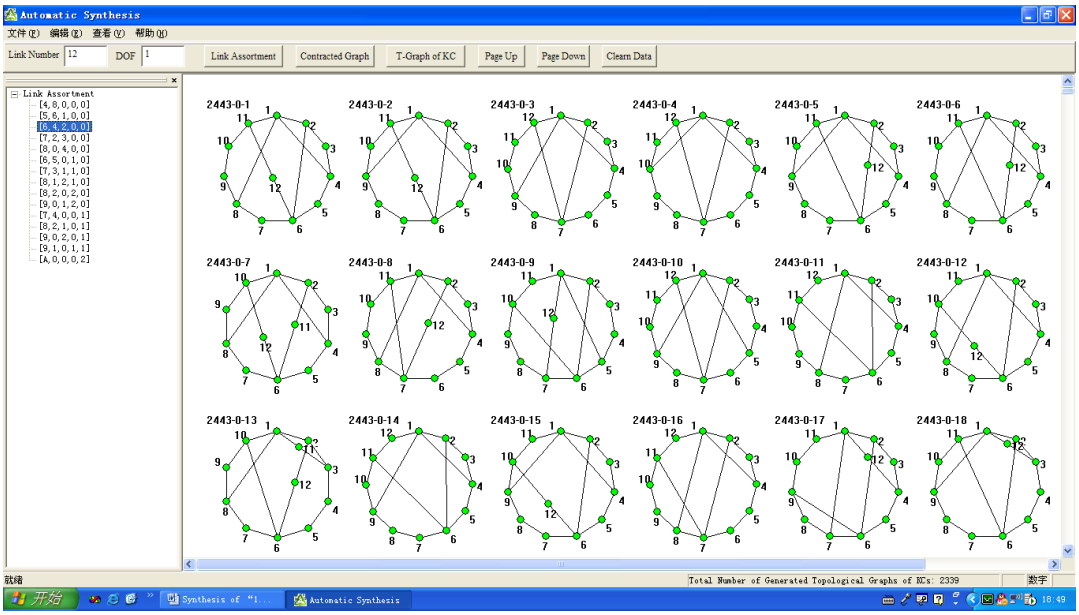

Fig. 4-7 Extract of the complete atlas database for planar 12-link 1-DOF kinematic chains

Fig. 4-8 shows an excerpt of the complete atlas database of planar 14-link 1-DOF kinematic chains. All the link assortments are shown in the left window. All the topological graphs corresponding to each link assortment can be synthesized automatically and are displayed in the right window. Displayed in Fig. 4-8 is an excerpt of all 89338 topological graphs corresponding to the link assortment "[6,6,2,0,0,0]".

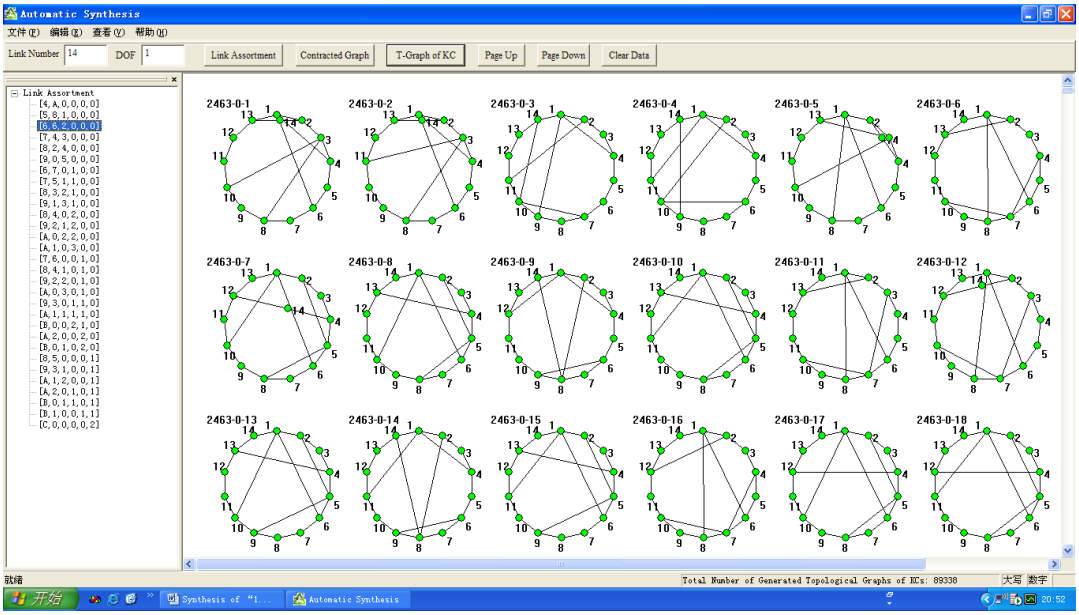

Fig. 4-8 Excerpt of the complete atlas database for planar 14-link 1-DOF kinematic chains

In the complete atlas database, all the valid topological graphs corresponding to a specified contracted graph can also be easily obtained. For example, Fig. 4-9 is a contracted graph for 12-link 1-DOF kinematic chains. All 157 valid topological graphs are obtained from the complete atlas database, part of which is shown in Fig. 4-10.

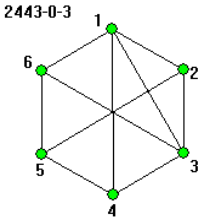

Fig. 4-9 Example of a contracted graph for a 12-link 1-DOF kinematic chain

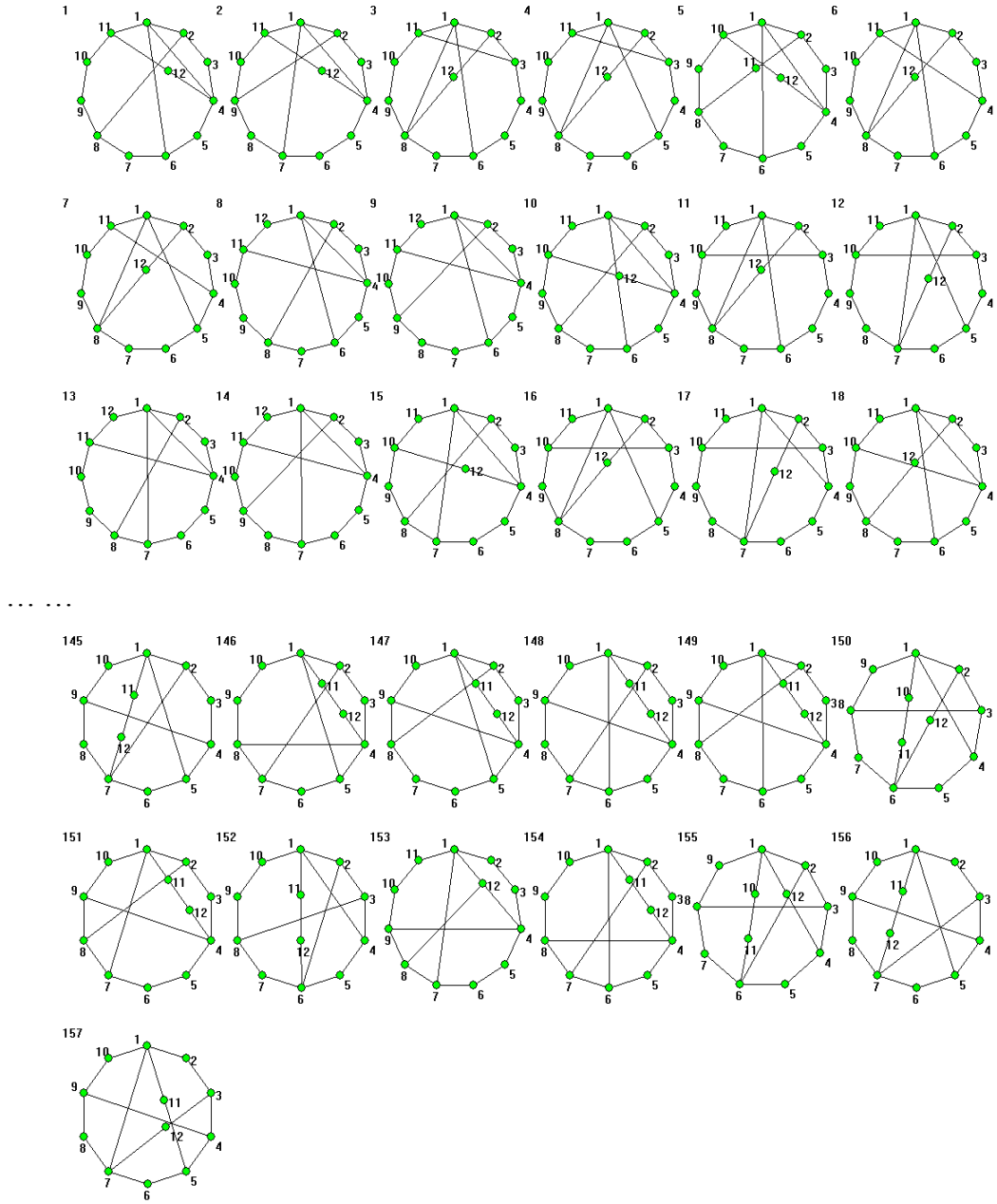

Fig. 4-10 Excerpt of 157 topological graphs corresponding to the contracted graph in Fig. 4-9

Fig. 4-11 is a contracted graph for 14-link 1-DOF kinematic chains. All 1930 valid topological graphs can also be obtained from the atlas database, some of which are shown in Fig. 4-12.

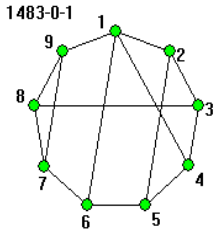

Fig. 4-11 Example of a contracted graph for a 14-link 1-DOF kinematic chains

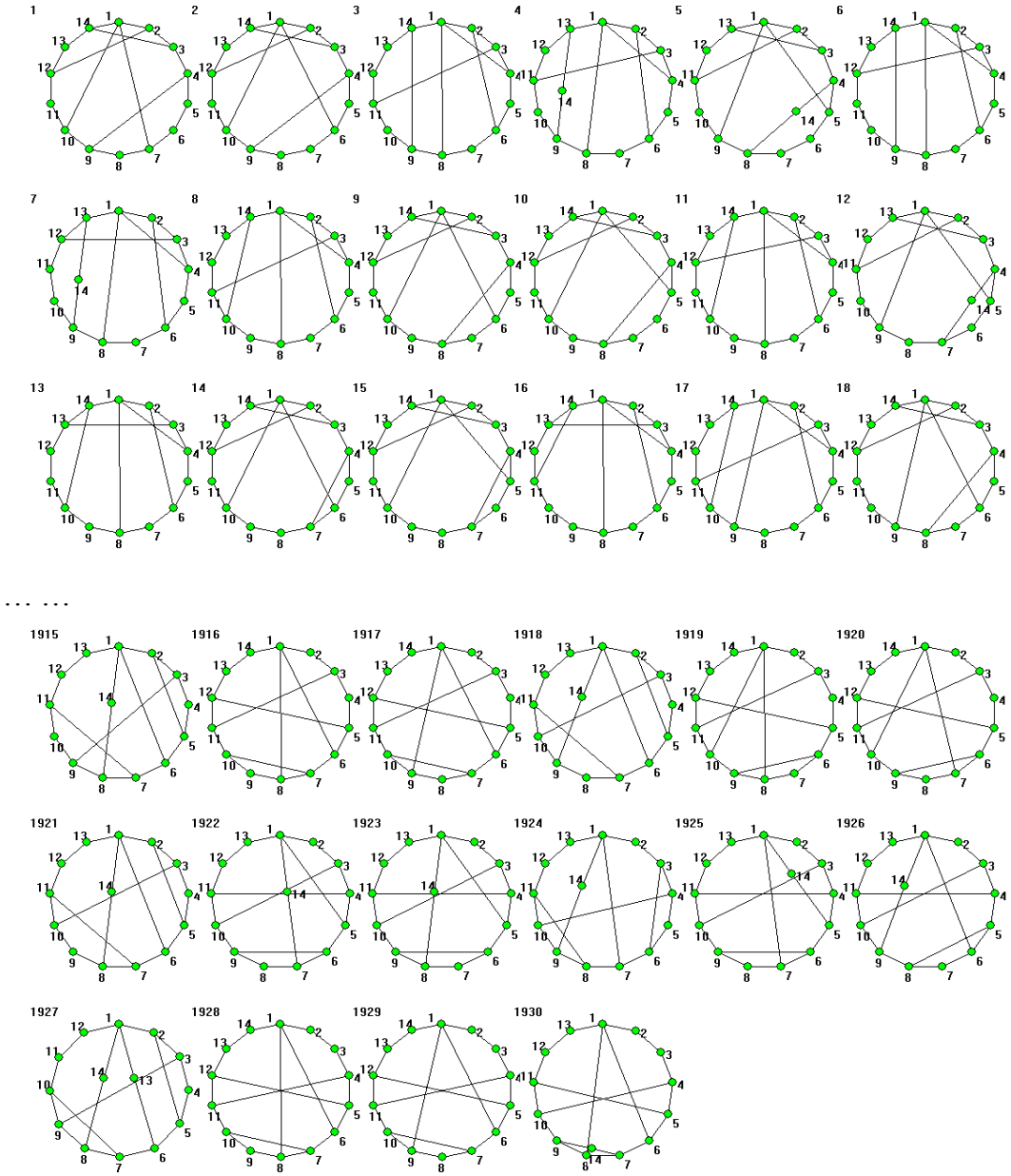

Fig. 4-12 Excerpt of the 1930 valid topological graphs for the contracted graph in Fig. 4-11

Table 4-2 presents the quantitative information concerning the topological graphs for 12-link 1-DOF kinematic chains. The total number of the topological graphs is in this case 6856. All the contracted graphs and the topological graphs are classified according to their link assortment (column 2). For each link assortment, the numbers of the multiple edges of the contracted graphs are used to further classify both contracted graphs and topological graphs (TG) (see columns 3, 4, 5). In column 4, the numbers of valid contracted graphs (VCG) are shown before the parentheses, and the numbers of contracted graphs (CG) are shown within the parentheses.

Tables 4-2, 4-3, 4-4 and 4-5 display the quantitative information for the atlas databases for 1-DOF kinematic chains of 6, 8, 10 and 14 links, respectively. The total numbers of the topological graphs are 2, 16, 230, and 318162, respectively.

Tab. 4-2 Numbers of topological graphs for 12-link 1-DOF kinematic chains

No.	Link assortment	No. of multiple edges	No. of VCG (CG)	No. of TG	No. of TG
1	[4,8,0,0,0]	0	5(5)	352	410
		1	4(4)	52	
		2	2(4)	6	
		3	0(2)	0	
		4	0(1)	0	
2	[5,6,1,0,0]	0	4(4)	1282	1873
		1	7(7)	536	
		2	5(7)	55	
		3	0(4)	0	
		4	0(1)	0	
3	[6,4,2,0,0]	0	3(3)	942	2339
		1	7(7)	1059	
		2	11(11)	308	
		3	5(7)	30	
		4	0(3)	0	
4	[7,2,3,0,0]	0	1(1)	111	648
		1	1(1)	231	
		2	4(4)	266	
		3	3(3)	40	
		4	0(2)	0	
5	[8,0,4,0,0]	2	1(1)	28	37
		4	2(2)	9	
6	[6,5,0,1,0]	0	1(1)	120	506
		1	2(2)	311	

		2	2(2)	69	
		3	1(2)	6	
7	[7,3,1,1,0]	1	2(2)	386	716
		2	3(3)	243	
		3	5(5)	87	
		4	0(1)	0	
8	[8,1,2,1,0]	2	1(1)	74	147
		3	2(2)	65	
		4	1(1)	8	
9	[8,2,0,2,0]	2	1(1)	32	63
		3	1(1)	21	
		4	2(2)	10	
10	[9,0,1,2,0]	4	1(1)	7	7
11	[7,4,0,0,1]	2	1(1)	40	49
		3	1(1)	9	
12	[8,2,1,0,1]	3	2(2)	46	46
13	[9,0,2,0,1]	4	1(1)	5	5
14	[9,1,0,1,1]	4	1(1)	8	8
15	[A,0,0,0,2]	1	1(1)	2	2

Tab. 4-3 Numbers of topological graphs for 6-link 1-DOF kinematic chains

No.	Link assortment	No. of multiple-edges	No. of VCG (CG)	No. of TG	No. of TG
1	[4,2]	2	1(1)	2	2

Tab. 4-4 Numbers of topological graphs for 8-link 1-DOF kinematic chains

No.	Link assortment	No. of multiple-edges	No. of VCG (CG)	No. of TG	No. of TG
1	[4,4,0]	0	1(1)	6	9
		2	1(1)	3	
2	[5,2,1]	2	1(1)	5	5
3	[6,0,2]	3	1(1)	2	2

Tab. 4-5 Numbers of topological graphs for 10-link 1-DOF kinematic chains

No.	link assortment	No. of multiple-edges	No. of VCG (CG)	No. of TG	No. of TG
1	[4,6,0,0]	0	2(2)	39	50
		1	1(1)	8	
		2	1(1)	3	
		3	0(1)	0	

2	[5,4,1,0]	0	1(1)	42	95
		1	1(1)	43	
		2	1(1)	10	
		3	0 (1)	0	
3	[6,2,2,0]	1	1(1)	32	57
		2	1(1)	15	
		3	2(2)	10	
4	[7,0,3,0]	3	1(1)	3	3
5	[6,3,0,1]	2	1(1)	15	15
6	[7,1,1,1]	3	1(1)	8	8
7	[8,0,0,2]	1	1(1)	2	2

Tab. 4-6 Numbers of topological graphs for 14-link 1-DOF kinematic chains

No.	link assortment	No. of multiple-edges	No. of VCG (CG)	No. of TG	No. of TG
1	[4,A,0,0,0,0]	0	18(18)	3994	4420
		1	16(18)	410	
		2	5(17)	16	
		3	0(9)	0	
		4	0(3)	0	
		5	0(1)	0	
2	[5,8,1,0,0,0]	0	25(25)	30510	38098
		1	48(50)	7192	
		2	27 (51)	396	
		3	0(27)	0	
		4	0(8)	0	
		5	0(1)	0	
3	[6,6,2,0,0,0]	0	27(27)	55825	89338
		1	68(68)	29270	
		2	80(91)	4103	
		3	21(60)	140	
		4	0(21)	0	
		5	0(3)	0	
4	[7,4,3,0,0,0]	0	11(11)	25653	62854
		1	31(31)	27516	
		2	53(54)	8915	
		3	35(47)	770	
		4	0(19)	0	
		5	0(3)	0	

5	[8,2,4,0,0,0]	0	2(2)	2509	12117
		1	5(5)	4900	
		2	14(14)	3789	
		3	16(16)	866	
		4	7(10)	53	
		5	0(3)	0	
6	[9,0,5,0,0,0]	0	1(1)	54	302
		2	1(1)	182	
		3	1(1)	56	
		4	1(1)	10	
		5	0(1)	0	
7	[6,7,0,1,0,0]	0	6(6)	8095	15215
		1	15(15)	6371	
		2	15(19)	721	
		3	4(11)	28	
		4	0(4)	0	
8	[7,5,1,1,0,0]	0	5(5)	13766	44871
		1	26(26)	23186	
		2	47(48)	7212	
		3	29 (38)	707	
		4	0(16)	0	
		5	0(1)	0	
9	[8,3,2,1,0,0]	0	2(2)	3183	28242
		1	10(10)	12707	
		2	29(29)	9831	
		3	37(37)	2405	
		4	10(21)	116	
		5	0(2)	0	
10	[9,1,3,1,0,0]	1	1(1)	861	3320
		2	3(3)	1245	
		3	8(8)	1076	
		4	6(6)	138	
		5	0(2)	0	
11	[8,4,0,2,0,0]	0	1(1)	309	4515
		1	3(3)	1877	
		2	10(10)	1846	
		3	11(11)	436	
		4	6 (7)	47	

		5	0 (2)	0	
12	[9,2,1,2,0,0]	1	1(1)	422	3083
		2	4(4)	1452	
		3	9(9)	1006	
		4	10(10)	203	
		5	0 (2)	0	
13	[A,0,2,2,0,0]	3	2(2)	158	216
		4	2(2)	36	
		5	3(3)	22	
14	[A,1,0,3,0,0]	3	1(1)	37	77
		4	1(1)	40	
15	[7,6,0,0,1,0]	0	1(1)	342	2672
		1	3(3)	1588	
		2	5(5)	692	
		3	3(5)	50	
		4	0(1)	0	
16	[8,4,1,0,1,0]	1	3(3)	2017	5120
		2	9(9)	2446	
		3	11(11)	625	
		4	3(6)	32	
17	[9,2,2,0,1,0]	2	4(4)	1078	1858
		3	6(6)	600	
		4	7(7)	180	
		5	0(1)	0	
18	[A,0,3,0,1,0]	3	1(1)	39	79
		4	1(1)	40	
19	[9,3,0,1,1,0]	2	2(2)	437	857
		3	4(4)	342	
		4	4(4)	78	
		5	0(1)	0	
20	[A,1,1,1,1,0]	3	1(1)	139	306
		4	4(4)	151	
		5	2(2)	16	
21	[B,0,0,2,1,0]	5	1(1)	7	7
22	[A,2,0,0,2,0]	3	1(1)	32	63
		4	1(1)	21	
		5	2(2)	10	
23	[B,0,1,0,2,0]	5	1(1)	7	7

24	[8,5,0,0,0,1]	2	1(1)	120	180
		3	1(1)	60	
25	[9,3,1,0,0,1]	3	3(3)	211	232
		4	1(1)	21	
26	[A,1,2,0,0,1]	4	2(2)	49	49
27	[A,2,0,1,0,1]	4	2(2)	46	46
28	[B,0,1,1,0,1]	5	1(1)	8	8
29	[B,1,0,0,1,1]	5	1(1)	8	8
30	[C,0,0,0,0,2]	1	1(1)	2	2

Mechanisms can further be synthesized from the atlas database of kinematic chains. For example, the total numbers of 1-DOF non-fractionated mechanisms are: 5 mechanisms for 6-link kinematic chains, 71 mechanisms for 8-link kinematic chains, 1834 mechanisms for 10-link kinematic chains, 75397 mechanisms for 12-link kinematic chains, and 4274510 mechanisms for 14-link kinematic chains. Table 4-7 displays the quantitative information for the atlas databases of non-fractionated kinematic chains and mechanisms with up to 19 links.

Tab. 4-7 Numbers of non-fractionated kinematic chains and mechanisms

N	*F*	No. of LAs	No. of VCGs	No. of KCs	Comfirms with others	No. of Mechanisms	Comfirms with others
6	1	1	1	2	Acknowledged	5	Acknowledged
7	2	1	1	3	Acknowledged	11	Acknowledged
8	1	3	4	16	Acknowledged	71	Acknowledged
	3	1	1	5	Acknowledged	18	Acknowledged
9	2	3	4	35	Acknowledged	220	Refs.[15],[125]
	4	1	1	6	Acknowledged	28	Ref.[125]
10	1	7	15	230	Refs.[15],[125]	1834	Refs.[15],[125]
	3	3	4	74	Acknowledged	517	Refs.[15],[125]
	5	1	1	8	Acknowledged	39	Ref.[125]
11	2	7	16	753	Refs.[15],[125]	7156	Refs.[15],[125]
	4	3	4	126	Ref.[125]	1056	Ref.[125]
	6	1	1	10	Acknowledged	55	Ref.[125]
12	1	15	97	6856	Refs.[15],[125]	75397	Refs.[15],[125]
	3	7	17	1962	Refs.[15],[125]	20737	Refs.[15],[125]
	5	3	4	212	Ref.[125]	1955	Ref.[125]
	7	1	1	12	New result	71	Refs.[15],[125]
13	2	15	109	27496	Refs.[15],[125]	335398	Refs.[15],[125]
	4	7	17	4356	Ref.[125]	51245	Ref.[125]
	6	3	4	325	Ref.[125]	3387	Ref.[125]

	8	1	1	14	New result	93	New result
14	1	30	923	318162	Ref.[125]	4274510	New result
	3	15	116	83547	Refs.[15],[125]	1105923	Refs.[15],[125]
	5	7	17	8846	Ref.[125]	113387	Ref.[125]
	7	3	4	490	New result	5550	New result
	9	1	1	17	New result	116	New result
15	2	30	1090	1432730	Ref.[125]	20737954	New result
	4	15	117	216291	Ref.[125]	3093027	New result
	6	7	17	16649	Ref.[125]	231664	Ref.[125]
	8	3	4	699	New result	8727	New result
	10	1	1	19	New result	145	New result
16	1	58	12612	19668033	New result		
	3	30	1169	4805764	Ref.[125]	74393277	New result
	5	15	118	504599	New result	7732861	New result
	7	7	17	29686	New result	444007	New result
	9	3	4	989	New result	13234	New result
	11	1	1	22	New result	175	New result
17	4	30	1188	13743920	Ref.[125]	226621724	New result
	6	15	118	1086580	New result	17773527	New result
	8	7	17	50484	New result	808720	New result
	10	3	4	1343	New result	19493	New result
	12	1	1	25	New result	213	New result
18	5	30	1196	35315327	New result	617745323	New result
	7	15	118	2199179	New result	38208747	New result
	9	7	17	82749	New result	1410661	New result
	11	3	2	1811	New result	27975	New result
	13	1	1	28	New result	251	New result
19	6	30	1197	83708033	New result		
	8	15	118	4226542	New result	77742656	New result
	10	7	17	131160	New result	2372955	New result
	12	3	2	2377	New result	39291	New result
	14	1	1	31	New result	298	New result

From Tab. 4-7 we can see that although great advancements have been made since the 1960s, which is also shown in the two review papers on structural synthesis [15,125], a lot of new results have been achieved with the new synthesis method, especially those kinematic chains or mechanisms with more complex structures. As for existing synthesis results reported in literature, the results here are the same as the widely acknowledged ones. There are also a lot of new results never obtained before, in particular for complex kinematic chains

and mechanisms.

4.8 Summary

In this chapter, an effective, fully-automatic and designer-friendly method is proposed to synthesize the whole family of planar non-fractionated kinematic chains and mechanisms with specified number of links and degrees of freedom. The effectiveness of the method is proved by successful synthesis of all the valid kinematic chains reported before. More importantly, with this method a lot of new results have been obtained, many of which are complex kinematic chains and mechanisms never synthesized otherwise before.

As so many topological structures of non-fractionated kinematic chains exist, for the sake of practical application in the conceptual stage of mechanisms, the corresponding atlas databases of non-fractionated kinematic chains and mechanisms are also established, which contains all the valid non-fractionated topological graphs classified by their structural characteristics.

5 Structural synthesis of fractionated kinematic chains

5.1 Foreword

Fractionated planar mechanisms, apart from the non-fractionated ones, are also widely used in engineering machinery and various robots. This chapter attempts to develop an automatic approach to synthesize the whole family of the kinematic structures of planar fractionated mechanisms with specified number of links and degrees of freedom. First, based on the structure characteristics of planar fractionated kinematic chains, the synthesis equation of fractionated kinematic chains is proposed. Then the synthesis of 2-DOF fractionated kinematic chains is proposed based on the combination algorithms of 1-DOF kinematic chains and the atlas databases of 1-DOF kinematic chains. The synthesis of 3-DOF or more fractionated kinematic chains is further proposed based on the combination of non-fractionated kinematic chains in their atlas databases. The whole family of the kinematic structures of planar fractionated planar mechanisms up to seven basic loops is also synthesized and given, while reportedly the largest number of basic loops of the fractionated kinematic chains synthesized so far is four [126-127].

5.2 Synthesis modeling

A fractionated kinematic chain can be separated into several non-fractionated kinematic chains or individual links at some links or joints. So any fractionated kinematic chain can be regarded as the assembly of several non-fractionated kinematic chains or links in series through link- or joint-connection to a basic non-fractionated kinematic chain. Here, the terminal part of a fractionated kinematic chain is a non-fractionated kinematic chain rather than an individual link.

The fractionation types (FT) of a fractionated kinematic chain can be represented by "*pL-qJ-rV*", which means the fractionated kinematic chain is the assembly of (p+q-r+1) non-fractionated kinematic chains and r individual links, comprising p link-connection and q joint-connection.

For example, Fig. 5-1(a) shows a 14-link 5-DOF fractionated kinematic chain. It can be separated into four parts: a 4-link 1-DOF kinematic chain (part 1), a binary link (part 2), a 6-link 1-DOF kinematic chain (part 3) and a 4-link 1-DOF kinematic chain

(part 4). Its fractionation type is "1*L*-2*J*-1*V*". If part 1 is selected as the basic non-fractionated kinematic chain, the whole fractionated kinematic chain can be constituted by first connecting a binary link (part 2) to it through joint-connection, then connecting a 6-link 1-DOF kinematic chain (part 3) to the binary link through joint-connection, finally, connecting a 4-link 1-DOF kinematic chain (part 4) to link 9 of the 6-link 1-DOF kinematic chain through link-connection, which can be seen from Fig. 5-1.

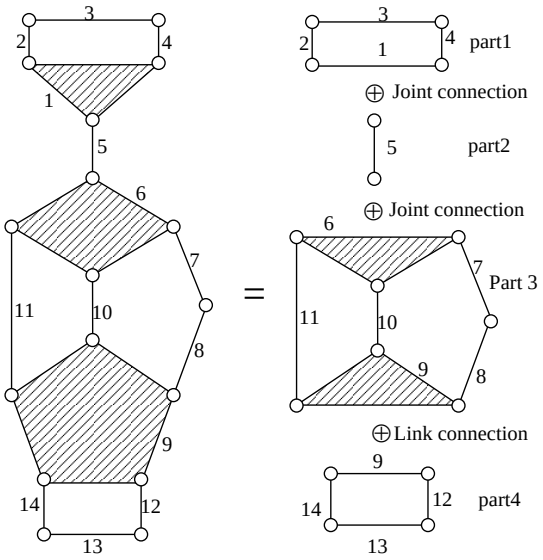

Fig. 5-1 A fractionated kinematic chain and its structure analysis

The corresponding topological graphs of Fig. 5-1 are shown in Fig. 5-2. From the view of topological graph, the progress can be more clearly: the topological graph of the 14-link 5-DOF fractionated kinematic chain can be constituted by first connecting vertex 5 (part 2) to vertex 1 of part 1, then connecting vertex 6 of part 3 to vertex 5, finally, connecting vertex 9 of part 4 to vertex 9 of part 3.

Suppose set {[N_i, F_i]} denotes the whole family of N_i-link F_i-DOF non-fractionated kinematic chains. For example, set {[6, 1]} contains two kinematic chain: the Watt chain and the Stephenson chain.

An N-link F-DOF fractionated kinematic chain can be separated into a basic N_B-link F_B-DOF non-fractionated kinematic chain, α non-fractionated kinematic chains of link-fractionation, i.e. coupled to the predecessor through a link connection, β non-fractionated kinematic chains of joint-fractionation, i.e. coupled to the

predecessor through a joint connection, and N_V individual links. The number of links and degrees of freedom of these kinematic chains satisfy

$$\begin{cases} N_B + (N_{L1} + N_{L2} \cdots + N_{L\alpha}) + (N_{J1} + N_{J2} \cdots + N_{J\beta}) + N_V = N + \alpha \\ F_B + (F_{L1} + F_{L2} \cdots + F_{L\alpha}) + (F_{J1} + F_{J2} \cdots + F_{J\beta}) + N_V = F - \beta \end{cases} \tag{5-1}$$

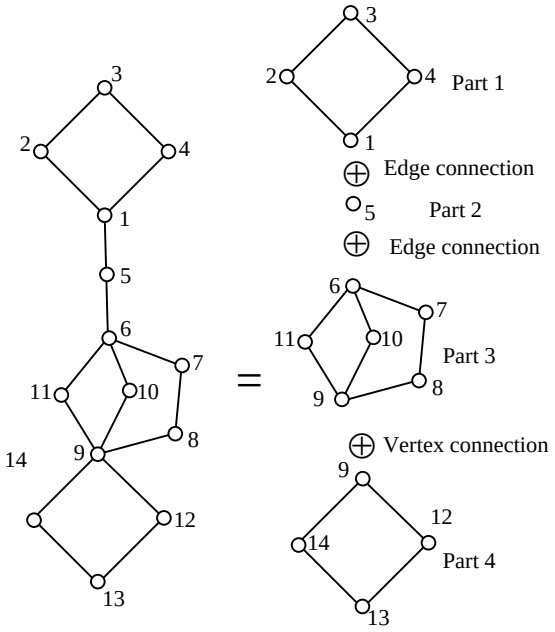

Fig. 5-2 Topological graphs of Fig. 5-1

Where N_i, F_i (i = $L1$, $L2$, …, $L\alpha$) are the number of links and degrees of freedom of the α non-fractionated kinematic chains, and N_j, F_j (j = $J1$, $J2$, …, $J\alpha$) are the number of links and degrees of freedom of the β non-fractionated kinematic chains. For the required N-link F-DOF fractionated kinematic chains, all possible combinations of non-fractionated kinematic chains can be obtained from Eq. (5-1), which becomes the synthesis constraint equation of fractionated kinematic chains.

5.3 Synthesis of 2-DOF fractionated kinematic chains

5.3.1 Rules of combination

According to the synthesis constraint equation of fractionated kinematic chains, the determination of all combinations of 2-DOF fractionated kinematic chains becomes simple. All 2-DOF fractionated kinematic chains can contain only one fractionated link, i.e. all 2-DOF fractionated kinematic chains can be synthesized by the combination of two appropriate 1-DOF kinematic chains.

In general, for the synthesis of *N*-link 2-DOF fractionated kinematic chains, the number of links of appropriate 1-DOF kinematic chains satisfies

$$\begin{cases} N_1 + N_2 = N + 1 \\ N_1 \le N_2 \\ N_i = 4, 6, 8, 10, \cdots \quad (i = 1, 2) \end{cases} \tag{5-2}$$

where N_1 and N_2 are the numbers of links of the appropriate 1-DOF kinematic chains. Without loss of generality, we suppose $N_1 \le N_2$.

For example, all 11-link 2-DOF fractionated kinematic chains can be synthesized by combining

(1)a 4-link 1-DOF kinematic chain with 16 possible 8-link 1-DOF kinematic chains;

(2) two possible 6-link 1-DOF kinematic chains.

In order to avoid isomorphism in the synthesis process, the vertices in each topological graph of 1-DOF kinematic chains are classified into different sets based on their topological symmetry. Two vertices are topologically symmetric if one can switch the labels of the two vertices and find a relabeling of the remaining vertices such that the resulting graph is the same as the original one, i.e. that they have the same adjacency matrices. A set S_i for which every pair of vertices in S_i is topologically symmetric is called a symmetry set. For a given topological graph, all its symmetry sets S_i (i=1, 2, … , r , where r is the number of sets) constitute the vertex-symmetry set (*VS*) of the topological graph, i.e. $VS = \{S_1, S_2, \ldots, S_r\}$. Each symmetry set S_i is an equivalent class that is uniquely determined by any representative vertex in this set. A set of one representative vertex from each S_i is called a vertex-asymmetry set *VA*. Obviously, any two vertices in *VA* are asymmetric.

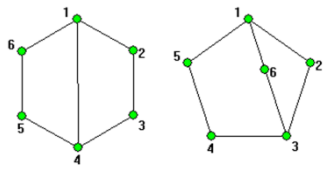

(a) (b)

Fig.5-3 Two 6-link 1-DOF kinematic chains

For the example of Fig.5-3(a), vertices 1 and 4 are symmetrical, and vertices 2, 3, 5 and 6 are also symmetrical. Thus, the vertex-symmetry set for the topological graph in

Fig.5-3(a) is VS_a={S_1, S_2}, where S_1={1, 4}, S_2={2, 3, 5, 6}. A possible vertex-asymmetry set of Fig.5-3(a) is for example VA_a={1, 2}, but VA_a can also be set equal to one of the sets of {1, 3}, {4, 2}, etc., which are equivalent.

Similarly, the vertex-symmetry set for the topological graph in Fig.5-3(b) is VS_b={S_1, S_2, S_3}, where S_1={1, 3}, S_2={2, 6}, and S_3={4, 5}, and a possible vertex-asymmetry set of Fig.5-3(b) is for example VA_b={1, 2, 4}.

Rule 5-1: For two different non-fractionated topological graphs whose vertex-asymmetry sets are VA_1 and VA_2, respectively, all different fractionated topological graphs through the combination of the two topological graphs can be obtained by letting every vertex in VA_1 coincide with every vertex in VA_2. Thus the total number of all different fractionated topological graphs for two different non-fractionated topological graphs is

$$n_{dg} = |VA_1| \cdot |VA_2| \tag{5-3}$$

where | *A* | denotes the cardinality of a set *A*, i.e. its number of elements.

Rule 5-2: For a non-fractionated topological graph whose vertex-asymmetry set is *VA*, all different fractionated topological graphs through the combination of the topological graph with itself can be obtained by letting the first vertex in *VA* coincide with all vertices in *VA*, the second vertex in *VA* coincide with all vertices in *VA* except the first, the third vertex in *VA* coincide with all vertices in *VA* except the first two, and so on. Thus the total number of all different fractionated topological graphs for two identical non-fractionated topological graphs is

$$n_{ig} = \sum_{i=1}^{|VA|} i = \frac{|VA|.(|VA|+1)}{2} \tag{5-4}$$

5.3.2 Combination of "AA" type

The type of combination by using 1-DOF kinematic chains with the same number of links to synthesize fractionated 2-DOF kinematic chains is defined as the combination of "*AA*" type. For example, if two 6-link 1-DOF kinematic chains are used to synthesize 11-link 2-DOF fractionated kinematic chains, this combination will be of "*AA*" type.

Suppose that the atlas database of *N*-link 1-DOF kinematic chains has *q* different kinematic chains and that the vertex-asymmetry sets for these topological graphs are VA_1, VA_2, …, VA_q, respectively. Based on Rule 5-1, all fractionated 2-DOF kinematic chains combined by any two different kinematic chains in the atlas database can be

obtained by coinciding every vertex in VA_i with every vertex in VA_j (where j=1, 2, …, q-1, i=j+1), and the total number is

$$\begin{aligned} DN &= \sum_{j=1}^{q-1}\sum_{i=j+1}^{q}|VA_i|\cdot|VA_j| \\ &= \frac{1}{2}\left[(\sum_{i=1}^{q}|VA_i|)^2-\sum_{i=1}^{q}|VA_i|^2\right] \end{aligned} \tag{5-5}$$

Based on Rule 5-2, the total number of all fractionated 2-DOF kinematic chains combined by every kinematic chain in the atlas database with itself is

$$SN=\sum_{j=1}^{q}\sum_{i=1}^{|VA_j|}i=\sum_{j=1}^{q}\frac{|VA_j|.(|VA_j|+1)}{2} \tag{5-6}$$

So altogether TN=DN+SN fractionated 2-DOF kinematic chains can be synthesized through the combination of q kinematic chains in the atlas database.

For example in Fig.5-3(a), $|VA_a|=3$ and thus altogether 3 fractionated topological graphs can be obtained through combining Fig.5-3(a) with itself. These topological graphs are shown in Fig. 5-4.

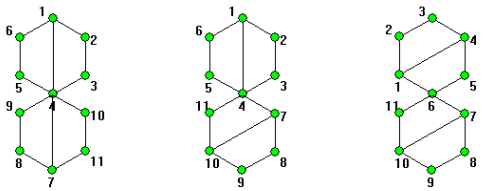

Fig.5-4 Three fractionated topological graphs by combining Fig.5-3(a) with itself

Also in Fig.5-3(b), $|VA_b|=3$, and thus altogether 6 fractionated topological graphs can be obtained by combining Fig.5-3(b) with itself, shown in Fig.5-5.

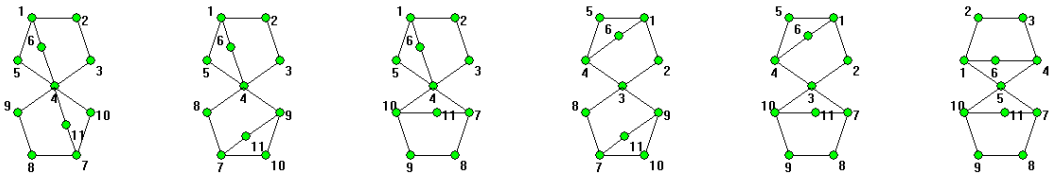

Fig.5-5 Six fractionated topological graphs by combining Fig.5-3(b) with itself

Finally, by combining Fig.5-3(a) and Fig.5-3(b), altogether 6 fractionated topological graphs can be obtained, shown in Fig. 5-6.

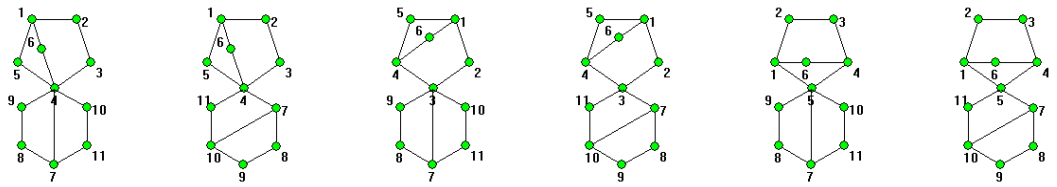

Fig.5-6 Six fractionated topological graphs by combining Figs.5-3(b) with 5-3(a)

5.3.3 Combination of "AB" type

The type of combination by using 1-DOF kinematic chains with different number of links to synthesize fractionated 2-DOF kinematic chains is defined as the combination of "*AB*" type. For example, if a 4-link kinematic chain and an 8-link 1-DOF kinematic chain are used to synthesize an 11-link 2-DOF fractionated kinematic chain, this combination will be of "*AB*" type.

Suppose the vertex-asymmetry sets for the q_1 kinematic chains in the atlas databases of N_1-link 1-DOF kinematic chains are VA_{a1}, VA_{a2}, …, VA_{aq_1}, and the vertex-asymmetry sets for the q_2 kinematic chains in the atlas databases of N_2-link 1-DOF kinematic chains are VA_{b1}, VA_{b2}, …, VA_{bq_2} (where $N_1 \neq N_2$). Based on Rule 5-1, all different fractionated topological graphs through the combination of two topological graphs from the two atlas databases can be obtained by letting every vertex in VA_{ai} coincide with every vertex in VA_{bj} (where i=1, 2, …, q_1 and j=1, 2, …, q_2), so the total number is

$$\begin{aligned} TN &= \sum_{i=1}^{q_1}\sum_{j=1}^{q_2}\left|VA_{ai}\right|\cdot\left|VA_{bj}\right| \\ &= \sum_{i=1}^{q_1}\left|VA_{ai}\right|\cdot\sum_{i=1}^{q_2}\left|VA_{bi}\right| \end{aligned} \tag{5-7}$$

For example, by combining a 4-link 1-DOF kinematic chain with 16 8-link 1-DOF kinematic chains, altogether 71 fractionated topological graphs of 11-link 2-DOF kinematic chains can be obtained. The 71 fractionated topological graphs are shown in Fig.5-7.

41-81-1

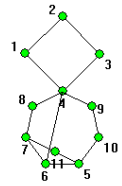

41-81-2

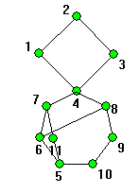

41-81-3

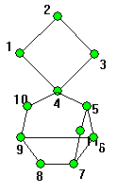

41-81-4

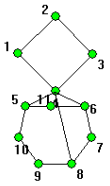

41-81-5

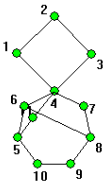

41-81-6

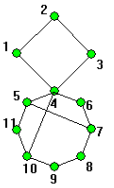

41-81-7

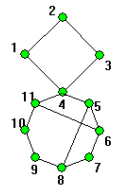

41-81-8

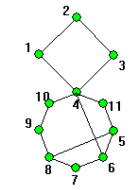

41-81-9

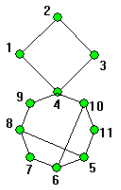

41-81-10

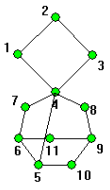

41-81-11

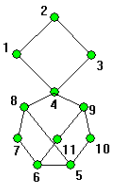

41-81-12

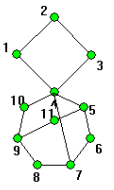

41-81-13

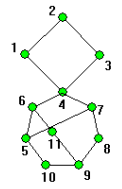

41-81-14

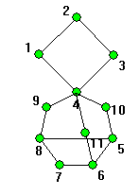

41-81-15

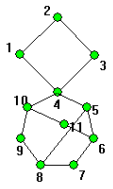

41-81-16

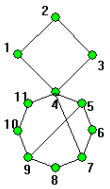

41-81-17

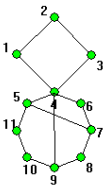

41-81-18

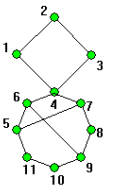

41-81-19

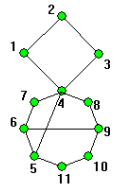

41-81-20

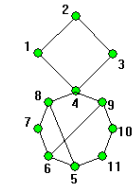

41-81-21

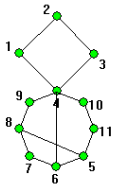

41-81-22

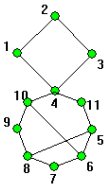

41-81-23

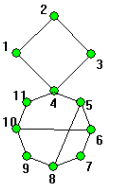

41-81-24

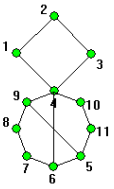

41-81-25

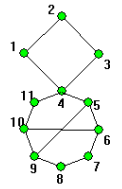

41-81-26

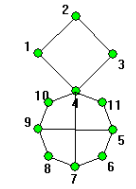

41-81-27

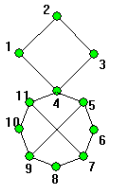

41-81-28

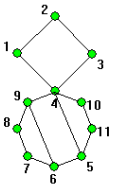

41-81-29

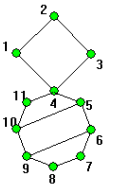

41-81-30

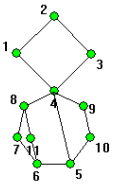

41-81-31

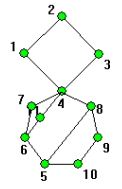

41-81-32

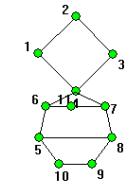

41-81-33

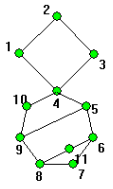

41-81-34

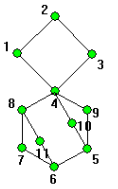

41-81-35

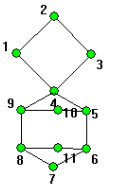

41-81-36

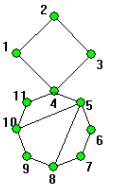

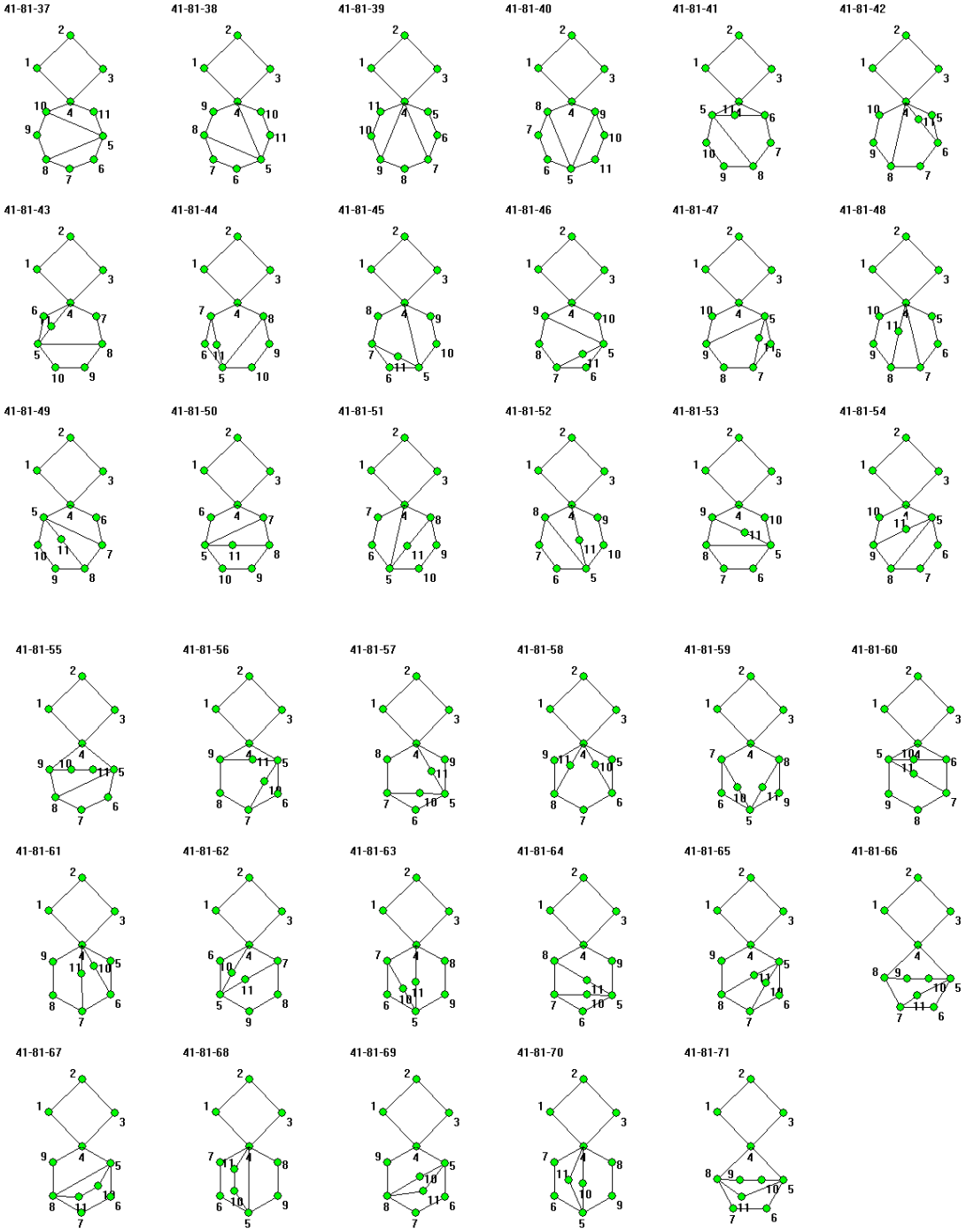

Fig.5-7 71 fractionated topological graphs through combination of 4-link and 8-link 1-DOF kinematic chains

5.3.4 Synthesis results of 2-DOF fractionated kinematic chains

In this way, the whole atlas database of fractionated 2-DOF kinematic chains can be established. Tab.5-1 shows the quantitative information concerning the whole family of fractionated 2-DOF kinematic chains up to seven basic loops (column 1) and 17

links (column 2). The fractionation types (FT) are shown in column 3: "*L*" denotes one fractionated link. Suppose operation "*" of two kinematic chain sets denotes the connection of all possible pairs of elements from the two sets by one fractionated link. For each fractionation type, the possible combinations of non-fractionated kinematic chains (non-FKCs) and the synthesized fractionated kinematic chains (FKCs) are shown in columns 4 and 5, respectively. For example, altogether 86 fractionated 11-link 2-DOF are synthesized, which consist of two parts: (1) 71 fractionated topological graphs are synthesized through the combination of 4-link kinematic chain with 8-link 1-DOF kinematic chains; (2) 15 fractionated topological graphs are synthesized through the combination of two 6-link 1-DOF kinematic chains.

The total number of 86 planar 11-link 2-DOF fractionated kinematic chains is confirmed by Mruthyunjaya [15] and Martins [127]. The complete sets of planar 2-DOF fractionated kinematic chains of 13, 15 and 17 links are obtained for the first time and the corresponding topological graphs and their numbers are also totally new.

Tab. 5-1 Numbers of 2-DOF fractionated kinematic chains and their classification

V	*N*	FT	Combination of kinematic chains	No. of FKCs	Total Number	Compared with other results
2	7	*L*	{[4,1]}*{[4,1]}	1	1	Acknowledged
3	9	*L*	{[4,1]}*{[6,1]}	5	5	Acknowledged
4	11	*L*	{[4,1]}*{[8,1]}	71	86	Confirmed by [15,127]
		L	{[6,1]}*{[6,1]}	15		
5	13	*L*	{[4,1]}*{[10,1]}	1834	2189	New result
		L	{[6,1]}*{[8,1]}	355		
6	15	*L*	{[4,1]}*{[12,1]}	75397	87123	New result
		L	{[6,1]}*{[10,1]}	9170		
		L	{[8,1]}*{[8,1]}	2556		
7	17	*L*	{[4,1]}*{[14,1]}	4274510	4781709	New result
		L	{[6,1]}*{[12,1]}	376985		
		L	{[8,1]}*{[10,1]}	130214		

5.4 Combination of three non-fractionated kinematic chains

Three non-fractionated kinematic chains used to form a fractionated chain must fit in with one of the three cases: (1) three identical kinematic chains, (2) two identical kinematic chains and another different one, (3) three different kinematic chains.

5.4.1 Combination rules for three identical kinematic chains

For a non-fractionated topological graph, assume its vertex-symmetry set is $VS=\{S_1, S_2, \ldots, S_r\}$, and its vertex-asymmetry set is $VA=\{V_1^*, V_2^*, \ldots, V_r^*\}$.

Case I Multiple fractionated link

Rule 5-3: All different fractionated topological graphs with multiple fractionated vertex through the combination of three identical non-fractionated topological graphs can be obtained by letting three vertices V_i^*, V_j^* and V_k^* coincide according to $1 \le i \le j \le k \le r$. The total number can be given by

$$n_{mv1} = \sum_{j=1}^{|VA|} \sum_{i=1}^{j} i = \sum_{j=1}^{|VA|} \frac{j(j+1)}{2} \tag{5-8}$$

For example, four different fractionated topological graphs can be obtained by combining three identical topological graphs of Fig.5-3(a), shown in Fig. 5-8.

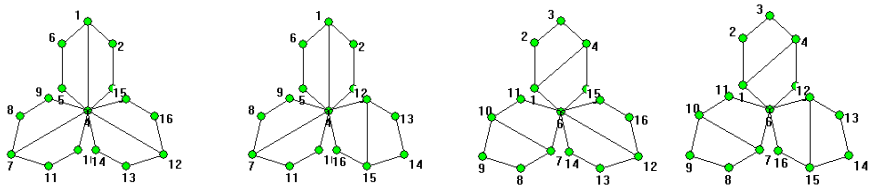

Fig. 5-8 Four fractionated topological graphs with multiple fractionated vertices

Case Ⅱ Two different fractionated vertices

In a topological graph, let any two vertices constitute a *vertex pair*, denoted as (V_i, V_j). An *asymmetrical pair* is constituted by two asymmetrical vertices. Two asymmetrical pairs are said to be equivalent pairs if they are topologically symmetrical. For example, the two asymmetrical pair (1,2) and (1,6) in Fig.5-3(a) are equivalent pairs. For a topological graph, a set constituted by all possible asymmetrical pairs without any equivalent pair is defined as the *set of asymmetrical vertex pairs* (*AP*) of the graph. It follows that no equivalent pairs exist in *AP*. For example, the set of asymmetrical vertex pairs for the topological graph in Fig.5-3(a) is $AP=\{(1,2),(1,3)\}$.

Rule 5-4: For a non-fractionated topological graph whose set of asymmetrical vertex pairs is *AP*, the total number of fractionated topological graphs obtained by letting two vertices of two non-fractionated graphs coincide with two asymmetrical vertices of the third graph is

$$n_{ap} = |AP| \cdot |VA|^2 \tag{5-9}$$

For example, eight different fractionated topological graphs can be obtained by combining three identical topological graphs of Fig.5-3(a) in this way, shown in Fig.5-9.

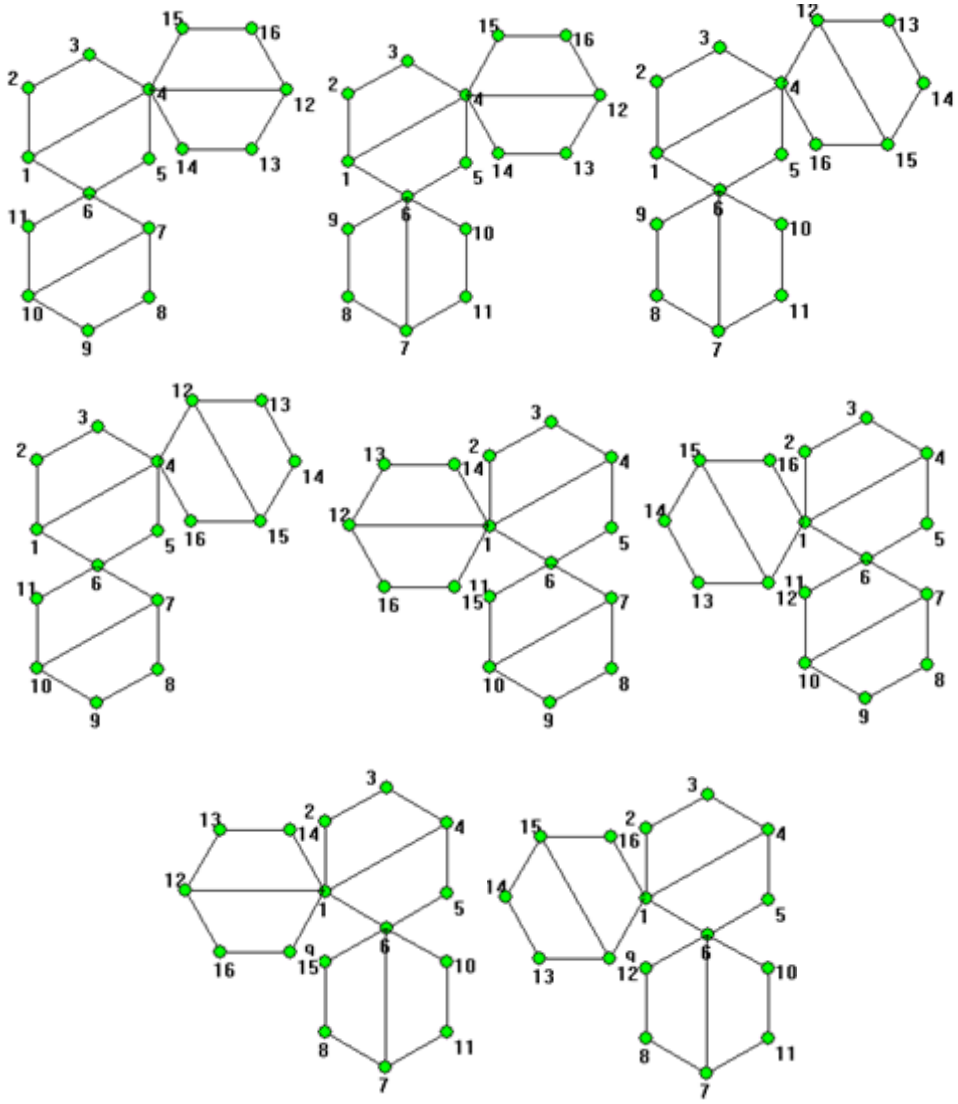

Fig.5-9 Eight fractionated topological graphs of two fractionated vertices

Similarly, a *symmetrical pair* is constituted by two symmetrical vertices. The *set of symmetrical vertex pairs* (*SP*) of a topological graph consists of all possible symmetrical pairs without any equivalent pair of the graph. For example, the set of symmetrical vertex pairs for the topological graph in Fig.5-3(a) is *SP*={(1,4)},(2,3),(2,5),(2,6)}.

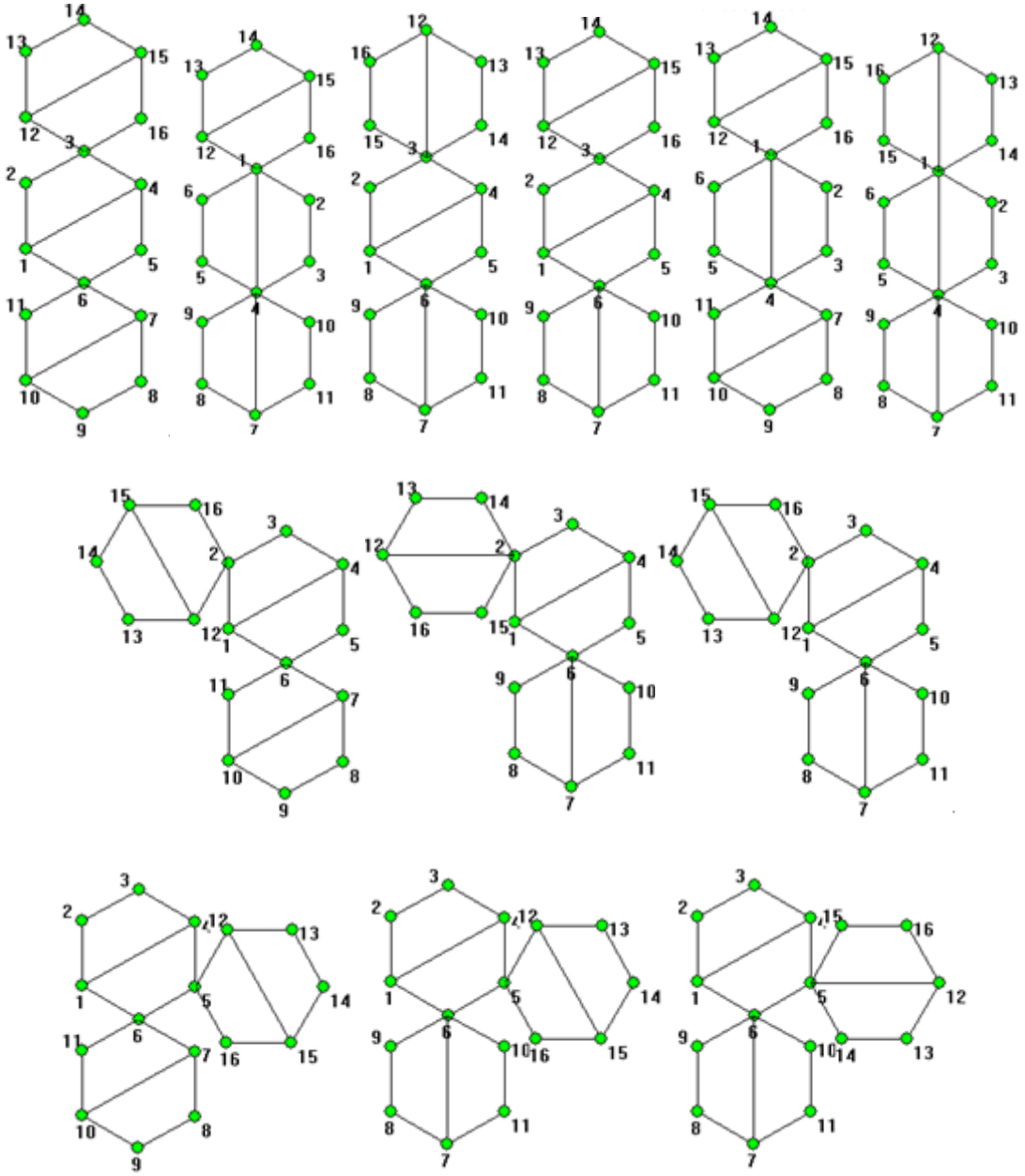

Fig. 5-10 12 fractionated topological graphs of two fractionated vertices

Rule 5-5: For a non-fractionated topological graph whose set of symmetrical vertex pairs is *SP*, the total number of fractionated topological graphs obtained by letting two vertices of two non-fractionated graphs coincide with two symmetrical vertices of the third graph is

$$n_{sp} = |SP| \cdot \sum_{i=1}^{|VA|} i = |SP| \cdot \frac{|VA|.(|VA|+1)}{2} \tag{5-10}$$

For example, 12 different fractionated topological graphs can be obtained by combining three topological graphs of Fig. 5-3(a) in this way, shown in Fig. 5-10.

So the total number of all different fractionated topological graphs with two different fractionated vertices through the combination of three identical non-fractionated topological graphs is

$$n_2 = n_{ap} + n_{sp} \tag{5-11}$$

5.4.2 Combination rules for two identical and a different one

Fractionated kinematic chains are constituted by the combination of two identical kinematic chains, A, and another different one, B. Assume that the vertex-asymmetry set for the two identical kinematic chains is VA_a, and that the vertex-asymmetry set for the third chain is VA_b.

Case I One multiple fractionated vertex

Rule 5-6: All different fractionated topological graphs with one multiple fractionated vertex through the combination of two identical topological graphs and a third different graph can be obtained by letting two vertices V_i^* and V_j^* in VA_a coincide according to $1 \le i \le j \le r$. The total number is

$$n_{mv2} = |VA_b| \cdot \sum_{i=1}^{|VA_a|} i = |VA_b| \cdot \frac{|VA_a|.(|VA_a|+1)}{2} \tag{5-12}$$

For example, nine different fractionated topological graphs with one multiple fractionated vertex can be obtained by combining two topological graphs of Fig. 5-3(a) and another different graph of Fig. 5-3(b), shown in Fig. 5-11.

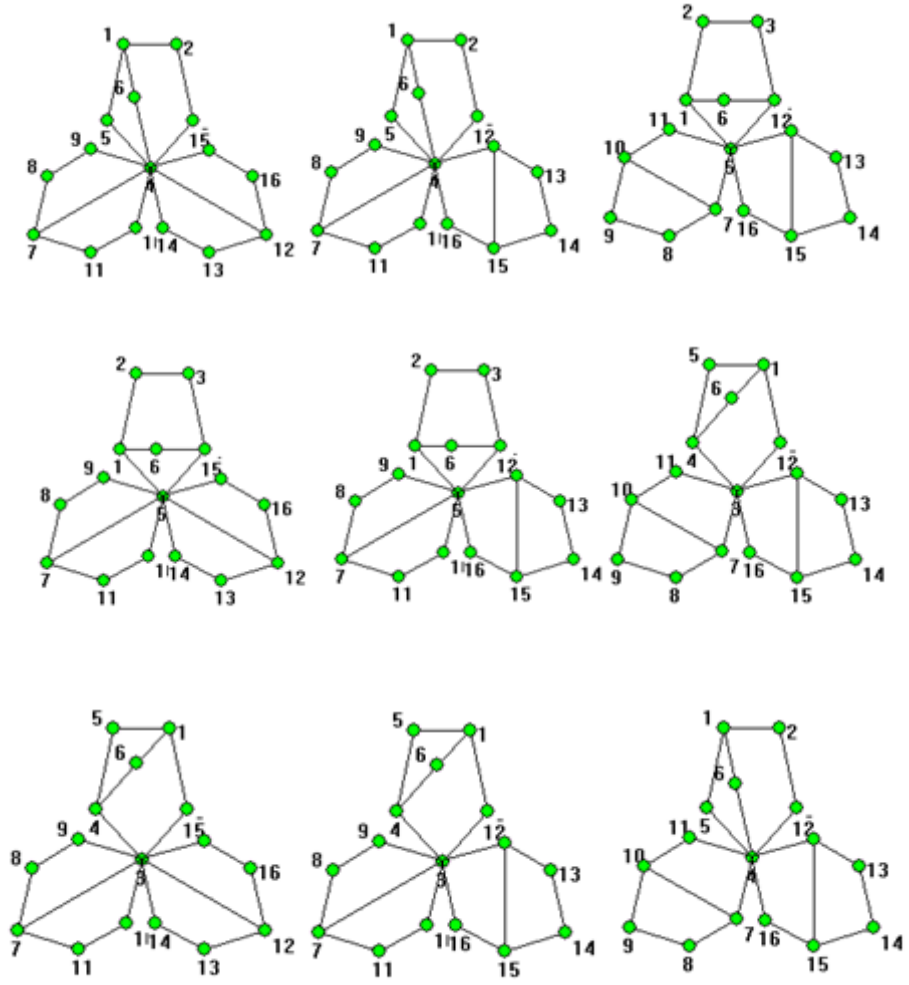

Fig. 5-11 Nine fractionated topological graphs with two fractionated vertices

Case II Two different fractionated vertices

Rule 5-7: Assume the sets of asymmetrical vertex pairs and symmetrical vertex pairs of kinematic chain A are AP_a and SP_a, respectively. The total number of different fractionated topological graphs obtained by combining the two identical kinematic chains A first and then with kinematic chain B is

$$W_4 = |SP_a| \cdot |VA_a| \cdot |VA_b| + 2|AP_a| \cdot |VA_a| \cdot |VA_b| \tag{5-13}$$

For example, 48 different fractionated topological graphs can be obtained by combining the kinematic chain A in Fig. 5-3(a) with itself first and then with kinematic chain B in Fig. 5-3(b), shown in Fig. 5-12.

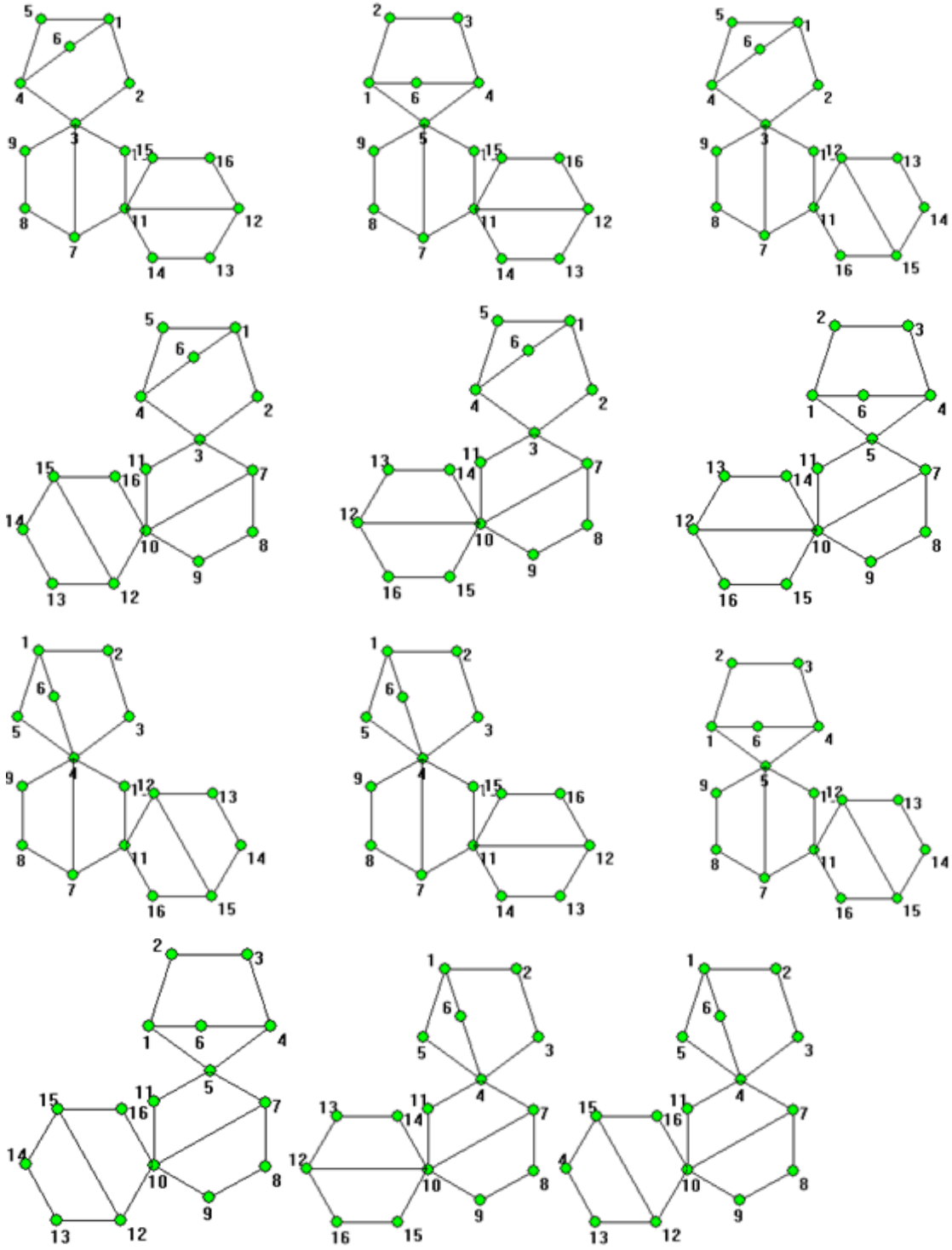

Fig. 5-12 Excerpt of 48 fractionated topological graphs of two fractionated vertices

Rule 8: Assume the sets of asymmetrical vertex pairs and symmetrical vertex pairs of kinematic chain B are AP_b and SP_b, respectively. The total number of different fractionated topological graphs obtained by letting two vertices of the two identical graphs A coincide with two different vertices of graph B is

$$W_5 = \left|SP_b\right| \cdot \sum_{i=1}^{\left|VA_a\right|} i + \left|AP_b\right| \cdot \left|VA_a\right|^2 \tag{5-14}$$

For example, 25 different fractionated topological graphs can be obtained by letting two vertices of the two identical graphs in Fig. 5-3(a) coincide with two different vertices of graph B in Fig. 5-3(b), shown in Fig. 5-13.

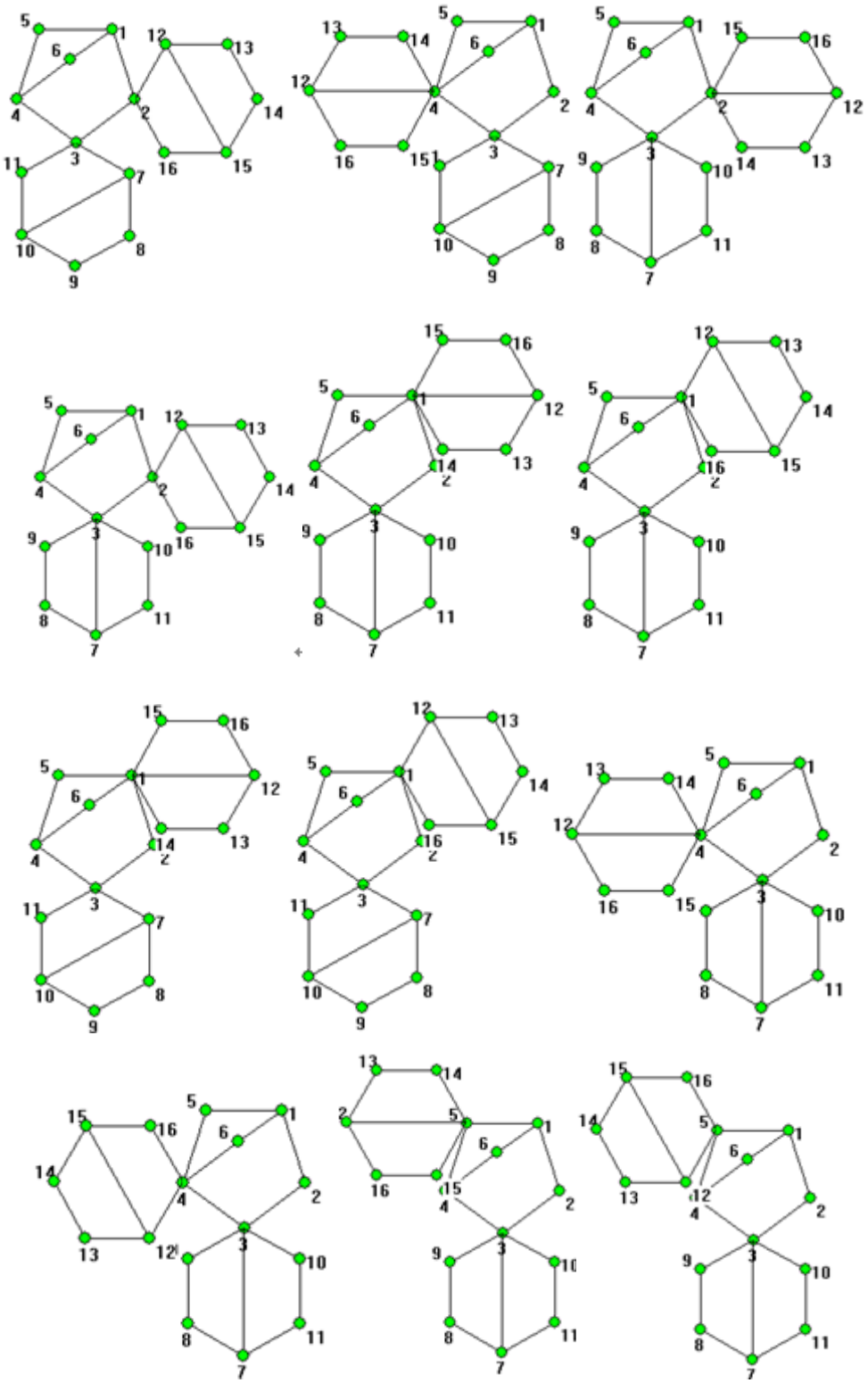

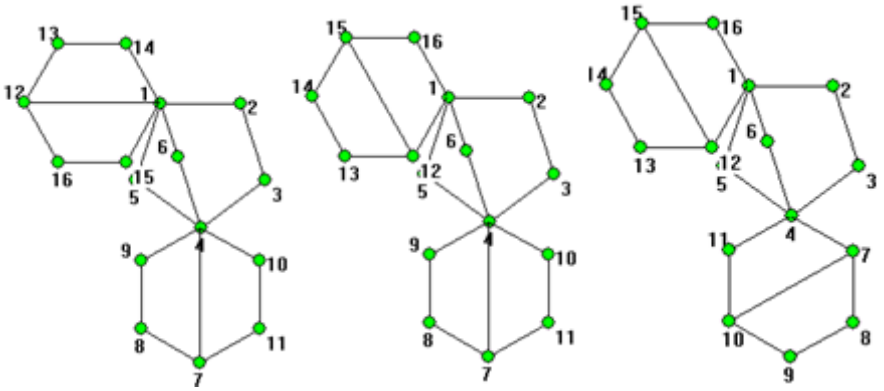

Fig. 5-13 Excerpt of 25 fractionated topological graphs of two fractionated vertices

5.4.3 Combination rules for three different kinematic chains

In this case, fractionated kinematic chains are constituted by the combination of three different non-fractionated kinematic chains A, B and C. Assume the vertex-asymmetry sets for kinematic chains A, B and C are VA_a, VA_b, and VA_c, respectively.

Case I One multiple fractionated vertex

Rule 9: The total number of all different fractionated topological graphs with one multiple fractionated vertex through the combination of three different topological graphs A, B and C is

$$n_{mv3} = |VA_a| \cdot |VA_b| \cdot |VA_c| \tag{5-15}$$

Case II Two different fractionated vertices

Rule 10: For three different kinematic chains A, B and C, assume their sets of asymmetrical vertex pairs are AP_a, AP_b and AP_c, respectively; their sets of symmetrical vertex pairs are SP_a, SP_b, and SP_c, respectively. The total number of different fractionated topological graphs with two different fractionated vertices by combining kinematic chains A, B and C and kinematic chain A in the middle is

$$W_{71} = |SP_a| \cdot |VA_b| \cdot |VA_c| + 2|AP_a| \cdot |VA_b| \cdot |VA_c| \tag{5-16}$$

the total number of different fractionated topological graphs with two different fractionated vertices and kinematic chain B in the middle is

$$W_{72} = |SP_b| \cdot |VA_a| \cdot |VA_c| + 2|AP_b| \cdot |VA_a| \cdot |VA_c| \tag{5-17}$$

the total number of different fractionated topological graphs with two different fractionated vertices and kinematic chain C in the middle is

$$W_{73} = \left|SP_c\right| \cdot \left|VA_a\right| \cdot \left|VA_b\right| + 2\left|AP_c\right| \cdot \left|VA_a\right| \cdot \left|VA_b\right| \tag{5-18}$$

So the total number of all different fractionated topological graphs through the combination of three different topological graphs with two different fractionated vertices is

$$W_7 = W_{71} + W_{72} + W_{73} \tag{5-19}$$

5.5 Synthesis of 3- DOF fractionated kinematic chains

According to the synthesis equation of fractionated kinematic chains, 3-DOF fractionated kinematic chains can be divided into three basic types, i.e. the type of (1)one fractionated link, (2) one fractionated joint, and (3) two fractionated links.

5.5.1 Synthesis of "L" type

In this case, an N-link 3-DOF fractionated kinematic chain is obtained by connecting an N_1-link 1-DOF kinematic chain with an N_2-link 2-DOF non-fractionated kinematic chain by one fractionated link. The numbers of links, N, N_1, N_2, of the fractionated, 1-DOF, and 2-DOF kinematic chain satisfy

$$\begin{cases} N_1 + N_2 = N + 1 \\ N_1 = 4, 6, 8, 10, \cdots \\ N_2 = 5, 7, 9, 11, \cdots \end{cases} \tag{5-20}$$

Suppose set $\{[N, F]\}$ denotes all N-link F-DOF non-fractionated kinematic chains and operation "*" of two sets of denotes the connection of all possible pairs of elements from the two sets by one fractionated link. So the whole family of N-link 3-DOF fractionated kinematic chains with one fractionated link, $\{[N, 3]\}_L$, can be synthesized by the "*" operation of the set of N_1-link 1-DOF kinematic chains and the set of N_2-link 2-DOF non-fractionated kinematic chains, that is

$$\{[N, 3]\}_L = \{[N_1, 1]\} * \{[N_2, 2]\} \tag{5-21}$$

For example, the whole family of 10-link 3-DOF fractionated kinematic chains with one fractionated link can be synthesized by $\{[4, 1]\} * \{[7, 2]\}$ and $\{[6, 1]\} * \{[5, 2]\}$. That is

$$\{[10, 3]\}_L = \{[4, 1]\} * \{[7, 2]\} \cup \{[6, 1]\} * \{[5, 2]\} \tag{5-22}$$

11 fractionated topological graphs can be synthesized by {[4, 1]}*{[7, 2]}, shown in Fig. 5-14; five fractionated topological graphs can be synthesized by {[6, 1]}*{[5, 2]}, shown in Fig. 5-15.

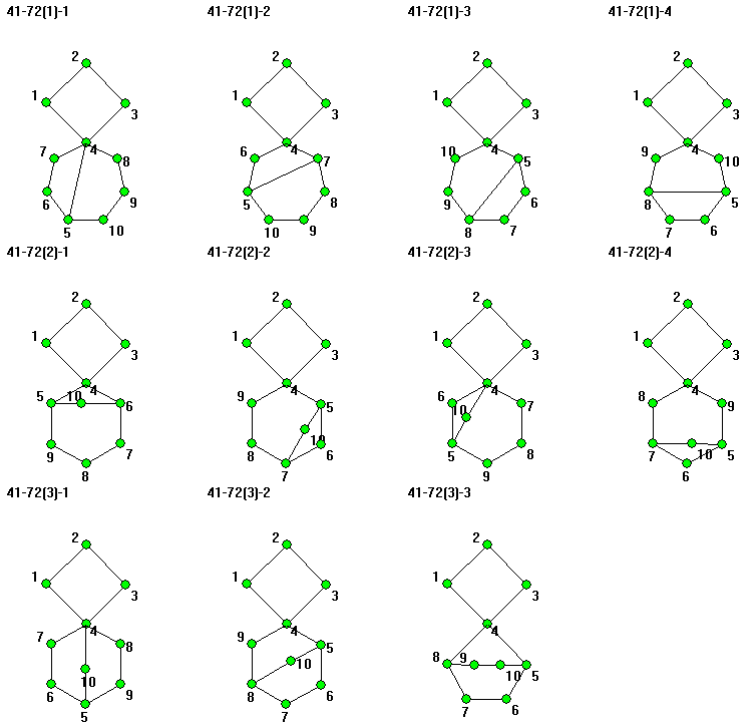

Fig. 5-14 11 fractionated topological graphs by {[4, 1]}*{[7, 2]}

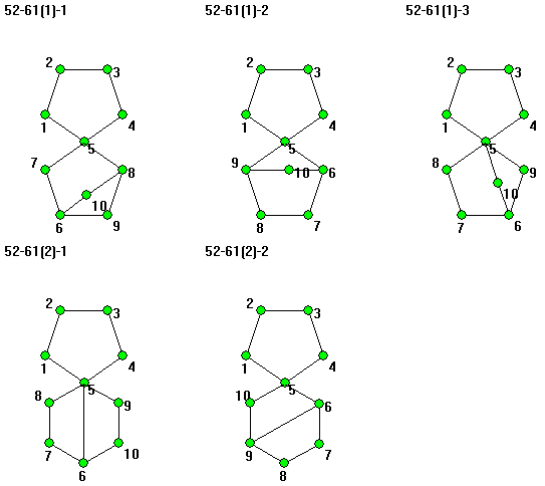

Fig. 5-15 five fractionated topological graphs by {[6, 1]}*{[5, 2]}

5.5.2 Synthesis of "J" type

In this case, an *N*-link 3-DOF fractionated kinematic chain is obtained by connecting two 1-DOF kinematic chains with N_1 and N_2 links by one fractionated joint. Without loss of generality, we suppose $N_1 \le N_2$. The numbers of links, N_1 and N_2, of the two 1-

DOF kinematic chains and the number of links, N, of the fractionated kinematic chain satisfy

$$\begin{cases} N_1 + N_2 = N \\ N_1 \le N_2 \\ N_i = 4, 6, 8, 10, \cdots \quad (i = 1, 2) \end{cases} \tag{5-23}$$

We suppose operation "~" of two kinematic chain sets denotes the connection of all possible pairs of elements from the two sets by one fractionated joint. So the whole family of N-link 3-DOF fractionated kinematic chains with one fractionated joint, $\{[N, 3]\}_J$, can be synthesized by

$$\{[N, 3]\}_J=\{[\{[N_1, 1]\}\sim\{[N_2, 1]\} \tag{5-24}$$

For example, the whole family of 10-link 3-DOF fractionated kinematic chains with one fractionated joint can be synthesized by {[4, 1]}~{[6, 1]}. Five fractionated topological graphs can be synthesized by {[4, 1]}~{[6, 1]}, which is shown in Fig. 5-16.

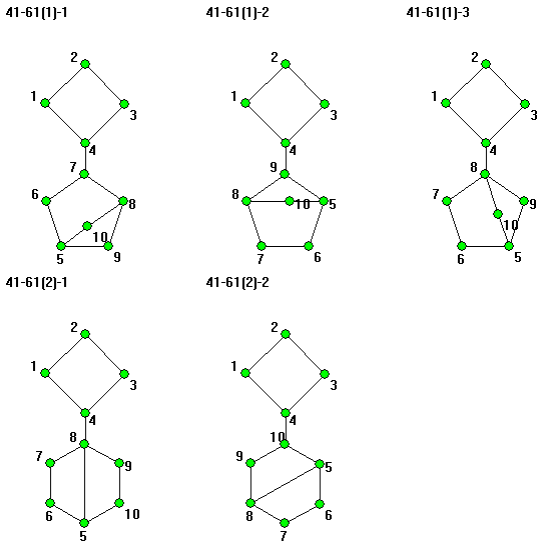

Fig. 5-16 Five fractionated topological graphs by {[4, 1]}~{[6, 1]}

5.5.3 Synthesis of "2L" type

Here, an N-link 3-DOF fractionated kinematic chain is obtained by connecting three 1-DOF kinematic chains with N_1, N_2 and N_3 links by two fractionated links. Without loss of generality, suppose $N_1 \le N_2 \le N_3$. The numbers of links, N_1, N_2 and N_3, of the three 1-DOF kinematic chains and the number of links, N, of the fractionated kinematic chain satisfy

$$\begin{cases} N_1 + N_2 + N_2 = N + 2 \\ N_1 \le N_2 \le N_3 \\ N_i = 4, 6, 8, 10, \cdots \quad (i = 1, 2, 3) \end{cases} \tag{5-25}$$

We suppose operation "&(S_1, S_2, S_3) "denotes the connection of three elements from the three sets in all possible ways by two fractionated links. So the whole family of N-link 3-DOF fractionated kinematic chains with two fractionated links, $\{[N, 3]\}_{TL}$, can be synthesized by

$$\{[N, 3]\}_{2L} = \&(\{[N_1, 1]\}, \{[N_2, 1]\}, \{[N_2, 1]\}) \tag{5-26}$$

For example, the whole family of 10-link 3-DOF fractionated kinematic chains with two fractionated links can be synthesized by &({[4, 1]}, {[4, 1]}, {[4, 1]}). Three fractionated topological graphs can be synthesized by the connection of the three 4-link kinematic chains, shown in Fig. 5-17.

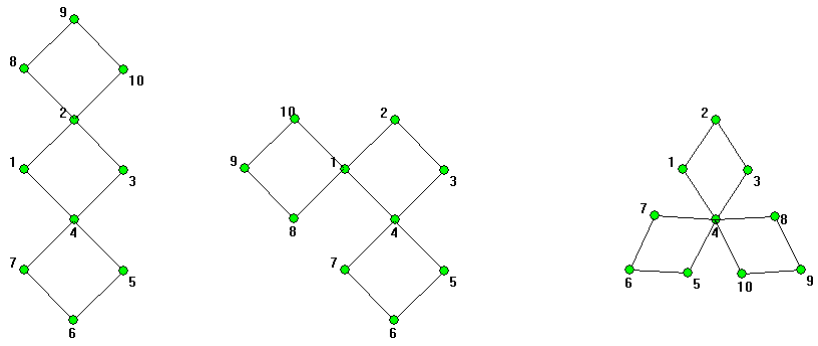

Fig. 5-17 Three fractionated topological graphs by &({[4, 1]}, {[4, 1]}, {[4, 1]})

5.5.4 Synthesis results of 3-DOF fractionated kinematic chains

Table 5-2 presents the quantitative information concerning the whole family of fractionated 3-DOF kinematic chains up to seven basic loops (column 1) and 18 links (column 2). The fractionation types (FT) are shown in column 3: "*L*" denotes one fractionated link, "*J*" denotes one fractionated joint, and "*2L*" denotes two fractionated links. For each fractionation type, the possible combinations of non-fractionated kinematic chains (non-FKCs) and the synthesized fractionated kinematic chains (FKCs) are shown in columns 4 and 5, respectively. The total number of 460 planar 12-link 3-DOF fractionated kinematic chains is confirmed by Mruthyunjaya [15] and Martins [127]. The complete sets of planar 3-DOF fractionated kinematic chains of 14, 16 and 18 links are obtained for the first time and the corresponding topological graphs and their numbers are totally new.

Tab. 5-2 Numbers of 3-DOF fractionated kinematic chains and their classification

V	*N*	FT	Combination of non-FKCs	No. of FKCs	Total Number	Compared with other's results
2	8	*L*	{[4,1]}*{[5,2]}	1	2	Acknowledged
		J	{[4, 1]}~{[4, 1]}	1		
3	10	*L*	{[4,1]}*{[7,2]}	11	24	Acknowledged
			{[6,1]}*{[5,2]}	5		
		2L	&({[4, 1]},{[4, 1]},{[4, 1]})	3		
		J	{[4, 1]}~{[6, 1]}	5		
4	12	*L*	{[4,1]}*{[9,2]}	220	460	Confirmed by [20,23]
			{[8,1]}*{[5,2]}	71		
			{[6,1]}*{[7,2]}	55		
		2L	&({[4, 1]},{[4, 1]},{[6, 1]})	28		
		J	{[4, 1]}~{[8, 1]}	71		
			{[6, 1]}~{[6, 1]}	15		
5	14	*L*	{[4,1]}*{[11,2]}	7156	13647	New result
			{[10,1]}*{[5,2]}	1834		
			{[6,1]}*{[9,2]}	1100		
			{[8,1]}*{[7,2]}	781		
		2L	&({[4, 1]},{[4, 1]},{[8, 1]})	447		
			&({[4, 1]},{[6, 1]},{[6, 1]})	140		
		J	{[4, 1]}~{[10, 1]}	1834		
			{[6, 1]}~{[8, 1]}	355		
6	16	*L*	{[4,1]}*{[13,2]}	335398	587627	New result
			{[12,1]}*{[5,2]}	75397		
			{[6,1]}*{[11,2]}	35780		
			{[10,1]}*{[7,2]}	20174		
			{[8,1]}*{[9,2]}	15620		
		2L	&({[4, 1]},{[4, 1]},{[10, 1]})	13336		
			&({[4, 1]},{[6, 1]},{[8, 1]})	4509		
			&({[6, 1]},{[6, 1]},{[6, 1]})	290		
		J	{[4, 1]}~{[12, 1]}	75397		
			{[6, 1]}~{[10, 1]}	9170		
			{[8, 1]}~{[8, 1]}	2556		

7	18	*L*	{[4,1]}*{[15,2]}	20737954	34027016	New result
			{[14,1]}*{[5,2]}	4274510		
			{[6,1]}*{[13,2]}	1676990		
			{[12,1]}*{[7,2]}	829367		
			{[10,1]}*{[9,2]}	403480		
			{[8,1]}*{[11,2]}	508076		
		2L	&({[4, 1]},{[4, 1]},{[12, 1]})	625887		
			&({[4, 1]},{[6, 1]},{[10, 1]})	138456		
			&({[4, 1]},{[8, 1]},{[8, 1]})	37417		
			&({[6, 1]},{[6, 1]},{[8, 1]})	13170		
		J	{[4, 1]}~{[14, 1]}	4274510		
			{[6, 1]}~{[12, 1]}	376985		
			{[8, 1]}~{[10, 1]}	130214		

5.6 Synthesis of 4- DOF fractionated kinematic chains

According to the synthesis equation of fractionated kinematic chains, 4-DOF fractionated kinematic chains can be divided into six basic types, i.e. the type of (1) "*L*", (2) "2*L*", (3) "3*L*", (4) "*J*", (5) "*L*-*J*", (6) "*J*-*V*".

5.6.1 Synthesis of "*L*" type

In this case, the synthesis equation of *N*-link 4-DOF fractionated kinematic chains is

$$\begin{cases} N_1 + N_2 = N + 1 \\ F_1 + F_2 = 4 \end{cases} \tag{5-27}$$

Obviously, an *N*-link 4-DOF fractionated kinematic chain can be obtained by connecting a 1-DOF kinematic chain with a 3-DOF non-fractionated kinematic chain or two 2-DOF kinematic chains.

(1) If an *N*-link 4-DOF fractionated kinematic chain is obtained by the combination of an N_1-link 1-DOF kinematic chain with an N_2-link 3-DOF non-fractionated kinematic chain through one fractionated link, the synthesis equation is

$$\begin{cases} N_1 + N_2 = N + 1 \\ N_1 = 4, 6, 8, 10, \cdots \\ N_2 = 6, 8, 10, 12, \cdots \end{cases} \tag{5-28}$$

In this case, $\{[N, 4]\}_L = \{[N_3, 1]\} * \{[N_4, 3]\}$.

(2) If an *N*-link 4-DOF fractionated kinematic chain is obtained by the combination of two 2-DOF kinematic chains through one fractionated link, the synthesis equation is

$$\begin{cases} N_3 + N_4 = N + 1 \\ N_3 \le N_4 \\ N_i = 5, 7, 9, 11, \cdots (i = 1, 2) \end{cases} \tag{5-29}$$

where N_3 and N_4 are the numbers of links of the two 2-DOF kinematic chains. Without loss of generality, suppose $N_3 \le N_4$. In this case, $\{[N, 4]\}_L = N_1, 2]\}*\{[N_2, 2]\}$.

For example, the whole family of 11-link 4-DOF fractionated kinematic chains with one fractionated link can be synthesized by {[4, 1]}*{[8, 3]}, {[6, 1]}*{[6, 3]} and {[5, 2]}*{[7, 2]}. That is

$$\{[11, 4]\}_L = \{[4, 1]\}*\{[8, 3]\} \cup \{[6, 1]\}*\{[6, 3]\} \cup \{[5, 2]\}*\{[7, 2]\} \tag{5-30}$$

11 fractionated topological graphs can be synthesized by {[5, 2]}*{[7, 2]}, shown in Fig. 5-18. Moreover, 18 fractionated topological graphs can be synthesized by {[4, 1]}*{[8, 3]}, and five fractionated topological graphs can be synthesized by {[6, 1]}*{[6, 3]}.

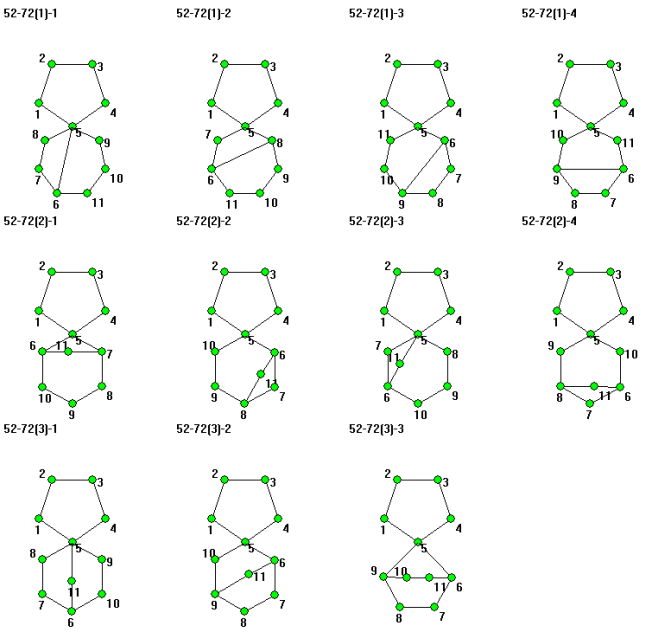

Fig. 5-18 11 fractionated topological graphs by {[5, 2]}*{[7, 2]}

5.6.2 Synthesis of "2*L*" type

In this case, the synthesis equation of *N*-link 4-DOF fractionated kinematic chains is

$$\begin{cases} N_1 + N_2 + N_3 = N + 2 \\ N_1 \le N_2 \\ N_i = 4, 6, 8, 10, \cdots \quad (i = 1, 2) \\ \mathrm{N}_3 = 5,7,9,11, \ldots \end{cases} \tag{5-31}$$

Obviously, an *N*-link 4-DOF fractionated kinematic chain can be obtained by connecting two 1-DOF kinematic chains (with N_1 and N_2 links and suppose $N_1 \le N_2$) and a 2-DOF kinematic chain (with N_3 links). That is

$$\{[N, 4]\}_{2L} = \&(\{[N_1, 1]\}, \{[N_2, 1]\}, \{[N_3, 2]\}) \tag{5-32}$$

For example, the whole family of 11-link 4-DOF fractionated kinematic chains with two fractionated links can be synthesized

$$\{[11, 4]\}_{2L} = \&(\{[4, 1]\}, \{[4, 1]\}, \{[5, 2]\}) \tag{5-33}$$

yielding the fractionated topological graphs, shown in Fig. 5-19.

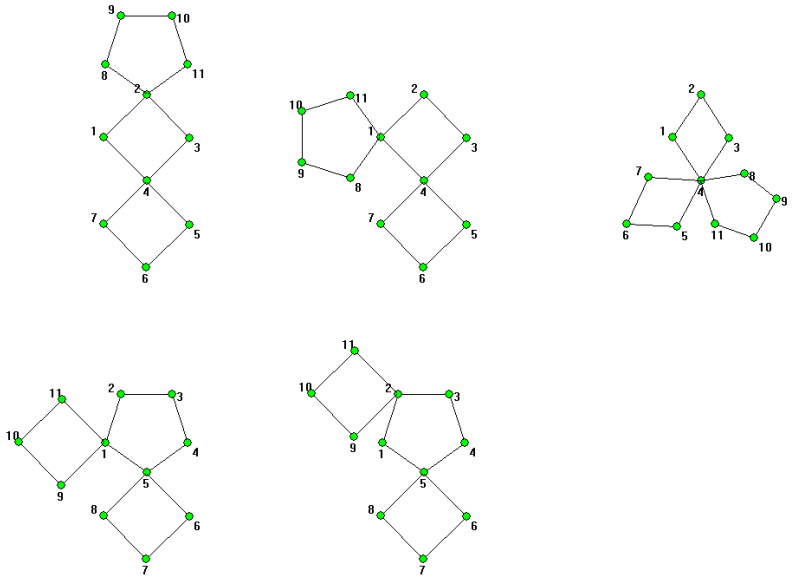

Fig. 5-19 Five fractionated topological graphs of $\{[11, 4]\}_{2L}$

5.6.3 Synthesis of "3*L*" type

In this case, the synthesis equation of *N*-link 4-DOF fractionated kinematic chains is

$$\begin{cases} N_1 + N_2 + N_3 + N_4 = N + 3 \\ N_1 \le N_2 \le N_3 \le N_4 \\ N_i = 4, 6, 8, 10, \cdots \quad (i = 1, 2, 3, 4) \end{cases} \tag{5-34}$$

Obviously, an N-link 4-DOF fractionated kinematic chain can be obtained by connecting four 1-DOF kinematic chains (with N_1, N_2, N_3, and N_4 links and suppose $N_1 \le N_2 \le N_3 \le N_4$). That is

$$\{[N, 4]\}_{3L}=\&(\{[N_1, 1]\}, \{[N_2, 1]\}, \{[N_3, 1]\}, \{[N_4, 1]\}) \quad (5\text{-}35)$$

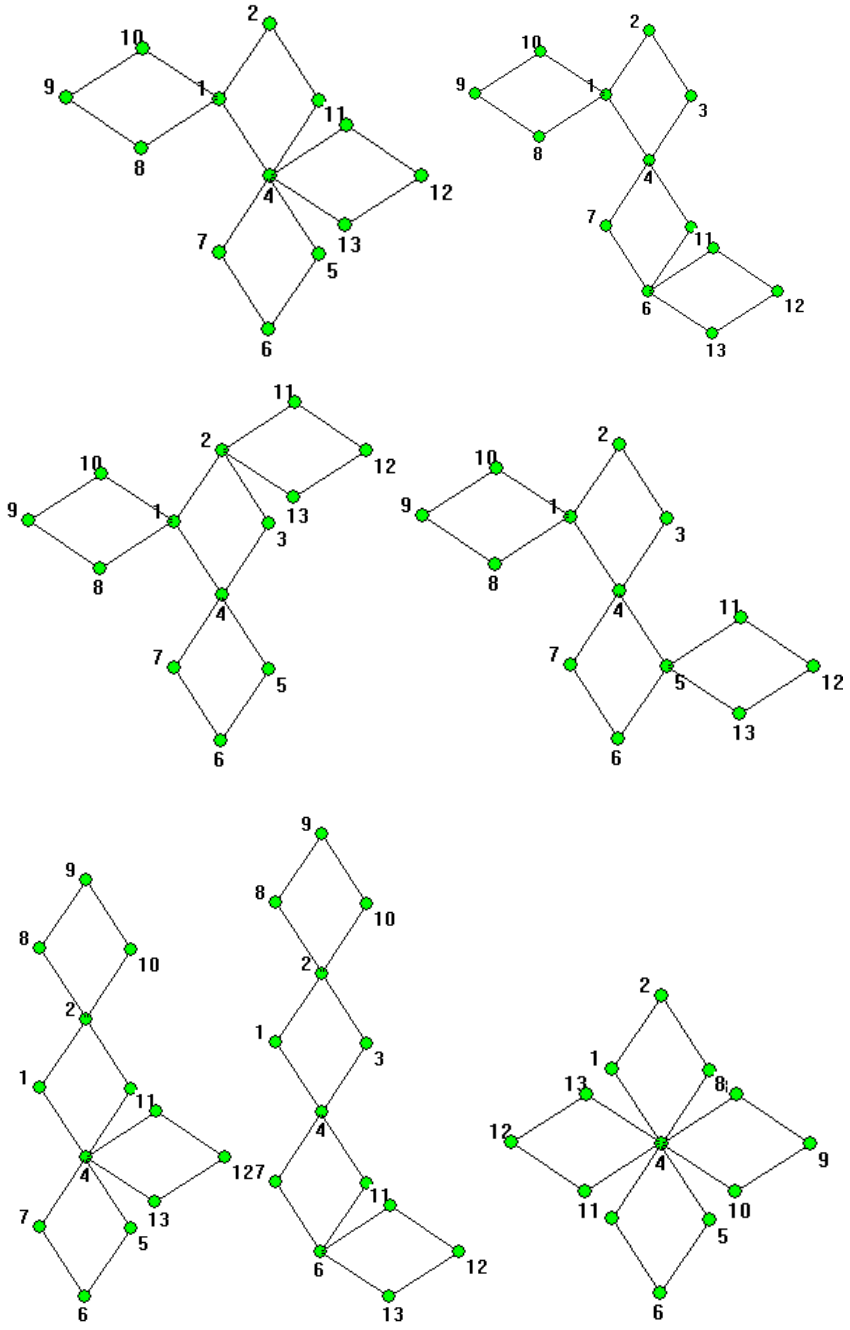

Fig. 5-20 Five fractionated topological graphs of $\{[13, 4]\}_{3L}$

For example, the whole family of 13-link 4-DOF fractionated kinematic chains with two fractionated links can be synthesized

$$\{[13, 4]\}_{3L}=\&(\{[4, 1]\}, \{[4, 1]\}, \{[4, 1]\}, \{[4, 1]\}) \quad (5\text{-}36)$$

yielding the seven fractionated topological graphs, shown in Fig. 5-20.

5.6.4 Synthesis of "*J*" type

In this case, the synthesis equation of *N*-link 4-DOF fractionated kinematic chains is

$$\begin{cases} N_1 + N_2 = N \\ N_1 = 4, 6, 8, 10, \cdots \\ N_2 = 5, 7, 9, 11, \cdots \end{cases} \quad (5\text{-}37)$$

Obviously, an *N*-link 4-DOF fractionated kinematic chain is obtained by connecting an N_1-link 1-DOF kinematic chain with and N_2-link 1-DOF kinematic chain, namely,

$$\{[N, 4]\}_J=\{[N_1, 1]\}\sim\{[N_2, 2]\} \quad (5\text{-}38)$$

For example, the whole family of 11-link 4-DOF fractionated kinematic chains with one fractionated joint can be synthesized by {[4, 1]}~{[7, 2]}and {[6, 1]}~{[5, 2]}. That is

$$\{[11, 4]\}_J=\{[4, 1]\}\sim\{[7, 2]\}\cup\{[6, 1]\}\sim\{[5, 2]\} \quad (5\text{-}39)$$

11 fractionated topological graphs can be synthesized by {[4, 1]}~{[7, 2]}. Five fractionated topological graphs can be synthesized by {[6, 1]}~{[5, 2]}, shown in Fig. 5-21.

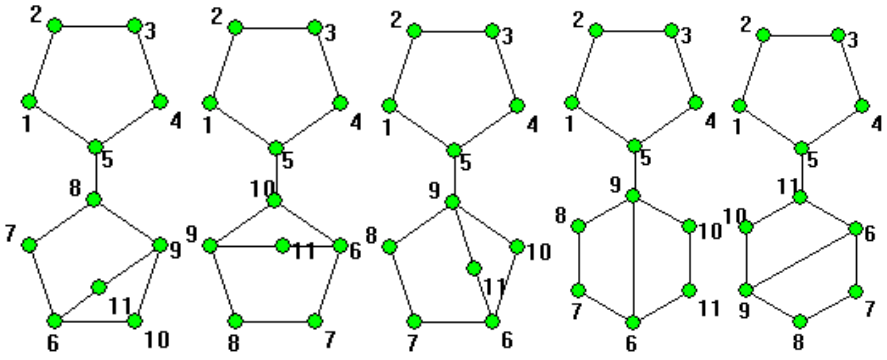

Fig. 5-21 Five fractionated topological graphs by {[6, 1]}~{[5, 2]}

5.6.5 Synthesis of "*L*-*J*" type

In this case, a fractionated kinematic chain contains a fractionated link and a fractionated joint. The synthesis equation of *N*-link 4-DOF fractionated kinematic chains of this type is

$$\begin{cases} N_1 + N_2 + N_3 = N\text{-}1 \\ N_1 \le N_2 \le N_3 \\ N_i = 4,6,8,10,\cdots (i = 1,2,3) \end{cases} \tag{5-40}$$

Obviously, an N-link 4-DOF fractionated kinematic chain of "*L-J*" type can be obtained by connecting three 1-DOF kinematic chains (with N_1, N_2, and N_3 links and suppose $N_1 \le N_2 \le N_3$). That is

$$\{[N, 4]\}_{L\text{-}J} = (\{[N_1, 1]\} * \{[N_2, 1]\} \sim \{[N_3, 1]\}) \cup (\{[N_1, 1]\} * \{[N_3, 1]\} \sim \{[N_2, 1]\})$$

$$\cup (\{[N_2, 1]\} * \{[N_3, 1]\} \sim \{[N_1, 1]\}) \tag{5-41}$$

For example, the whole family of 13-link 4-DOF fractionated kinematic chains of "*L-J*" type can be synthesized by {[4, 1]}*{[4, 1]}~{[6, 1]}and {[4, 1]}*{[6, 1]}~{[4, 1]}. That is

$$\{[13, 4]\}_{L\text{-}J} = (\{[4, 1]\} * \{[4, 1]\} \sim \{[6, 1]\}) \cup (\{[4, 1]\} * \{[6, 1]\} \sim \{[4, 1]\}) \tag{5-42}$$

Thus, 15 fractionated topological graphs can be synthesized by {[4, 1]}*{[4, 1]}~{[6, 1]}, as shown in Fig. 5-22.

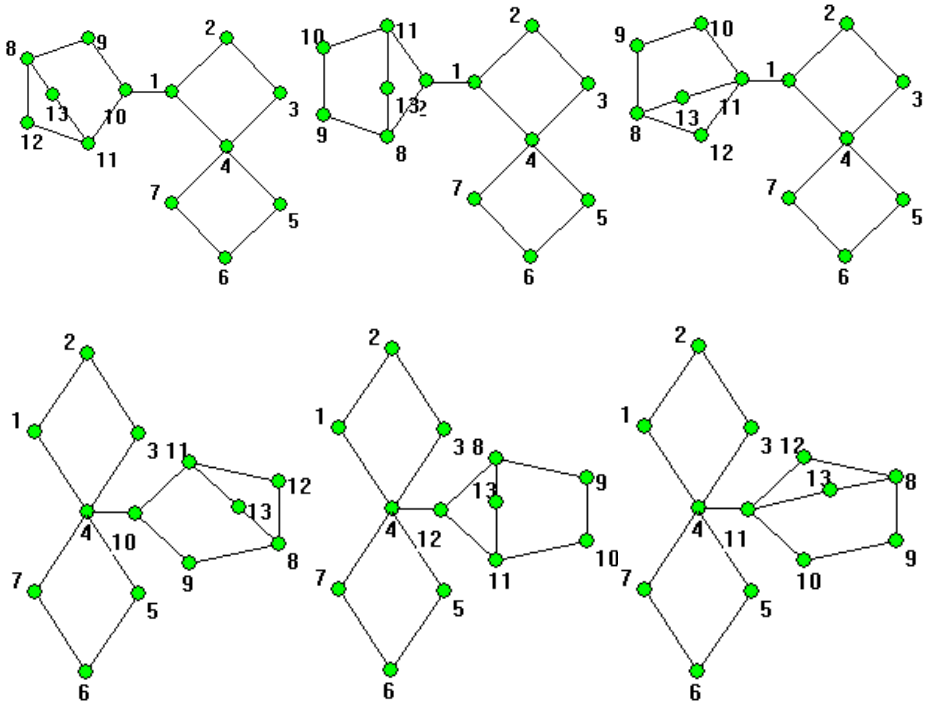

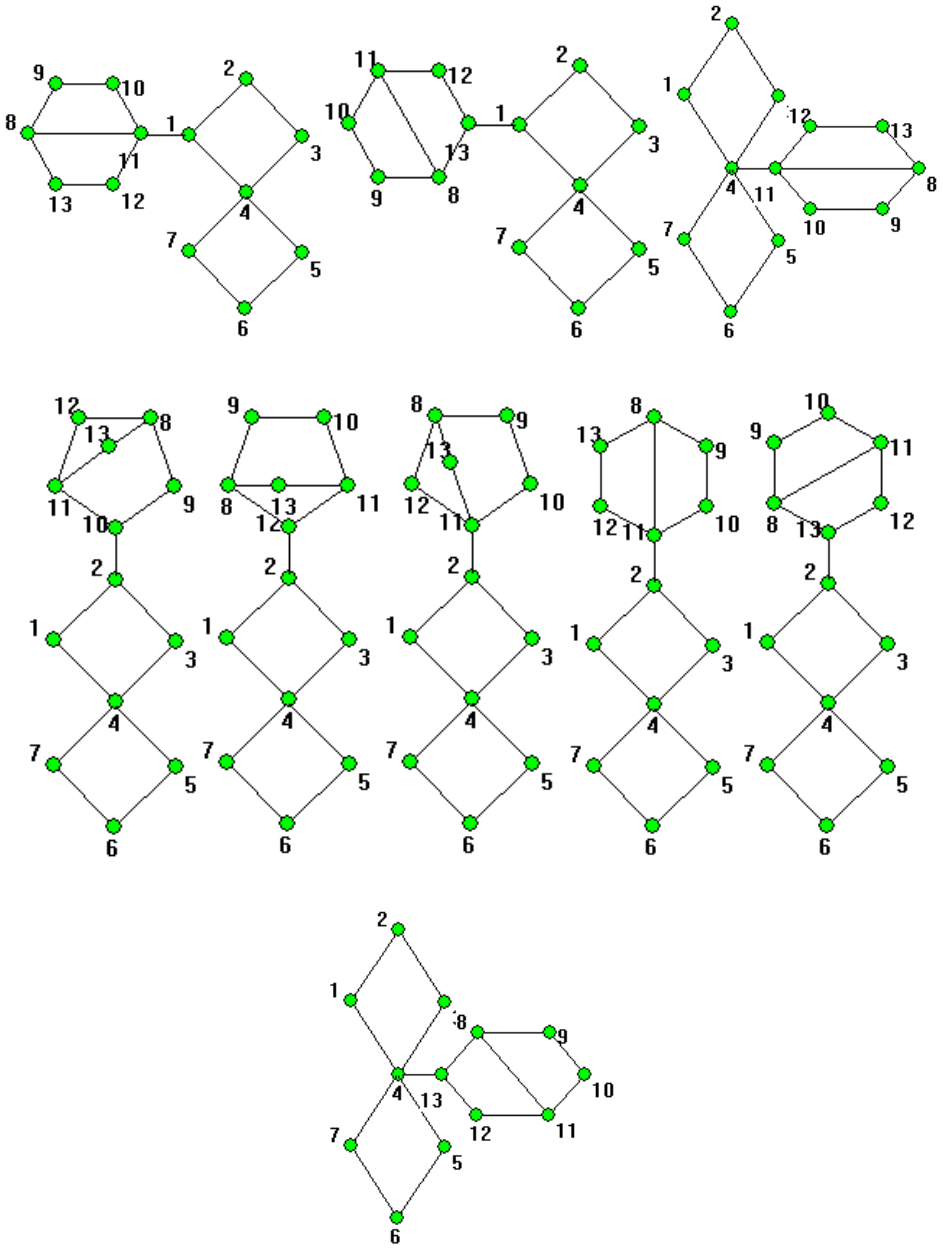

Fig. 5-22 Fifteen fractionated topological graphs by {[4, 1]}*{[4, 1]}~{[6, 1]}

5.6.6 Synthesis of "*J*-*V*" type

In this case, a fractionated kinematic chain contains a fractionated joint and an independent link. The synthesis equation of *N*-link 4-DOF fractionated kinematic chains of this type is

$$\begin{cases} N_1 + N_2 = N - 1 \\ N_1 \le N_2 \\ N_i = 4, 6, 8, 10, \cdots (i = 1, 2) \end{cases} \tag{5-43}$$

Obviously, an N-link 4-DOF fractionated kinematic chain of "*J*-*V*" type can be obtained by connecting two 1-DOF kinematic chains (with N_1 and N_2 links and suppose $N_1 \leq N_2$) through two joints to a link. That is

$$\{[N, 4]\}_{J\text{-}V} = \{[N_1, 1]\} \sim \mathrm{V} \sim \{[N_2, 1]\} \tag{5-44}$$

For example, the whole family of 11-link 4-DOF fractionated kinematic chains of "*J*-*V*" type can be synthesized by {[4, 1]}~V~{[6, 1]}. That is

$$\{[11, 4]\}_{J\text{-}V} = \{[4, 1]\} \sim \mathrm{V} \sim \{[6, 1]\} \tag{5-45}$$

Thus, five fractionated topological graphs can be synthesized by {[4, 1]}~V~{[6, 1]}, shown in Fig. 5-23.

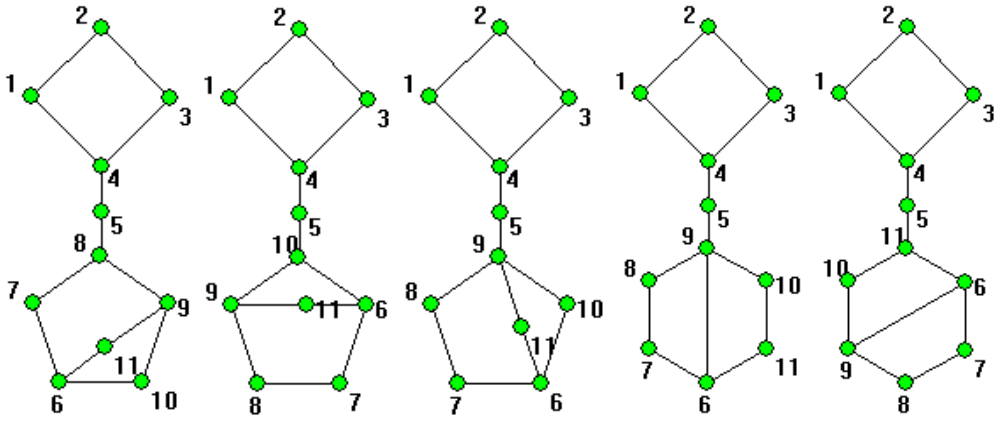

Fig. 5-23 Five fractionated topological graphs by {[4, 1]}~V~{[6, 1]}

5.6.7 Synthesis results of 4-DOF fractionated kinematic chains

Table 5-3 presents the quantitative information concerning the whole family of fractionated 4-DOF kinematic chains up to seven basic loops (column 1) and 19 links (column 2). The fractionation types (FT) are shown in column 3: "*L*" denotes one fractionated link, "*2L*" denotes two fractionated links, "3*L*" denotes three fractionated link, "*J*" denotes one fractionated joint, and "*L*-*J*" denotes a fractionated link and a fractionated joint, and "*J*-*V*" denotes a fractionated joint and an independent link. For each fractionation type, the possible combinations of non-fractionated kinematic chains (non-FKCs) and the synthesized fractionated kinematic chains (FKCs) are shown in columns 4 and 5, respectively. The total number of 1559 planar 13-link 4-DOF fractionated kinematic chains is confirmed by Mruthyunjaya [15] and Martins [127]. The complete sets of planar 4-DOF fractionated kinematic chains of 15, 17 and 19 links are obtained for the first time and the corresponding topological graphs and their numbers are totally new.

Tab. 5-3 Numbers of 4-DOF fractionated kinematic chains and their classification

V	*N*	*FT*	Combination of non-FKCs	No. of FKCs	Total Number
2	9	*L*	{[4,1]}*{[6,3]}	1	4
			{[5,2]}*{[5,2]}	1	
		J	{[4, 1]}~{[5, 2]}	1	
		J-V	{[4, 1]}≈{[4, 1]}	1	
3	11	*L*	{[4,1]}*{[8,3]}	18	63
			{[5,2]}*{[7,2]}	11	
			{[6,1]}*{[6,3]}	5	
		2*L*	&({[4, 1]},{[4, 1]},{[5, 2]})	5	
		J	{[4, 1]}~{[7, 2]}	11	
			{[5, 2]}~{[6, 1]}	5	
		L-J	{[4,1]}*{[4,1]}~{[4, 1]}	3	
		J-V	{[4, 1]}≈{[6, 1]}	5	
4	13	*L*	{[4,1]}*{[10,3]}	517	1559
			{[5,2]}*{[9,2]}	220	
			{[6,1]}*{[8,3]}	90	
			{[6,3]}*{[8,1]}	71	
			{[7,2]}*{[7,2]}	66	
		2*L*	&({[4, 1]},{[4, 1]},{[7, 2]})	63	
			&({[4, 1]},{[5, 2]},{[6, 1]})	44	
		3*L*	&({[4, 1]},{[4, 1]}, {[4, 1]},{[4, 1]})	7	
		J	{[4, 1]}~{[9, 2]}	220	
			{[5, 2]}~{[8, 1]}	71	
			{[6, 1]}~{[7, 2]}	55	
		L-J	{[4,1]}*{[4,1]}~{[6, 1]}	15	
			{[4,1]}*{[6,1]}~{[4, 1]}	34	
		J-V	{[4, 1]}≈{[8, 1]}	71	
			{[6, 1]}≈{[6, 1]}	15	
5	15	*L*	{[4,1]}*{[12,3]}	20737	53334
			{[5,2]}*{[11,2]}	7156	
			{[6,1]}*{[10,3]}	2585	
			{[6,3]}*{[10,1]}	1834	
			{[7,2]}*{[9,2]}	2420	
			{[8,1]}*{[8,3]}	1278	
		2*L*	&({[4, 1]},{[4, 1]},{[9, 2]})	1475	
			&({[4, 1]},{[5, 2]},{[8, 1]})	774	

			&({[4, 1]},{[6, 1]},{[7, 2]})	624	
			&({[6, 1]},{[6, 1]},{[5, 2]})	140	
		3*L*	&({[4, 1]},{[4, 1]},{[4, 1]},{[6, 1]})	126	
		J	{[4, 1]}~{[11, 2]}	7156	
			{[5, 2]}~{[10, 1]}	1834	
			{[6, 1]}~{[9, 2]}	1100	
			{[7, 2]}~{[8, 1]}	781	
		L-J	{[4,1]}*{[4,1]}~{[8, 1]}	213	
			{[4,1]}*{[6,1]}~{[6, 1]}	170	
			{[4,1]}*{[8,1]}~{[4, 1]}	632	
			{[6,1]}*{[6,1]}~{[4, 1]}	110	
		J-V	{[4, 1]}≈{[10, 1]}	1834	
			{[6, 1]}≈{[8, 1]}	355	
6	17	*L*	{[4,1]}*{[14,3]}	1105923	2514094
			{[5,2]}*{[13,2]}	335398	
			{[6,1]}*{[12,3]}	103685	
			{[6,3]}*{[12,1]}	75397	
			{[7,2]}*{[11,2]}	78716	
			{[8,1]}*{[10,3]}	36707	
			{[8,3]}*{[10,1]}	33012	
			{[9,2]}*{[9,2]}	24310	
		2*L*	&({[4, 1]},{[4, 1]},{[11, 2]})	55471	
			&({[4, 1]},{[5, 2]},{[10, 1]})	24390	
			&({[4, 1]},{[6, 1]},{[9, 2]})	15175	
			&({[4, 1]},{[8, 1]},{[7, 2]})	10502	
			&({[6, 1]},{[5, 2]},{[8, 1]})	4509	
			&({[6, 1]},{[6, 1]},{[7, 2]})	1860	
		3*L*	&({[4, 1]},{[4, 1]}, {[4, 1]},{[8, 1]})	2460	
			&({[4, 1]},{[4, 1]}, {[6, 1]},{[6, 1]})	940	
		L-J	{[4,1]}*{[4,1]}~{[10, 1]}	5502	
			{[4,1]}*{[6,1]}~{[8, 1]}	2414	
			{[6,1]}*{[6,1]}~{[6, 1]}	550	
			{[6,1]}*{[8,1]}~{[4, 1]}	3799	
			{[4,1]}*{[10,1]}~{[4, 1]}	20722	
			{[4,1]}*{[8,1]}~{[6, 1]}	3160	
		J	{[4, 1]}~{[13, 2]}	335398	
			{[5, 2]}~{[12, 1]}	75397	
			{[6, 1]}~{[11, 2]}	35780	

			{[7, 2]}~{[10, 1]}	20174	
			{[8, 1]}~{[9, 2]}	15620	
		J-V	{[4, 1]}≈{[12, 1]}	75397	
			{[6, 1]}≈{[10, 1]}	9170	
			{[8, 1]}≈{[8, 1]}	2556	
7	19	*L*	{[4,1]}*{[16,3]}	74393277	154527061
			{[5,2]}*{[15,2]}	20737954	
			{[6,1]}*{[14,3]}	4274510	
			{[6,3]}*{[14,1]}	5529615	
			{[7,2]}*{[13,2]}	3689378	
			{[8,1]}*{[12,3]}	1472327	
			{[8,3]}*{[12,1]}	1357146	
			{[9,2]}*{[11,2]}	1574320	
			{[10,1]}*{[10,3]}	948178	
		2*L*	&({[4, 1]},{[4, 1]},{[13, 2]})	2950613	
			&({[4, 1]},{[5, 2]},{[12, 1]})	1169661	
			&({[4, 1]},{[6, 1]},{[11, 2]})	577794	
			&({[4, 1]},{[7, 2]},{[10, 1]})	319642	
			&({[4, 1]},{[8, 1]},{[9, 2]})	248309	
			&({[6, 1]},{[5, 2]},{[10, 1]})	138456	
			&({[5, 2]},{ [8, 1]},{[8, 1]})	37417	
			&({[6, 1]},{[6, 1]},{[9, 2]})	43665	
			&({[6, 1]},{[7, 2]},{[8, 1]})	59539	
		3*L*	&({[4, 1]},{[4, 1]}, {[4, 1]},{[10, 1]})	85771	
			&({[4, 1]},{[4, 1]}, {[6, 1]},{[8, 1]})	42106	
			&({[4, 1]},{[6, 1]}, {[6, 1]},{[6, 1]})	4615	
		L-J	{[4,1]}*{[4,1]}~{[12, 1]}	226191	
			{[4,1]}*{[6,1]}~{[10, 1]}	62356	
			{[4,1]}*{[8,1]}~{[8, 1]}	44872	
			{[4,1]}*{[10,1]}~{[6, 1]}	103610	
			{[4,1]}*{[12,1]}~{[4, 1]}	1018867	
			{[6,1]}*{[6,1]}~{[8, 1]}	7810	
			{[6,1]}*{[8,1]}~{[6, 1]}	18995	
			{[6,1]}*{[10,1]}~{[4, 1]}	120116	
			{[8, 1]} *{[8,1]}~ {[4,1]}	32305	
		J	{[4, 1]}~{[15, 2]}	20737954	
			{[5, 2]}~{[14, 1]}	4274510	
			{[6, 1]}~{[13, 2]}	1676990	

			{[7, 2]}~{[12, 1]}	829367	
			{[8, 1]}~{[11, 2]}	533636	
			{[9, 2]}~{[10, 1]}	403480	
		J-V	{[4, 1]}≈{[14, 1]}	4274510	
			{[6, 1]}≈{[12, 1]}	376985	
			{[8, 1]}≈{[10, 1]}	130214	

By this way, planar fractionated kinematic chains with more DOFs can also be synthesized.

5.7 Summary

In this chapter, based on the structural synthesis of planar non-fractionated kinematic chains and their atlas database, a fully-automatic approach is proposed to synthesize the whole family of planar fractionated kinematic chains with specified number of links and degrees of freedom. The synthesis equation of planar fractionated kinematic chains is proposed, and for wanted fractionated kinematic chains, all possible combination ways of non-fractionated kinematic chains can be obtained according to the synthesis equation. Isomorphism-free combination algorithms of non-fractionated kinematic chains are proposed. With this algorithm, isomorphism identification, one of the most difficult problems in structural synthesis, is rendered unnecessary in the synthesis of planar fractionated kinematic chains. The whole family of the kinematic structures of planar fractionated planar mechanisms with up to seven basic loops (the mechanisms synthesized so far with other methods contain only four basic loops) is also given, showing the effectiveness of the method.

6 Structural synthesis of multiple joint kinematic chains

6.1 Foreword

Kinematic chains with multiple joints are also widely used in engineering machinery and various robots. This chapter attempts to develop a new structural synthesis method for kinematic chains with multiple joints based on the structural synthesis theory of simple joint kinematic chains and theirs atlas database. First, the relationship between the topological graphs of multiple joint kinematic chains and the topological graphs of simple joint kinematic chains is revealed. Then the structural synthesis method for kinematic chains with multiple joints is proposed, which is derived from the structural synthesis method of simple joint kinematic chains. Examples are given to show how to obtain all multiple joint kinematic chains with specified number of links and multiple joints, and degrees of freedom from the atlas database of corresponding simple joint kinematic chains.

6.2 Relationship of simple and multiple joint kinematic chains

A multiple joint kinematic chain is represented by a bicolor topological graph by using solid vertices which denote links of the chain and hollow vertices which denote multiple joints. So if the difference between solid vertices and hollow vertices is ignored, the bicolor topological graph of a multiple joint kinematic chain is converted into the topological graph of a simple joint kinematic chain, which is defined as the *basic topological graph* of the multiple joint kinematic chain.

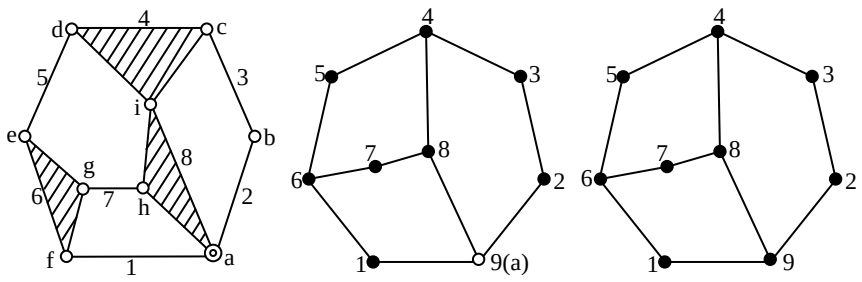

(a) (b) (c)

Fig. 6-1 (a) A multiple joint kinematic chain, (b) its bicolor topological graph, (c) its basic topological graph

For example, Fig. 6-1(a) is a 8-link 1-DOF kinematic chain with one multiple joint and Fig. 6-1(b) is its bicolor topological graph. Fig. 6-1(b) becomes the topological graph of a simple joint kinematic chain if its hollow vertex 9 is converted into a solid vertex, shown in Fig. 6-1(c). Fig. 6-1(c) is the *basic topological graph* for the multiple joint kinematic chain in Fig. 6-1(a).

For a multiple joint kinematic chain with one link grounded, the degrees of freedom (F_{BG}) of its *basic topological graph* are

$$\begin{aligned} F_{BG} &= 3\times(N+J-1)-2\times(M+J) \\ &= [3\times(N-1)-2\times M]+J \\ &= F+J \end{aligned} \tag{6-1}$$

where N is the number of links, M is the number of kinematic pairs, J is the number of multiple joints, and F is the DOFs of the multiple joint kinematic chain.

It can be seen that the DOFs (F_{BG}) of the *basic topological graph* increase by J compared with the DOFs (F) of the multiple joint kinematic chain.

The model of the bicolor topological graph enlightens us on a new synthesis method of the structures of multiple joint kinematic chains: they may be synthesized in batch directly based on the developed structural synthesis theories of the simple joint kinematic chains and their atlas database. For example, in the topological graph of a 9-link 2-DOF simple joint kinematic chain, if a vertex whose degree is greater than or equal to 3 is converted into a hollow vertex, the new bicolor topological graph of an 8-link 1-DOF multiple joint kinematic chain is obtained, and the corresponding multiple joint kinematic chain is synthesized.

Fig. 6-2 (a) is a 10-link kinematic chain with two multiple joints. Its bicolor topological graph and *basic topological graph* are shown in Fig. 6-2 (b) and (c), respectively. Its characteristic perimeter topological graph and the characteristic perimeter topological graph of its *basic topological graph* are shown in Fig. 6-2 (d) and (e), respectively. It is clear that such a 10-link kinematic chain with 2 multiple joints can be synthesized from the topological graphs of a 12-link 3-DOF simple joint kinematic chain.

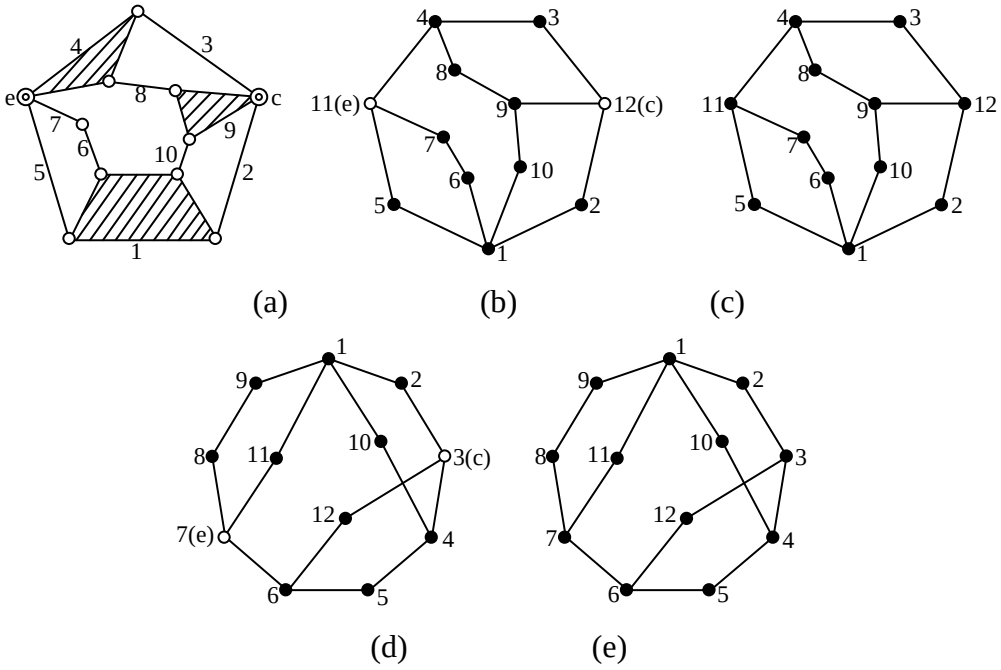

Fig. 6-2 (a) A 10-link multiple joint kinematic chain, (b) its new bicolor topological graph, (c) its basic topological graph, (d) the CPTG of (b), (e) the CPTG of (c)

6.3 Synthesis method

The objective of the new synthesis theory is to generate all multiple joint kinematic chains of specified DOFs and numbers of links and joints from simple joint chains of certain numbers of links and DOFs from the established atlas database, and those simple joint chains from the atlas database are called the *basic chains*.

For example, Fig. 6-3(a) is the characteristic perimeter topological graph of a simple joint kinematic chain from the established atlas database. It is the *basic topological graph* for the synthesis of multiple joint kinematic chains. If one of its vertices is converted into a hollow vertex, it becomes the characteristic perimeter topological graph of a multiple joint kinematic chain [Fig. 6-3(b)]. Fig. 6-3(c) and 6-3 (d) are the new bicolor topological graph and the resulting multiple joint kinematic chain (Here Fig. 6-3(c) is another drawing and labeling ways of the graph Fig. 6-3(b)).

In general, all *N*-vertex, *F*-DOF, and *J* hollow vertice(s) new bicolor topological graphs of multiple joint chains can be synthesized from the topological graphs of (*N*+*J*)-vertex, (*F*+*J*)-DOF simple joint chains if *J* vertice(s) whose degrees are greater than or equal to 3 are converted into hollow vertices. Reversely, all (*N*+*J*)-vertex,

(*F*+*J*)-DOF topological graphs of simple joint chains can be obtained from the new bicolor topological graphs of multiple joint kinematic chains with *N*-vertex, *F*-DOF and *J* hollow vertice(s) if all the hollow vertices are converted into solid vertices. The conversion relationships between the topological graphs of simple joint and multiple joint kinematic chains can be expressed by

$$[N+J, F+J, 0] \rightleftharpoons [N, F, J] \tag{6-2}$$

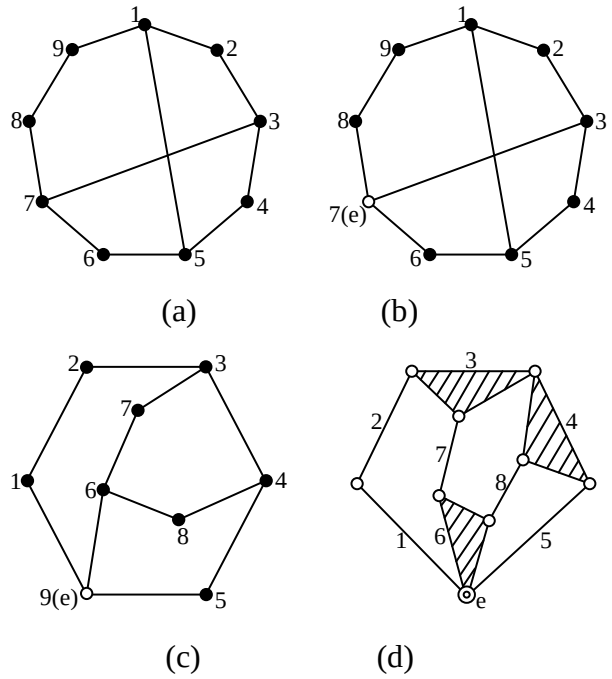

Fig. 6-3 (a) The CPTG of a simple joint kinematic chain, (b) the CPTG of the generated multiple joint chain, (c) the bicolor topological graph of the generated chain, (d) the generated multiple joint kinematic chain

Tab. 6-1 Conversion relationship between the S.J. and M.J. kinematic chains

M.J. kinematic chains			S.J. kinematic chains		
Number of Links (*N*)	DOFs (*F*)	Number of M.J. (*J*)	Number of Links (*N*+*J*)	DOFs (*F*+*J*)	Number of links converted to M.J at a time (*J*)
6	1	1	7	2	1
6	1	2	8	3	2
7	2	1	8	3	1
7	2	2	9	4	2
8	1	1	9	2	1
8	1	3	11	4	3

8	3	1	9	4	1
9	2	1	10	3	1
8	1	2	10	3	2
11	2	1	12	3	1
10	1	2	12	3	2
11	4	1	12	5	1
12	1	1	13	2	1
13	2	1	14	3	1
14	1	1	15	2	1
15	2	1	16	3	1
16	1	1	17	2	1

(S.J.: simple joint; M.J.: multiple joint)

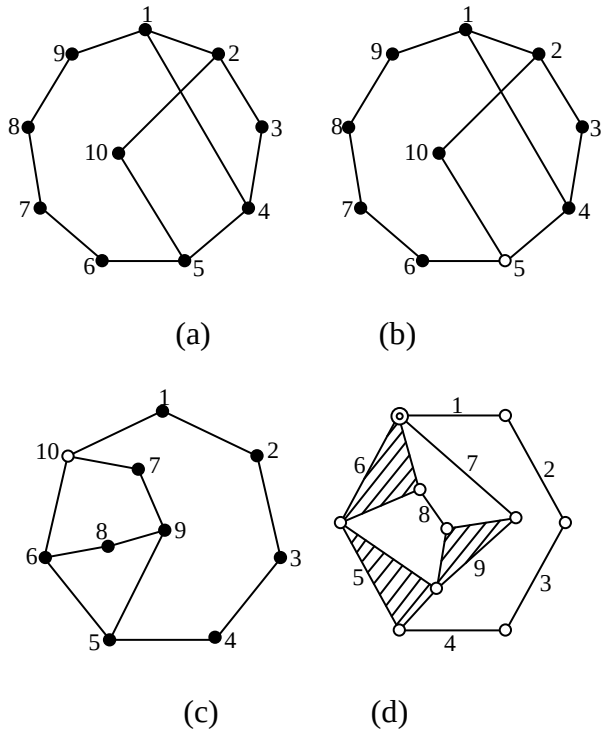

Fig. 6-4 (a) The CPTG of a simple joint chain , (b) the CPTG of the generated multiple joint chain, (c) another form of (b), (d) the generated multiple joint kinematic chain

Some of the conversion relationships are given in Tab.6-1. In the table, all the distinct multiple joint kinematic chains with specified numbers of links(*N*), DOFs(*F*) and multiple joints (*J*) can be generated from their corresponding simple joint chains. For example, all 6-link 1-DOF 1-multiple joint kinematic chains can be generated from all 7-link 2-DOF simple joint kinematic chains when all links whose degrees are

greater than or equal to 3 are converted into multiple joints, one link converted at a time.

Not all the multiple joint kinematic chains synthesized with this method are valid. Sometimes rigid sub-chains come into existence. For example, Fig. 6-4 (a) is the characteristic perimeter topological graph of a simple joint kinematic chain from the atlas database. If vertex 5 is converted into a hollow vertex, it becomes the characteristic perimeter topological graph of a multiple joint kinematic chain [Fig. 6-4 (b)], which can also be drawn in the form of Fig. 6-4 (c). The generated multiple joint kinematic chain is shown in Fig. 6-4 (d). Obviously, there exists a rigid sub-chain. However, rigid sub-chains can be detected easily with the method in literature [115].

6.4 Unique representation and isomorphism identification

The isomorphism identification is also required with this synthesis method. Here the characteristic number string (*CNS*) of bicolor topological graphs is proposed to represent multiple joint kinematic chains uniquely and detect isomorphism in the synthesis process. The steps to obtain the characteristic number string of bicolor topological graphs are as follows.

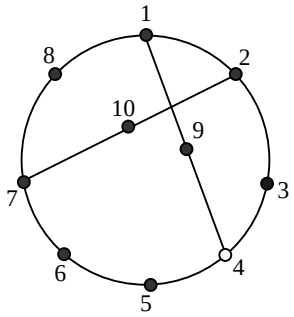

Fig. 6-5 A bicolor topological graph

Step 1: Obtain the perimeter loops of a bicolor topological graph with the start vertex of multiple joint.

In a bicolor topological graph, the loops with the most vertices or edges are defined as its *maximum loops*. For example, the bicolor topological graph in Fig. 6-5 has two maximum loops with the start vertex of four: the first is constituted by vertices 4,9,1,2,10,7,6,5 and the second is by vertices 4,3,2,1,8,7,6,5.

The degree-sequence of a maximum loop is the degree permutation of vertices sequenced one by one from a starting vertex along the loop clockwise or counterclockwise. In Fig. 6-5 the degree-sequence for the first maximum loop is 32332322, and the degree-sequence for the second is also 32332322.

A degree-sequence can be viewed as a number. For a bicolor topological graph, the largest of the degree-sequences of the maximum loops is defined as the *canonical perimeter degree-sequence* and the corresponding loop is defined as the perimeter loop. Obviously, both maximum loops are perimeter loops in Fig. 6-5.

Step 2: Obtain the perimeter graph.

The perimeter graph bicolor topological graph is drawn as follows.

(1) Draw the perimeter loop as the outmost loop in the form of an equilateral polygon.

(2) Put the remaining vertices of the graph inside the perimeter loop.

For example, the two perimeter graphs corresponding to the two perimeter loops in Fig. 6-5 are shown in Fig. 6-6.

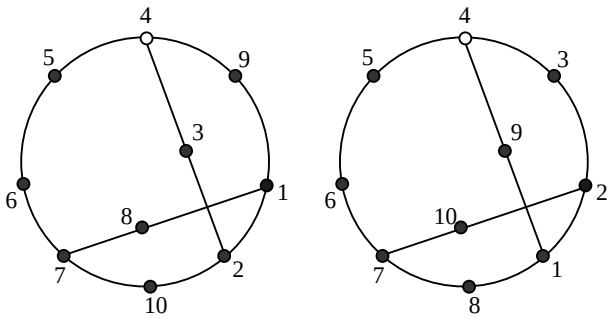

(a) (b)

Fig. 6-6 The two perimeter graphs for Fig. 6-5

Step 3: Obtain the canonical perimeter graphs and canonical adjacency matrices.

Assign natural numbers 1~t in turn to each vertex as its new label on the perimeter loop according to the perimeter degree-sequence. An inner sub-chain can be viewed as a directed path. Here, the starting vertex of the inner sub-chain is assumed to connect with the vertex on the perimeter loop which has the smaller new label. Here, relabel the vertices on inner sub-chains by the following rules in turn.

(1) Relabel the inner sub-chain containing a vertex with the biggest degree first, then the inner sub-chain containing a vertex with the second biggest degree, and so on.

(2) Relabel the inner sub-chain containing the most vertices first, and so on.

(3) Relabel the inner sub-chain whose starting vertex is connected with the vertex on the perimeter loop having the smallest new label first, and so on.

(4) Relabel the inner sub-chain whose end vertex is connected with the vertex on the perimeter loop having the smallest new label first, and so on.

(5) In an inner sub-chain, the relabel sequence is from the starting vertex to the end vertex.

The perimeter graph labeled in the above way is defined as the *canonical perimeter graph*. The corresponding adjacency matrix is defined as the *canonical adjacency matrix*. The canonical perimeter graphs for Figs. 6-6 (a) and (b) are the same, and their shared canonical perimeter graph is shown in Fig. 6-7.

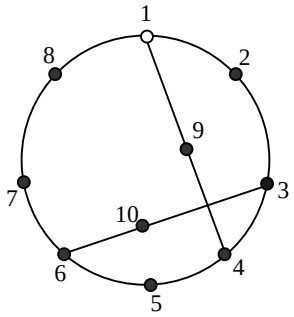

Fig. 6-7 The shared canonical perimeter graph for the two graphs in Fig. 6-6

Step 4: Obtain characteristic number string.

From a bicolor topological graph, the matrix with the largest value of the number string concatenated by the upper-right triangle of the matrix among the canonical adjacency matrices is defined as the *characteristic adjacency matrix (CAM)*, and the corresponding canonical perimeter graph is defined as the *characteristic perimeter graph(CPG).*

Obviously, the characteristic adjacency matrix of a bicolor topological graph is unique. The number string concatenated by the upper-right triangle of the characteristic adjacency matrix is defined as the *characteristic number string* (*CNS*), which is used to identify isomorphism in the synthesis process.

For only one canonical perimeter graph exists for the bicolor topological graph in Fig. 6-5, the canonical perimeter graph is also the characteristic perimeter graph. The characteristic adjacency matrix and characteristic number string of the graph in Fig. 6-5 are

$$CAM = \begin{bmatrix} 3 & 1 & 0 & 0 & 0 & 0 & 0 & 1 & 1 & 0 \\ 1 & 0 & 1 & 0 & 0 & 0 & 0 & 0 & 0 & 0 \\ 0 & 1 & 0 & 1 & 0 & 0 & 0 & 0 & 0 & 1 \\ 0 & 0 & 1 & 0 & 1 & 0 & 0 & 0 & 1 & 0 \\ 0 & 0 & 0 & 1 & 0 & 1 & 0 & 0 & 0 & 0 \\ 0 & 0 & 0 & 0 & 1 & 0 & 1 & 0 & 0 & 1 \\ 0 & 0 & 0 & 0 & 0 & 1 & 0 & 1 & 0 & 0 \\ 1 & 0 & 0 & 0 & 0 & 0 & 1 & 0 & 0 & 0 \\ 1 & 0 & 0 & 1 & 0 & 0 & 0 & 0 & 0 & 0 \\ 0 & 0 & 1 & 0 & 0 & 1 & 0 & 0 & 0 & 0 \end{bmatrix}$$

CNS = 3100000110 010000000 01000001 0100010 010000 01001 0100 000 00 0

Two bicolor topological graphs of 13-link multiple joint kinematic chains are shown in Fig. 6-8. They have the same characteristic number string, shown as follows. So they are isomorphic. Their shared characteristic perimeter graph is shown in Fig. 6-8 (c).

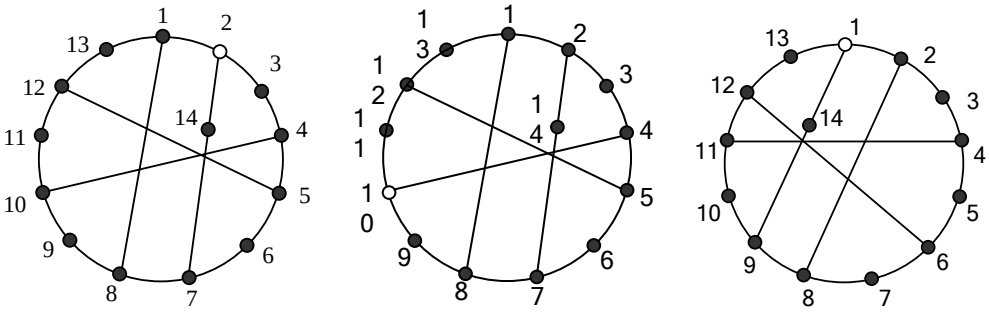

(a) (b) (c)

Fig. 6-8 (a) A bicolor topological graph, (b) another bicolor topological graph, (c) their shared characteristic perimeter graph

CNS (a,b)= 31000000000011 0100001000000 010000000000 01000001000 0100000000 010000100 01000000 0100000 010001 01000 0100 010 00 0

6.5 Synthesis process

Based on the conversion relationship between simple joint and multiple joint kinematic chains, all *N*-link, *F*-DOF chains of *J* multiple joint(s) can be synthesized from the atlas database of (*N*+*J*)-link, (*F*+*J*)-DOF simple joint chains as follows:

Phase 1: All (*N*+*J*-1)-link, (*F*+*J*-1)-DOF chains of 1 multiple joint are synthesized from the atlas database of (*N*+*J*)-link, (*F*+*J*)-DOF simple joint chains (with 0 multiple joint), namely,

$$[N+J,\ F+J,\ 0] \Rightarrow [N+J\text{-}1,\ F+J\text{-}1,\ 1] \tag{6-3}$$

Phase 2: All (*N*+*J*-2)-link, (*F*+*J*-2)-DOF chains of 2 multiple joints are synthesized from the atlas database of (*N*+*J*-1)-link, (*F*+*J*-1)-DOF chains with 1 multiple joint, namely,

$$[N+J\text{-}1,\ F+J\text{-}1,\ 1] \Rightarrow [N+J\text{-}2,\ F+J\text{-}2,\ 2] \tag{6-4}$$

……

Phase *J*: All *N*-link, *F*-DOF multiple joint chains of *J* multiple joint(s) are synthesized from the atlas database of (*N*+1)-link, (*F*+1)-DOF chains with (*J*-1) multiple joint(s), namely,

$$[N+1, F+1, J-1] \Rightarrow [N, F, J] \tag{6-5}$$

Hence all required N-link, F-DOF chains of J multiple joint(s) are synthesized.

The synthesis steps involved in each phase are similar, so here only those in the first phase are given in detail as an illustration.

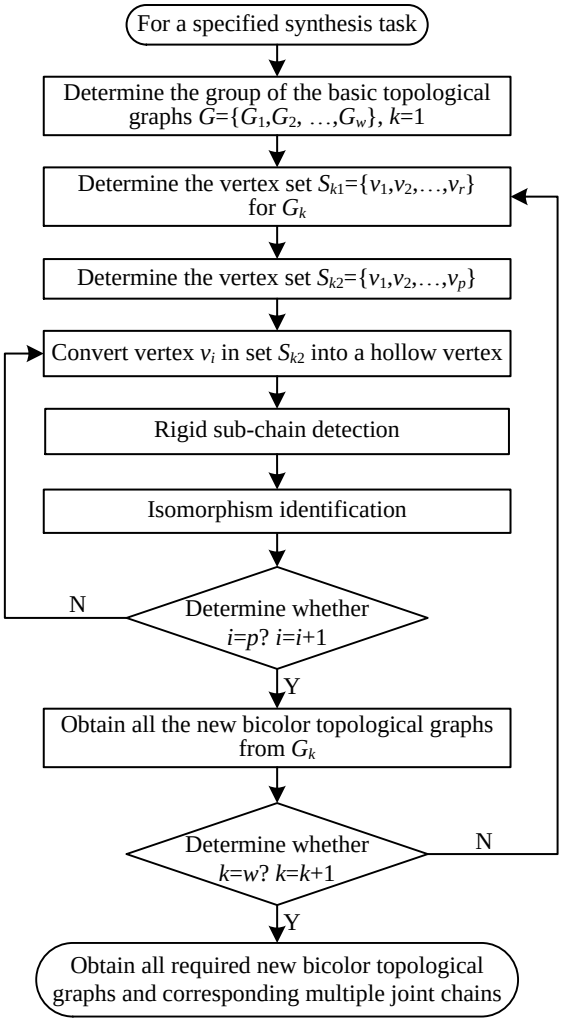

Fig. 6-9 The synthesis flowchart with the unified structural synthesis mothod

Step 1: Determine the *basic topological graph* group, $G=\{G_1,G_2,\ldots,G_w\}$, of the simple joint kinematic chains according to the specified task and $[N+J, F+J, 0] \Rightarrow [N+J-1, F+J-1, 1]$. Suppose $k=1$.

Step 2: Get all the vertices in graph G_k from group G whose degrees are greater than or equal to 3 into the vertex set $S_{k1}=\{v_1,v_2,\ldots,v_r\}$.

Step 3: Determine the vertex set $S_{k2}=\{v_1,v_2,\ldots,v_p\}$ by deleting from set S_{k1} all solid vertices in the loops whose sub-dimensions (i.e. the number of solid vertices the loop contains) are 4.

Step 4: Convert vertex v_i in S_{k2} into a hollow vertex.

Step 5: Detect rigid sub-chains in the obtained new bicolor topological graph. If there are no rigid sub-chains, store the graph; otherwise delete it.

Step 6: Obtain the characteristic number string of the new bicolor topological graph and use it to detect isomorphism. If it is the same with any of the former ones, delete it; otherwise store the graph.

Step 7: Determine whether $i=p$. If $i=p$, then all the new bicolor topological graphs from the graph G_k are obtained; go to step 8. Otherwise $i=i+1$, and return to step 4.

Step 8: Determine whether $k=w$. If $k=w$, then all the new bicolor topological graphs derivable from group G are obtained; end the phase. Otherwise $k=k+1$, and return to step 2.

The synthesis flowchart of kinematic chains with one multiple joint is shown in Fig. 6-9. If chains of n multiple joints are to be synthesized, take the new bicolor topological graphs of the synthesized (n-1) multiple joint chains as the *basic topological graph* group, and repeat the synthesis steps 1~8.

These procedures followed, all the multiple joint kinematic chains with certain specifications can be synthesized in batch.

For example, the synthesis of all 8-link, 1-DOF kinematic chains with one multiple joint can be generated from the atlas database of 9-link, 2-DOF simple joint kinematic chains, that is

$$[9,\ 2,\ 0] \Rightarrow [8,\ 1,\ 1]$$

Altogether 22 distinct topological graphs of 8-link, 1-DOF kinematic chains with one multiple joint are generated, shown in Fig. 6-10, and the corresponding 22 multiple joint kinematic chains are shown in Fig. 6-11.

Another example, the synthesis of all 8-link 1-DOF kinematic chains with 2 multiple joints can be generated from the atlas database of 10-link, 3-DOF simple joint kinematic chains. Two synthesis phases are involved: first, all 9-link, 2-DOF chains of one multiple joint are synthesized from the atlas database of 10-link, 3-DOF simple joint chains (with zero multiple joint), namely,

$$[10,\ 3,\ 0] \Rightarrow [9,\ 2,\ 1]$$

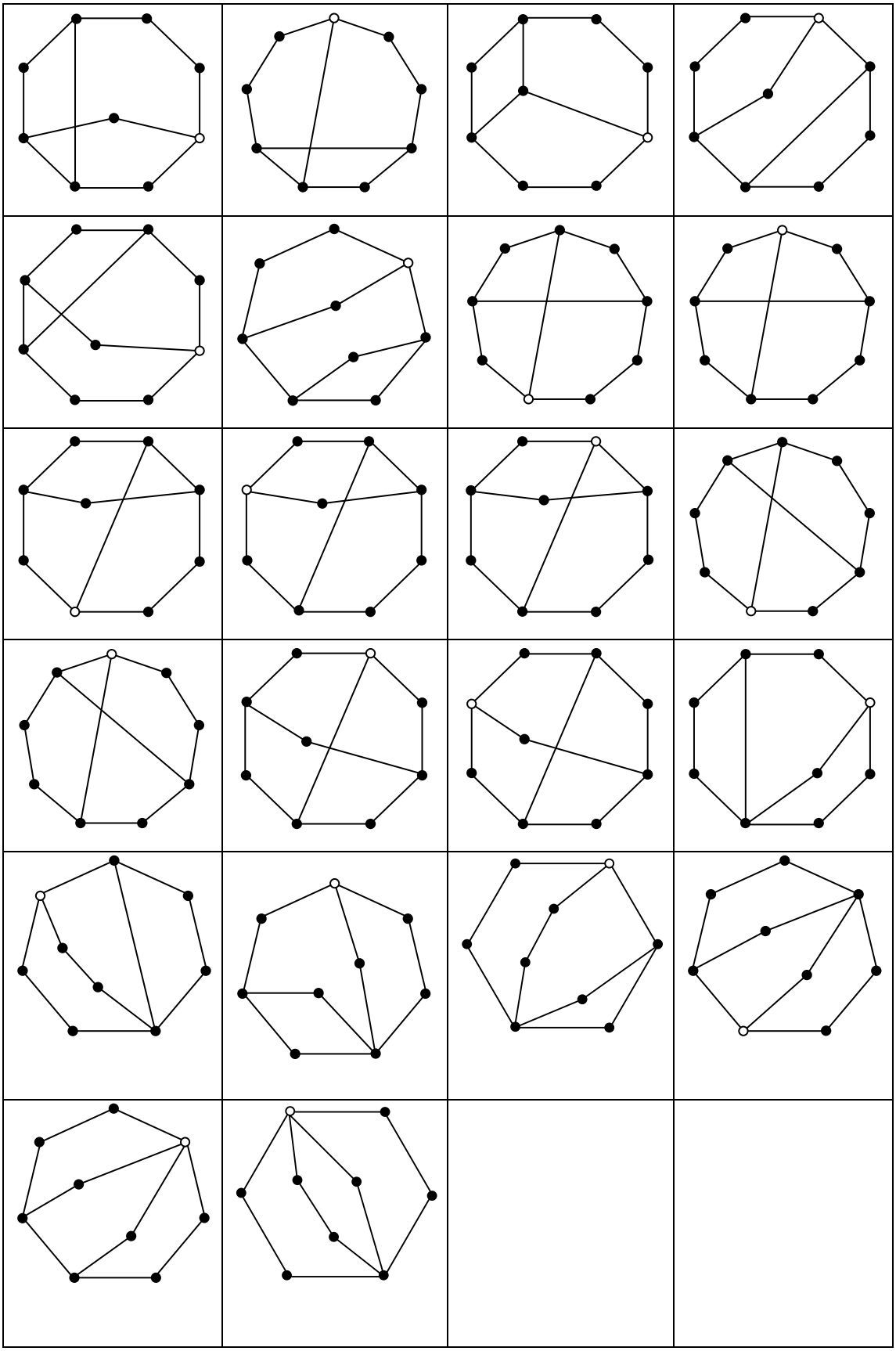

Fig. 6-10 All *CPGs* of 8-link, 1-DOF chains with one multiple joint

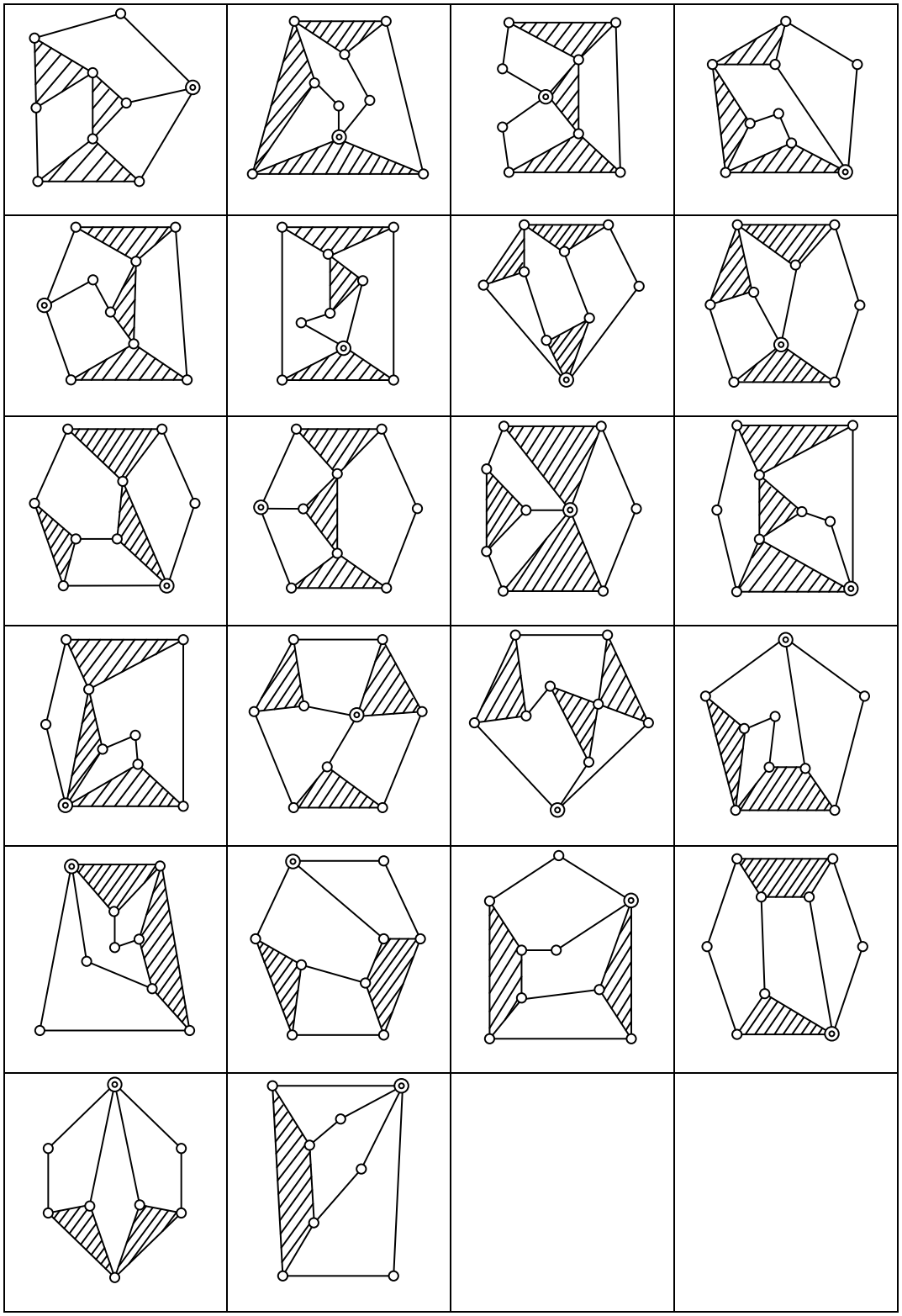

Fig. 6-11　22 8-link, 1-DOF kinematic chains with one multiple joint

Second, all 8-link, 1-DOF chains of two multiple joints are synthesized from the atlas database of 9-link, 2-DOF chains with one multiple joint, namely,

$$[9,\ 2,\ 1] \Rightarrow [8,\ 1,\ 2]$$

Altogether 18 multiple joint kinematic chains are synthesized, shown in Fig. 6-12.

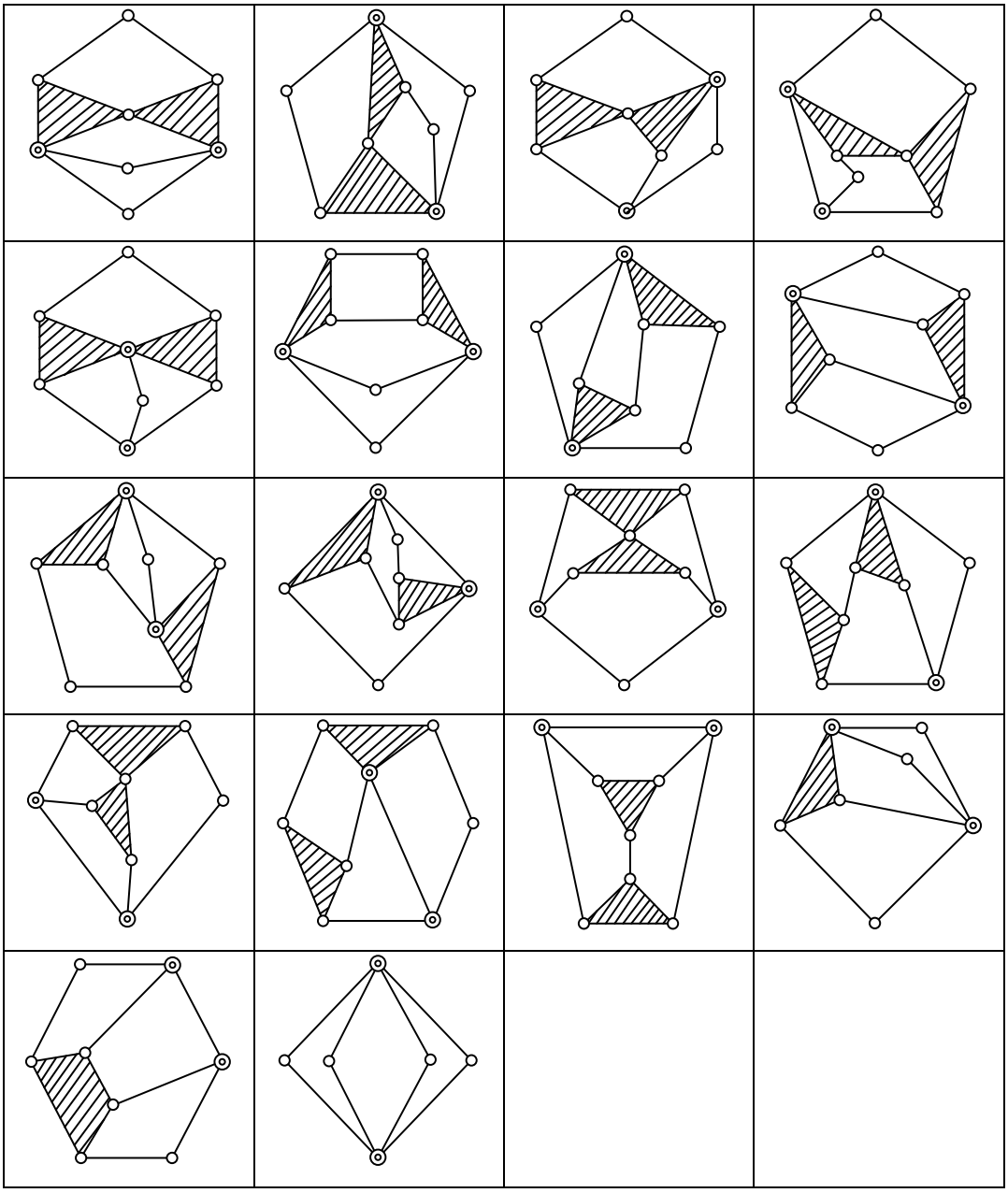

Fig. 6-12 18 8-link, 1-DOF kinematic chains with 2 multiple joints

6.6 Automatic synthesis and classified atlas databases

If the number of links, degrees of freedom, and the number of multiple joints are specified, the whole family of multiple joint kinematic chains can be synthesized in batch from the topological graphs of the corresponding simple joint kinematic chains. As we have developed automatic structural synthesis for simple joint kinematic chains

and established their classified atlas databases, the automatic synthesis of multiple joint kinematic chains is much more easily to carry out.

Based on the above method, a synthesis program has been developed to synthesize multiple joint kinematic chains from the atlas databases of planar non-fractionated kinematic chains. For example, there are 25 topological graphs corresponding to the link assortment of "[7,2,1]" in the atlas database of 10-link 3-DOF simple joint kinematic chains. Altogether 24 9-link 2-DOF kinematic chains with one multiple joint can be synthesized from the 25 topological graphs, shown in Fig. 6-13.

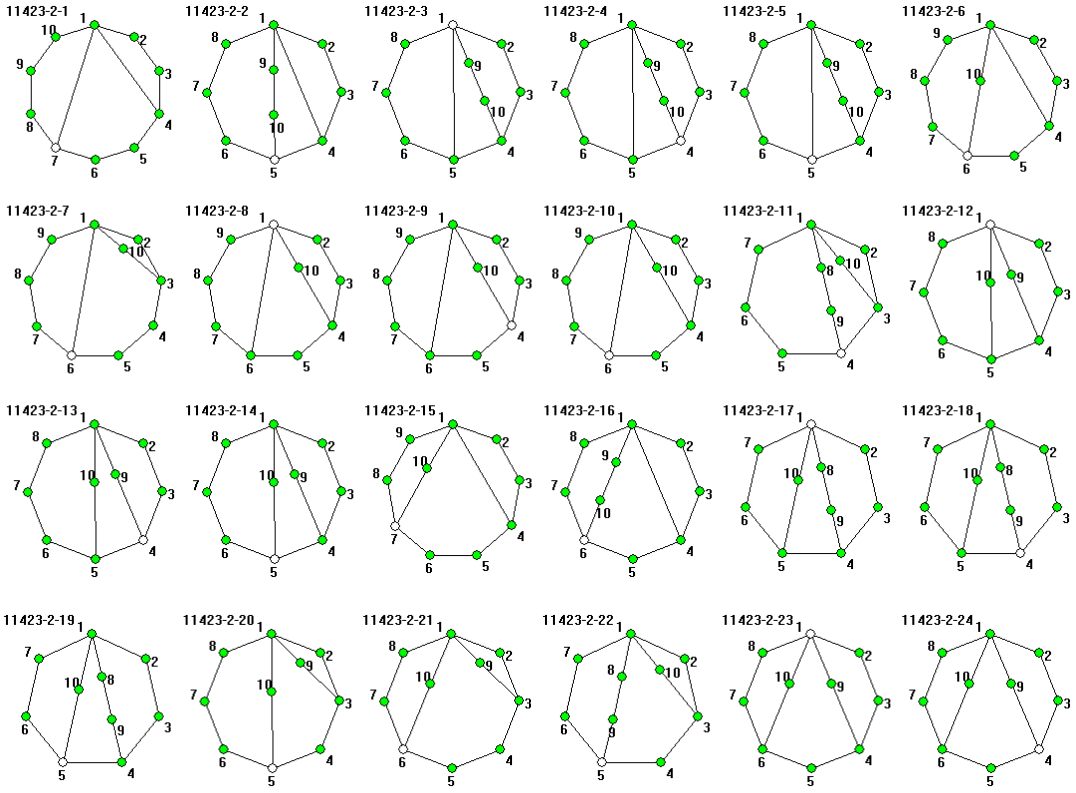

Fig. 6-13 24 multiple joint kinematic chains synthesized from "[7,2,1]"

In the atlas database of 14-link 3-DOF simple joint kinematic chains, there are 5658 topological graphs corresponding to the link assortment of "[6,8,0,0,0]". From these topological graphs, altogether 21004 13-link 2-DOF kinematic chains with one multiple joint can be synthesized. The former 24 bicolor topological graphs of the generated multiple joint kinematic chains are shown in Fig. 6-14.

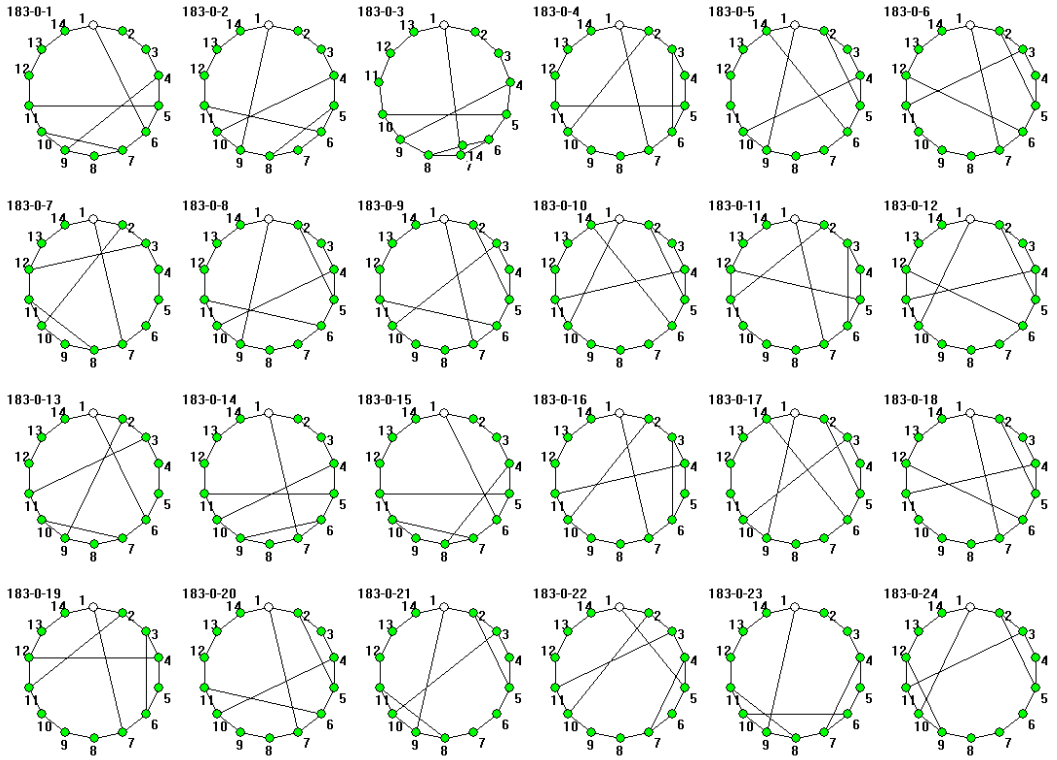

Fig. 6-14 Excerpt of 21004 multiple joint kinematic chains from "[6,8,0,0,0]"

At present, multiple joint kinematic chains with no more than 10 links were synthesized and reported by other methods [15, 57, 128]. However, the whole family of multiple joint kinematic chains with up to 16 links can be synthesized by the method.

Table 6-2 presents the quantitative information concerning the bicolor topological graphs for 9-link 2-DOF kinematic chains with one multiple joint. The total number of the bicolor topological graphs is 79. All the bicolor topological graphs are classified according to their link assortment (column 2). For each link assortment, the numbers of the multiple edges of the bicolor topological graphs are used to further classify bicolor topological graphs (see columns 3 and 4). The total numbers of bicolor topological graphs corresponding to link assortment are shown in column 5.

Tables 6-3, 6-4, 6-5 and 6-6 display the quantitative information for the atlas databases of 1-DOF one multiple joint kinematic chains of 8, 10, 12 and 14 links, respectively. The total numbers of the topological graphs are 22, 763, 38880, and 2580435, respectively.

The total quantitative information for the atlas databases of one multiple joint kinematic chains with up to 16 links is given in Tab. 6-7. The multiple joint kinematic chains with more than 10 links are synthesized here for the first time.

Tab. 6-2 Numbers of 9-link 2-DOF kinematic chains with one multiple joint

No.	Link assortment	No. of Multi-edges	No. of multiple joint kinematic chains	Total number
1	[6,4,0]	0	38	53
		2	15	
2	[7,2,1]	2	24	24
3	[8,0,2]	3	2	2

Tab. 6-3 Numbers of 8-link 1-DOF kinematic chains with one multiple joint

No.	Link assortment	No. of Multi-edges	No. of multiple joint kinematic chains	Total number
1	[5,4,0]	0	13	15
		2	2	
2	[6,2,1]	2	6	6
3	[7,0,2]	3	1	1

Tab. 6-4 Numbers of 10-link 1-DOF kinematic chains with one multiple joint

No.	Link assortment	No. of Multi-edges	No. of multiple joint kinematic chains	Total number
1	[5,6,0,0]	0	214	252
		1	33	
		2	5	
2	[6,4,1,0]	0	181	371
		1	162	
		2	28	
3	[7,2,2,0]	1	70	98
		2	20	
		3	8	
4	[8,0,3,0]	3	2	2
5	[7,3,0,1]	2	28	28
6	[8,1,1,1]	3	11	11
7	[9,0,0,2]	4	1	1

Tab. 6-5 Numbers of 12-link 1-DOF kinematic chains with one multiple joint

No.	Link assortment	No. of Multi-edges	No. of multiple joint kinematic chains	Total number
1	[5,8,0,0,0]	0	4102	4597

		1	472	
		2	23	
2	[6,6,1,0,0]	0	10954	15502
		1	4200	
		2	342	
		3	6	
3	[7,4,2,0,0]	0	5171	11529
		1	5131	
		2	1172	
		3	55	
4	[8,2,3,0,0]	0	404	1890
		1	753	
		2	665	
		3	68	
5	[9,0,4,0,0]	2	32	34
		3	2	
6	[7,5,0,1,0]	0	604	2509
		1	1599	
		2	284	
		3	22	
7	[8,3,1,1,0]	1	1327	2237
		2	730	
		3	180	
8	[9,1,2,1,0]	2	146	235
		3	81	
		4	8	
9	[9,2,0,2,0]	2	70	104
		3	26	
		4	8	
10	[A,0,1,2,0]	4	4	4
11	[8,4,0,0,1]	2	111	135
		3	24	
12	[9,2,1,0,1]	3	86	86
13	[A,0,2,0,1]	4	6	6
14	[A,1,0,1,1]	4	11	11
15	[B,0,0,0,2]	5	1	1

(In link assortment array, A=10, B=11, C=12, etc.)

Tab. 6-6 Numbers of 14-link 1-DOF kinematic chains with one multiple joint

No.	Link assortment	No. of Multi-edges	No. of multiple joint kinematic chains	Total number
1	[5,A,0,0,0,0]	0	81880	89374
		1	7296	
		2	198	
2	[6,8,1,0,0,0]	0	444316	550376
		1	100638	
		2	5360	
		3	62	
3	[7,6,2,0,0,0]	0	555489	861015
		1	270848	
		2	33760	
		3	918	
4	[8,4,3,0,0,0]	0	178263	400409
		1	171006	
		2	47857	
		3	3275	
		4	8	
5	[9,2,4,0,0,0]	0	11791	46832
		1	20065	
		2	12828	
		3	2075	
		4	73	
6	[A,0,5,0,0,0]	0	155	622
		2	372	
		3	81	
		4	14	
7	[7,7,0,1,0,0]	0	76990	145096
		1	61621	
		2	6218	
		3	267	
8	[8,5,1,1,0,0]	0	92415	288594
		1	151315	
		2	41469	
		3	3373	
		4	22	

9	[9,3,2,1,0,0]	0	15070	115687
		1	56208	
		2	36876	
		3	7299	
		4	234	
10	[A,1,3,1,0,0]	1	2519	7768
		2	3033	
		3	2046	
		4	170	
11	[9,4,0,2,0,0]	0	1187	18908
		1	8805	
		2	7398	
		3	1443	
		4	75	
12	[A,2,1,2,0,0]	1	1353	7827
		2	3946	
		3	2212	
		4	316	
13	[B,0,2,2,0,0]	3	192	228
		4	28	
		5	8	
14	[B,1,0,3,0,0]	3	58	99
		4	41	
15	[8,6,0,0,1,0]	0	2035	16537
		1	10012	
		2	4217	
		3	273	
16	[9,4,1,0,1,0]	1	8756	21505
		2	10607	
		3	2044	
		4	98	
17	[A,2,2,0,1,0]	2	3152	4845
		3	1368	
		4	325	
18	[B,0,3,0,1,0]	3	54	95
		4	41	
19	[A,3,0,1,1,0]	2	1442	2524

		3	922	
		4	160	
20	[B,1,1,1,1,0]	3	278	479
		4	185	
		5	16	
21	[C,0,0,2,1,0]	5	4	4
22	[B,2,0,0,2,0]	3	70	104
		4	26	
		5	8	
23	[C,0,1,0,2,0]	5	4	4
24	[9,5,0,0,0,1]	2	436	671
		3	235	
25	[A,3,1,0,0,1]	3	569	631
		4	62	
26	[B,1,2,0,0,1]	4	92	92
27	[B,2,0,1,0,1]	4	86	86
28	[C,0,1,1,0,1]	5	11	11
29	[C,1,0,0,1,1]	5	11	11
30	[D,0,0,0,0,2]	6	1	1

(In link assortment array, A=10, B=11, C=12, etc.)

Tab. 6-7 Numbers of kinematic chains with one multiple joint and all possible DOFs

Number of links	DOFs	No. of multiple joint kinematic chains
6	1	1
7	2	3
8	1	22
	3	4
9	2	79
	4	6
10	1	763
	3	189
	5	8
11	2	3258
	4	374
	6	10
12	1	38880

	3	9595
	5	664
	7	12
13	2	182628
	4	23270
	6	1087
	8	15
14	1	2580435
	3	604965
	5	49820
	7	1685
	9	17
15	2	12935612
	4	1662457
	6	97603
	8	2501
	10	20
16	3	46268464
	5	4037727
	7	178768
	9	3584
	11	23

6.7 Summary

In this chapter, based on the structural synthesis theory of simple joint kinematic chains and their atlas database, a new structural synthesis method of multiple joint kinematic chains is proposed. The inter-conversion of the bicolor topological graphs of multiple joint kinematic chains and the topological graphs of simple joint kinematic chains is analysed. All multiple joint kinematic chains with specified numbers of links and degrees of freedom can be synthesized from the atlas database of corresponding simple joint kinematic chains. The whole family of multiple joint kinematic chains with up to 16 links is obtained for the first time, far more than other methods applicable only to multiple joint kinematic chains with no more than 10 links.

7 Conceptual creative design of mechanisms

7.1 Foreword

The first phase in the design of a product is the conceptual design in which the designer explores as many and diverse design concepts as possible. Traditionally it was accomplished on the designer's intuition, ingenuity and experience. Later, some systematic methods were proposed to generate feasible mechanisms for a given design task [5,129,130]. However, the mechanisms generated with these methods are relatively simple in terms of the structures. In this chapter, based on the established classified atlas databases of planar kinematic chains with simple and multiple joints, a systematic method is proposed to generate all feasible mechanisms for both simple and complex mechanisms. More complex mechanisms are created in this way, such as 2-DOF main mechanisms for road tractors, 3-DOF hydraulic robots and 6-DOF forging manipulators, provided as examples to demonstrate the effectiveness of the method.

7.2 Design procedure

As we have known, design is the creation of synthesized solutions in the form of products or systems that satisfy customer's requirements [5]. In mechanical design the conceptual creative design can be regarded as the mapping of the customer's requirements into one or several mechanisms. When a specified design task is given, the designer tries to make the best of his knowledge and the information available to transform the design task into detailed design specifications, such as knowledge of the existing mechanisms, relative mechanisms, or some preliminary ideas if no relative mechanisms are available. Design specifications are usually of three coherent categories, namely functional requirements, structural characteristics and design constraints [129,130]. The main goal is to transform as many of the design specifications of these three categories as possible into the selection constraints. Once the selection constraints are given, search automatically all possible mechanisms in the established classified atlas databases. The designer may have to search several times until all selection constraints are considered and all possible mechanisms are obtained. Then the obtained mechanisms are evaluated against the remaining design specifications, those that cannot meet these requirements are ruled out, and the rest constitutes a complete set of the feasible mechanisms for this design task. Hence the creative design of mechanisms is fulfilled with a systematic method, which is based strictly on the structural synthesis and classified atlas databases of simple and multiple joint kinematic chains. The main steps of the creative design method can be outlined as [5]:

Step 1: Identify design specifications according to the customer's requirements.

Step 2: Determine structural characteristics that meet the design specifications based on existing mechanisms, relative mechanisms, or preliminary ideas.

Structural characteristics usually include the number of links, degrees of freedom (DOF), the nature of motion (i.e. planar, spherical or spatial mechanism), the fractionated types (link-fractionated, joint-fractionated, etc.), the number of basic loops and the admissible types of joints, and so on.

Step 3: Determine functional requirements that meet the design specifications based on existing or relative mechanisms or preliminary ideas.

Functional requirements are defined as "the general input/output relationship of a mechanism whose purpose is to perform a task" [131] and the "Motion requirements of a set of functioning links, such as the ground, input and output links" [130].

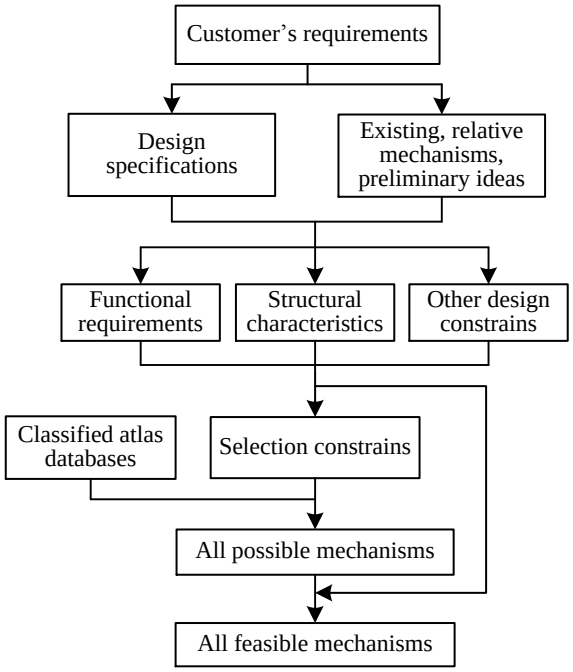

Fig. 7-1 The procedure of the creative design based on classified atlas databases

Step 4: Determine other design constraints that meet the design specifications based on existing or relative mechanisms or preliminary ideas.

Design specifications based on particular engineering reasoning and imposing restrictions on the mechanism are considered as other design constraints.

Step 5: Choose those structural characteristics, functional requirements and design constraints which can be represented in mathematical forms to formulate the selection constraints.

Step 6: Search automatically all possible mechanisms that safisfy the selection constraints in the classified atlas databases.

Step 7: Evaluate all the obtained mechanisms against the remaining structural characteristics, functional requirements and other design constraints, and rule out those invalid.

After accomplishing these steps, all feasible mechanisms for a certain design task are obtained hence.

A flowchart for the creative design with this method is shown in Fig. 7-1.

7.3 Creative design of 2-DOF mechanisms for road tractors

Consider the road tractor shown in Fig. 1-1(a) [13]. Its main mechanism is a 2-DOF link-fractionated mechanism with 11 links. One can get all feasible mechanisms for this type of road tractor with the above method.

The structural characteristics for the main mechanism are shown in Tab.7-1, where the fractionated type is specified as SC1, the number of links as SC2 , the degrees of freedom as SC3, the nature of motion as SC4, the admissible types of joints as SC5 and the number of basic loops as SC6 .

Tab. 7-1 Structural characteristics of the main mechanism for Fig. 1-1(a)

No.	Structural characteristics
SC1	The mechanism is link-fractionated.
SC2	The number of links is 11.
SC3	The mechanism has two DOFs.
SC4	The mechanism is confined to planar nature of motion, namely *d* equals three.
SC5	The type of joints is limited to revolute joints and prismatic joints only.
SC6	There are four basic loops.

The functional requirements for the main mechanism are shown in Tab.7-2. The assortments of the frame and the output links are specified as FR1 and FR2. The relationships of the output link and the fractionated link are specified as FR3 and FR4.

Tab. 7-2 Functional requirements for the main mechanism for Fig. 1-1(a)

No.	Functional requirements
FR 1	The frame link is a multiple-pair link.
FR 2	The output link is a binary link.
FR 3	The output link is connected with the fractionated link.
FR 4	The fractionated link is connected with the frame link.

Binary vertices in a topological graph may be connected in series to form a binary path. The first and last vertices of a binary path are necessarily connected to nonbinary vertices. The number of binary vertices in a binary path is defined as the length of the binary path. Binary path of length 0, 1, 2 and 3 are called the *E, Z, D* and *V* path, respectively.

The other design constraints for the main mechanism are shown in Tab.7-3. The mechanism is driven by two hydraulic cylinders, so there are two *D*-paths in the tological graph of the mechanism, specified as OC1. Each fractionated part has at least one DOF, so

each part has a prismatic joint, specified as OC2. Obviously, the output link and the frame link cannot be placed at the same fractionated part, specified as OC3.

Tab. 7-3 Other design constraints for the main mechanism for Fig. 1-1(a)

No.	Other design constraints
OC 1	There are two *D*-paths.
OC 2	Each fractionated part has one hydraulic cylinder (prismatic joint).
OC 3	The output link and the frame link cannot be placed at the same fractionated part.
OC 4	There are no useless (redundant) sub-structures.

The selection constraints are constituted by SC1~SC4, SC6, FR1~ FR4 and OC1~OC2. According to SC1, SC2, SC3, SC4 and SC6, all the required kinematic structures can be obtained from the atlas database of 11-link 2-DOF fractionated kinematic chains with the combination of two 6-link 1-DOF kinematic chains, shown in Fig. 7-2.

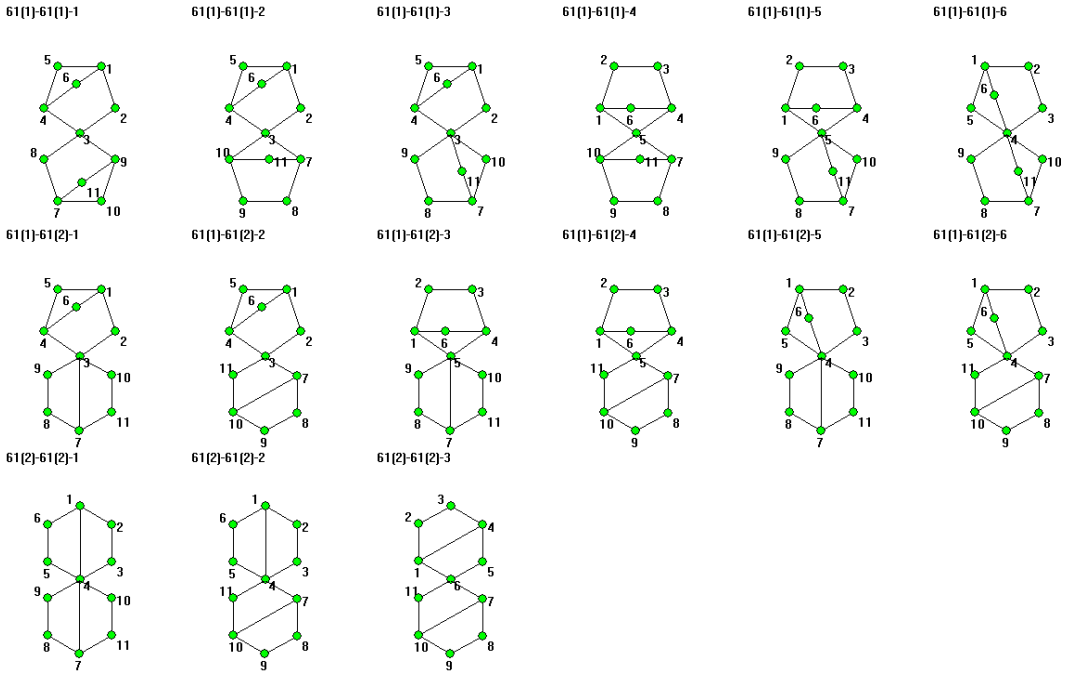

Fig. 7-2 All topological graphs in the class of {[6,1]}*{[6,1]}

According to OC1 and OC2, the chains of Figs.10 (b), (d), (e), (i) and (j) are ruled out as no appropriate driving pairs can be found. According to FR1 and FR4, the chain of Fig.10 (a) is ruled out as it has no appropriate frame. According to FR2 and FR3, the chain of Fig.10 (f) is ruled out as it has no appropriate output link. From the remaining structures, altogether nine possilbe mechanisms of 11-link 2-DOF road tractors are obtained, shown in Fig. 7-3.

According to OC4, Figs. 7-3(b), (f) and (g) are ruled out because they contain useless sub-structrues. Altogether six feasible mechanisms, namely Fig. 7-2(a), (c), (d), (e), (h) and (i), for 11-link 2-DOF road tractors are obtained, including the mechanism in Fig.1-1(b).

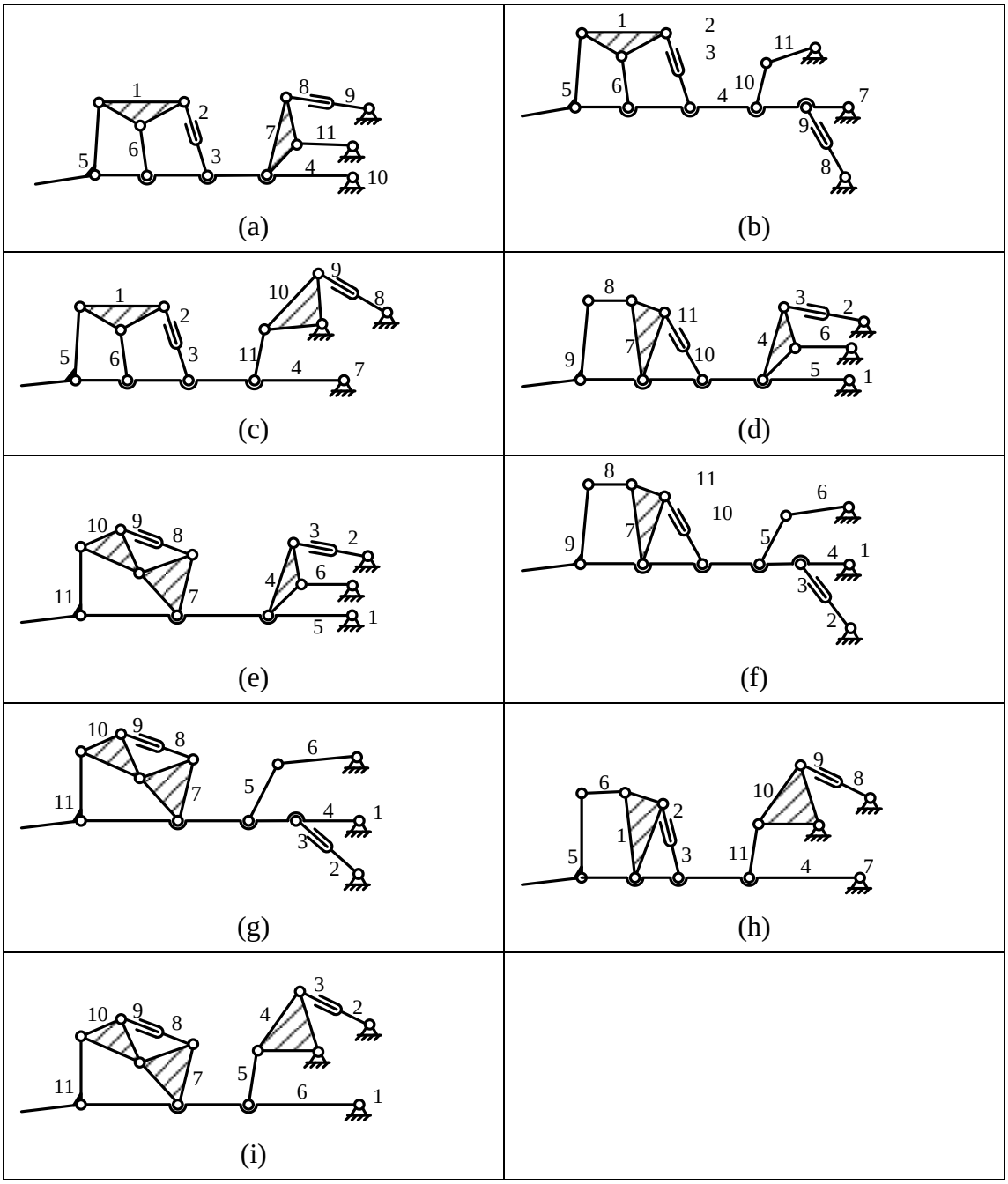

Fig. 7-3 Nine possible mechanisms for 11-link 2-DOF road tractors

Similarly, all three feasible mechanisms of 9-link 2-DOF fractionated mechanisms for road tractors can be obtained in this way, shown in Fig. 7-4.

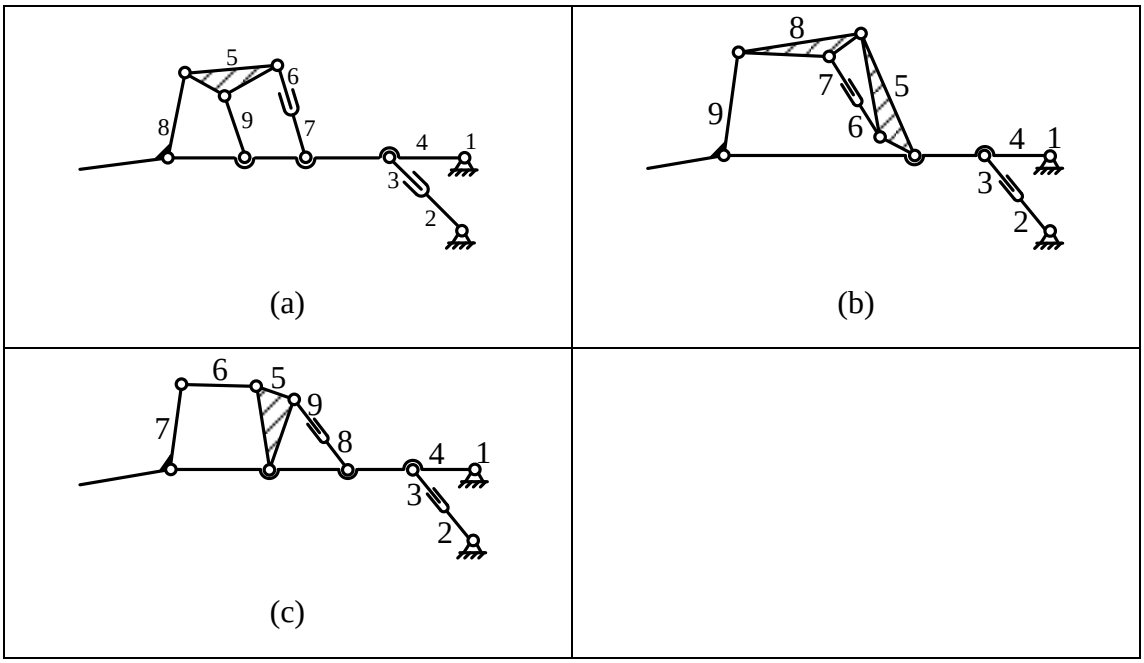

Fig. 7-4 Three feasible mechanisms for 9-link 2-DOF road tractors

If one wants to find all feasible mechanisms for this type of road tractor with non-fractionated structures, the creative design can also be achieved with the same method.

The structural characteristics of the main mechanism are shown in Tab.7-4, where the fractionated type is specified as SC1, the number of links as SC2 , the degrees of freedom as SC3, the nature of motion as SC4, the admissible types of joints as SC5 and the number of basic loops as SC6.

Tab. 7-4 Structural characteristics for the non-fractionated main mechanism of a road tractor

No.	Structural characteristics
SC1	The mechanism is non-fractionated.
SC2	The number of links is 9.
SC3	The mechanism has two DOFs.
SC4	The mechanism is confined to planar nature of motion, namely *d* equals three.
SC5	The type of joints is limited to revolute joints and prismatic joints only.
SC6	There are three basic loops.

The functional requirements for the main mechanism are shown in Tab.7-5. The assortments of the frame and the output links are specified as FR1 and FR2. The relationships of the output link and the big arm are specified as FR3 and FR4.

Tab. 7-5 The functional requirements for the main mechanism

No.	Functional requirements
FR 1	The frame link is a multiple-pair link.
FR 2	The output link is a binary link.
FR 3	The output link cannot connect directly with the hydraulic cylinder.
FR 4	The big arm is connected with the frame link.

The other design constraints for the main mechanism are shown in Tab.7-6. The mechanism is driven by two hydraulic cylinders, so there are two *D*-paths in the tological graph of the mechanism, specified as OC1. Both the output link and the big arm are driven by an individual hydraulic cylinder, so the *D*-paths cannot be placed in a basic loop, specified as OC2.

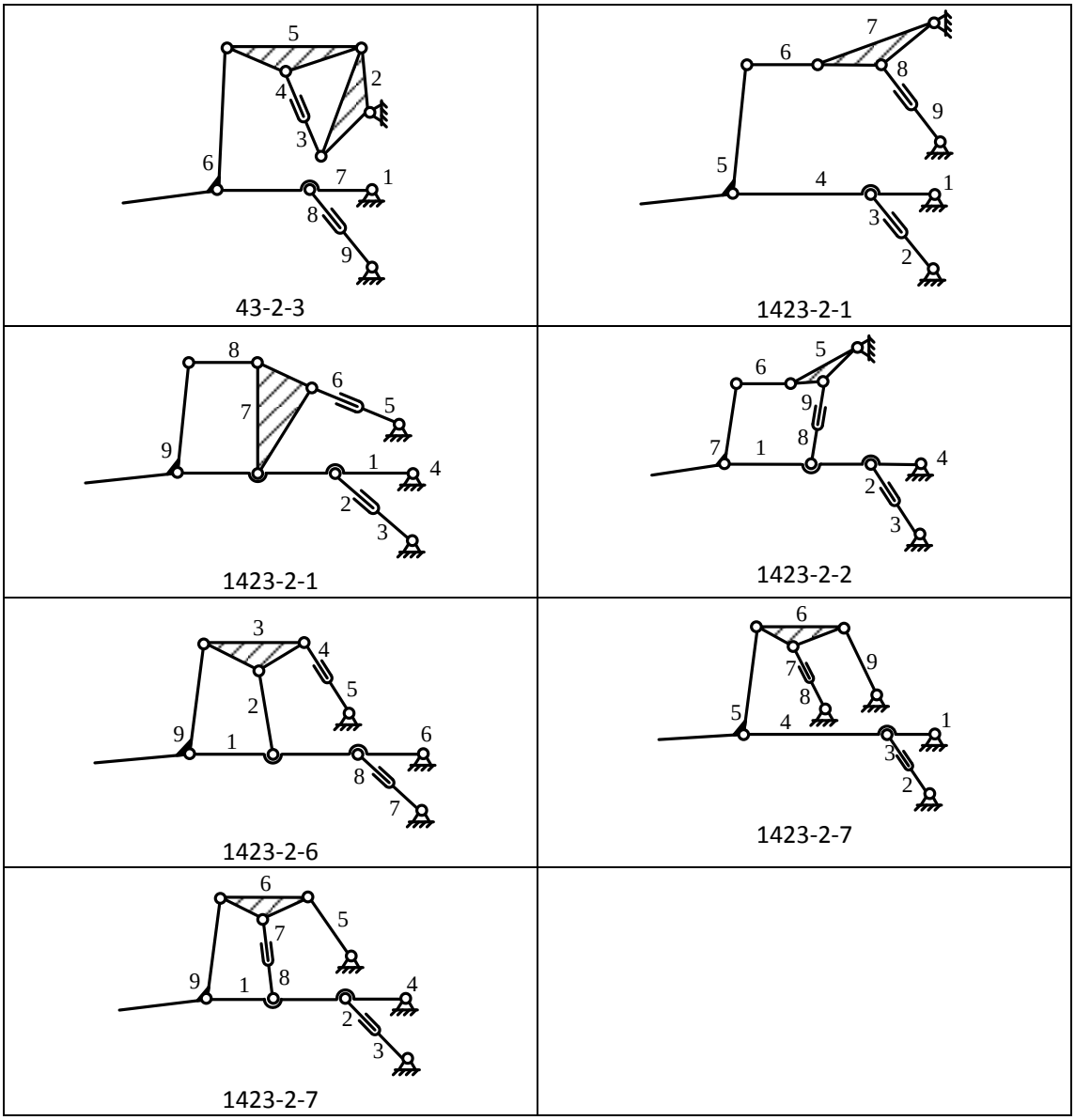

Fig. 7-5 Seven feasible mechanisms for 9-link 2-DOF road tractors

Tab. 7-6 Other design constraints for the main mechanism

No.	Other design constraints
OC 1	There are two *D*-paths.
OC 2	The two *D*-paths cannot be placed in a basic loop.
OC 3	There are no useless sub-structures.

Altogether seven feasible mechanisms for 9-link 2-DOF non-fractionaged road tractors are obtained, shown in Fig. 7-5. Some 3D graphs are shown in Fig. 7-6.

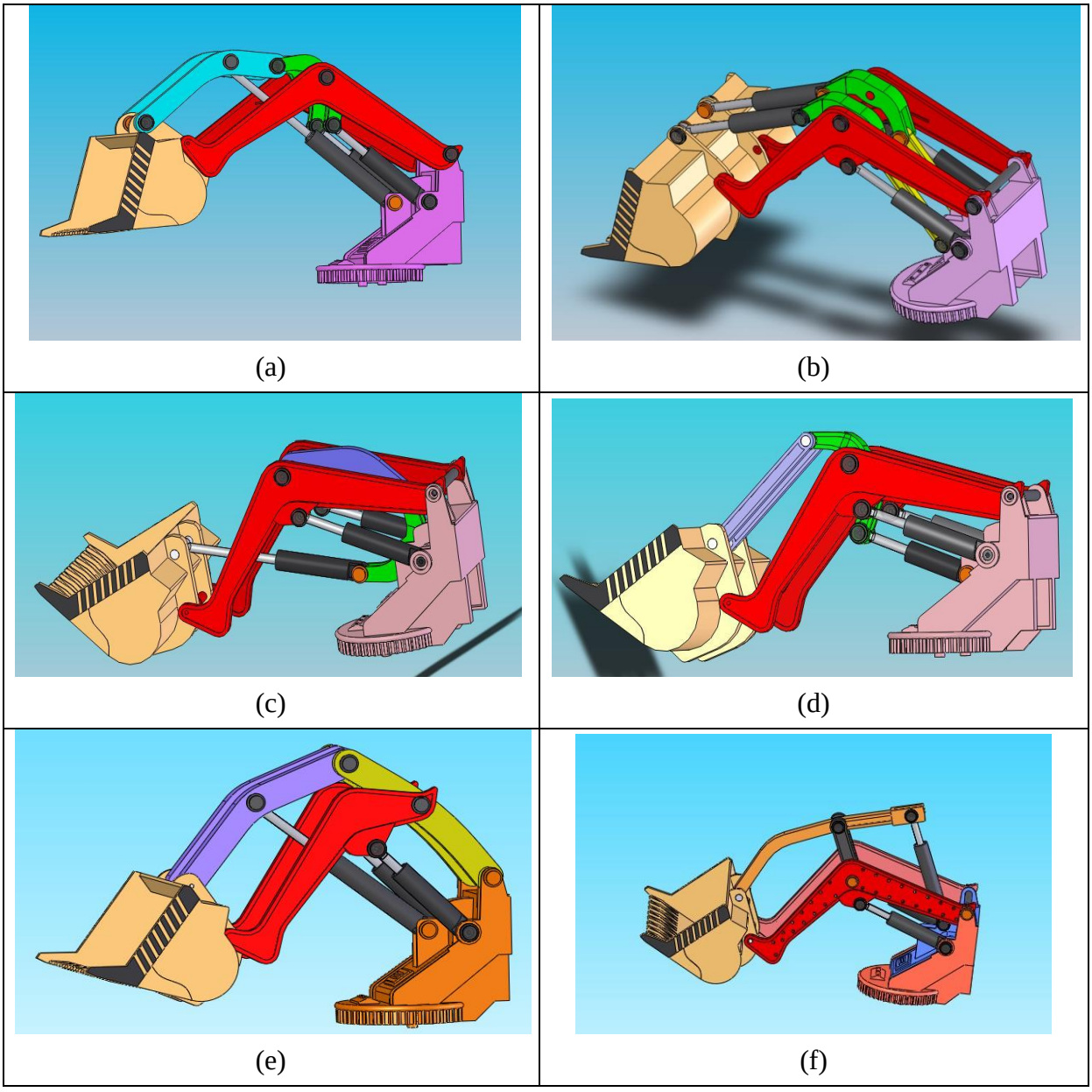

Fig. 7-6 3D graphs for non-fractionated road tractors

7.4 Creative design of 3-DOF hydraulic driven robots

3-DOF hydraulic driven mechanisms are widely used in various heavy-load robots, hydraulic excavators, etc. All feasible 3-DOF hydraulic driven robots can also be obtained with this creative design method.

The structural characteristics for 3-DOF hydraulic driven robots are shown in Tab.7-7, where the fractionated type is specified as SC1, the number of links as SC2, the degrees of freedom as SC3, the nature of motion as SC4, the admissible types of joints as SC5 and the number of basic loops as SC6.

Tab. 7-7 The structural characteristics for 3-DOF hydraulic driven robots

No.	Structural characteristics
SC1	The mechanism is non-fractionated.
SC2	The number of links is 12.
SC3	The mechanism has three DOFs.
SC4	The mechanism is confined to planar nature of motion, namely d equals three.
SC5	The type of joints is limited to revolute joints and prismatic joints only.
SC6	There are four basic loops.

The functional requirements for 3-DOF hydraulic driven robots are shown in Tab.7-8. The assortments of the frame and the output links are specified as FR1 and FR2. The relationships of the end effector and the base are specified as FR3.

Tab. 7-8 The functional requirements for 3-DOF hydraulic driven robots

No.	Functional requirements
FR 1	The frame link is a ternary link.
FR 2	The output link is a binary link.
FR 3	The connectivity between the end effector and the base is three.

The other design constraints for the main mechanism are shown in Tab.7-9. The mechanism is driven by three hydraulic cylinders, so there are three *D*-paths in the tological graph of a mechanism, specified as OC1. The end effector and the base cannot be placed at a basic loop, specified as OC2.

Tab. 7-9 The other design constraints for 3-DOF hydraulic driven robots

No.	Other design constraints
OC 1	There are three *D*-paths.
OC 2	The the end effector and the base cannot be placed at a basic loop.
OC 3	There are no useless sub-structures.

All feasible kinematic structures of such robots can be obtained from the atlas database of 12-link 3-DOF kinematic chains. For example, there are 128 topological graphs corresponding to the contracted graph of Fig. 2-1(e) in the atlas database. From the 128 topological graphs, altogether 25 feasible kinematic structures (including the structure in Fig.2-1(b)) can be obtained by taking the trinary link as the base. The other 24 feasible kinematic structures of these hydraulic robots apart from the one in Fig.2-1(b) are shown in Fig. 7-7.

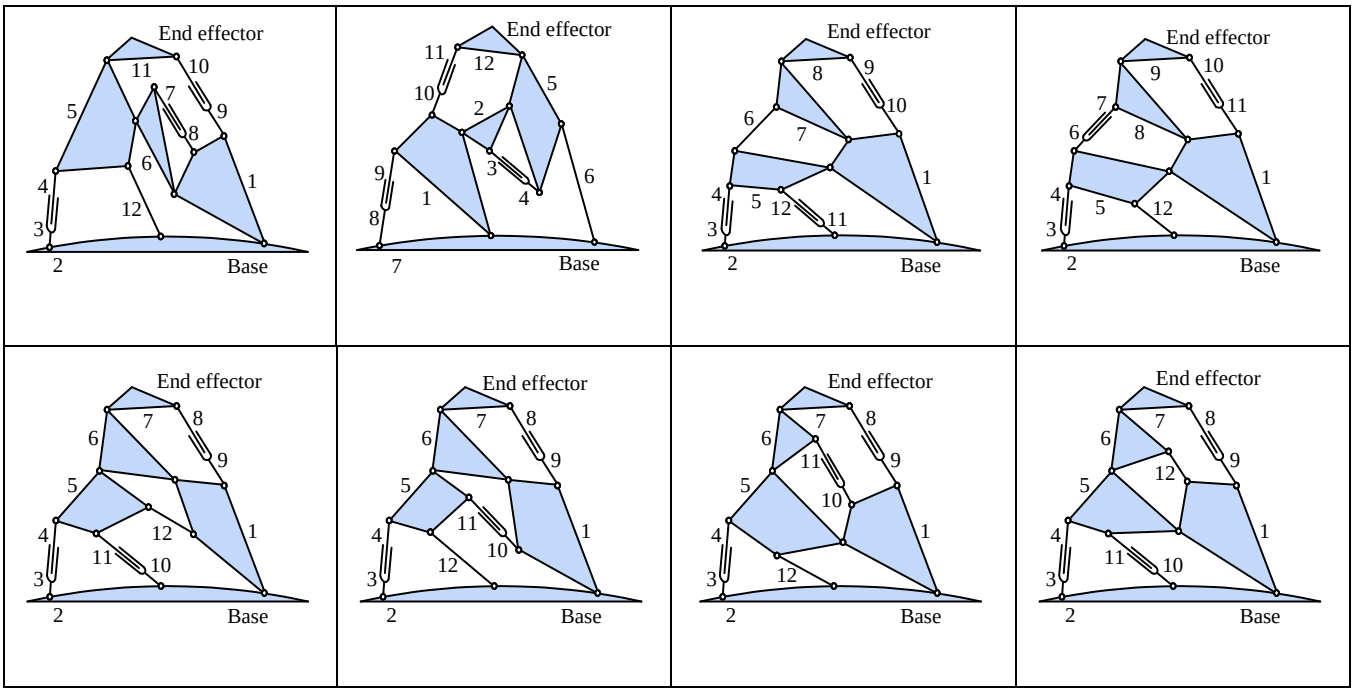

Fig. 7-7 Other 24 feasible mechanisms of 3-DOF hydraulic driven robots

From the 3-DOF hydraulic driven robots in Fig. 7-7, new hydraulic excavators can be achieved. Some virtual prototypes for four different new hydraulic excavators are shown in Fig. 7-8.

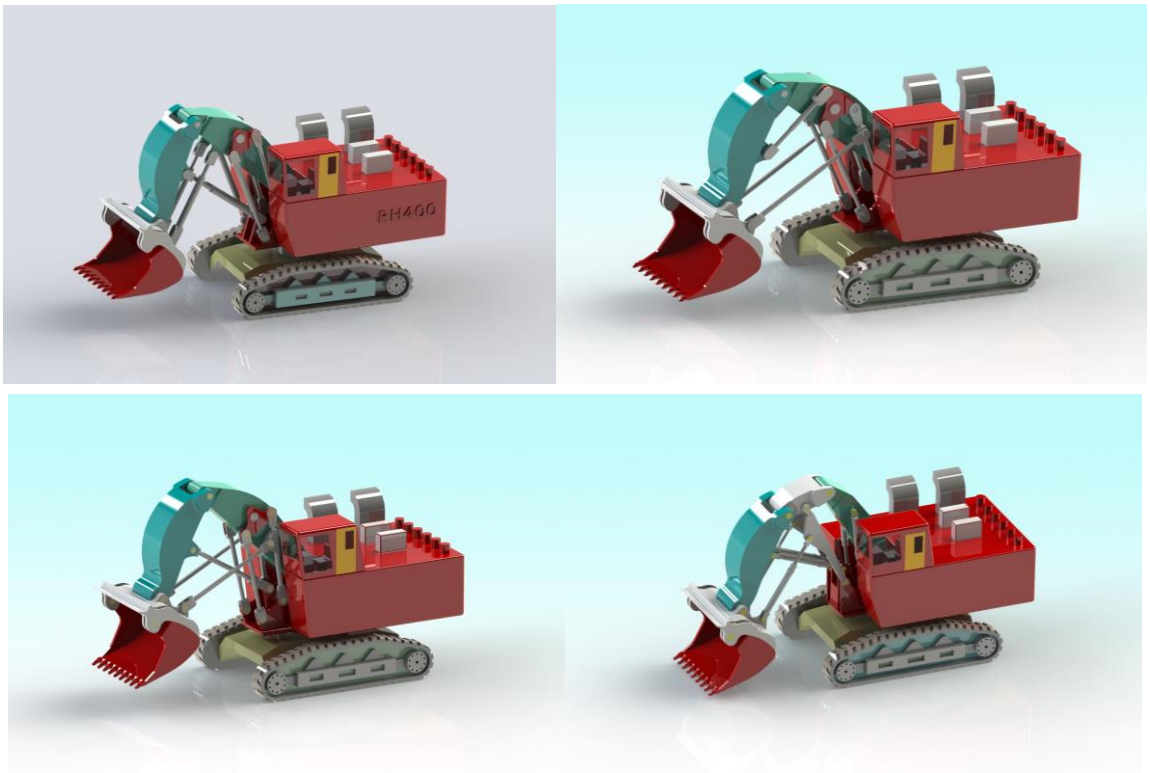

Fig. 7-8 Virtual prototypes of four new types of hydraulic excavators

7.5 Creative design of forging manipulators

Forging manipulators are heavy industrial robots whose main task is to hold and manipulate heavy forged pieces during the forging process. The forging manipulators can cooperate with the forging press and are widely used in the forging industry. The use of forging manipulators can boost the efficiency of the metal free forging and reduce energy consumption.

The gripper of a forging manipulator is connected to the gripper-support by a serially articulated rotation joint. The function of the gripper of a forging manipulator is to realize six essential motions, namely the lifting, pitching, lateral translation, yawing, horizontal translation, and rolling, as shown in Fig. 1. The horizontal translation, lifting and pitching are three main motions. The mechanism realizing the three main motions in a forging manipulator is defined as the major-motion mechanism.The forging manipulator built by Dango & Dienenthal [132] and its main kinematic mechanism are shown in Fig. 7-10 (a) and (b). SMS Meer [133] also built a forging manipulator, shown in Fig. 7-11 (a) and (b).

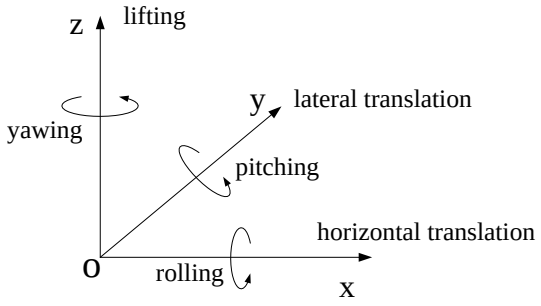

Fig. 7-9 Motion requirements of forging manipulators

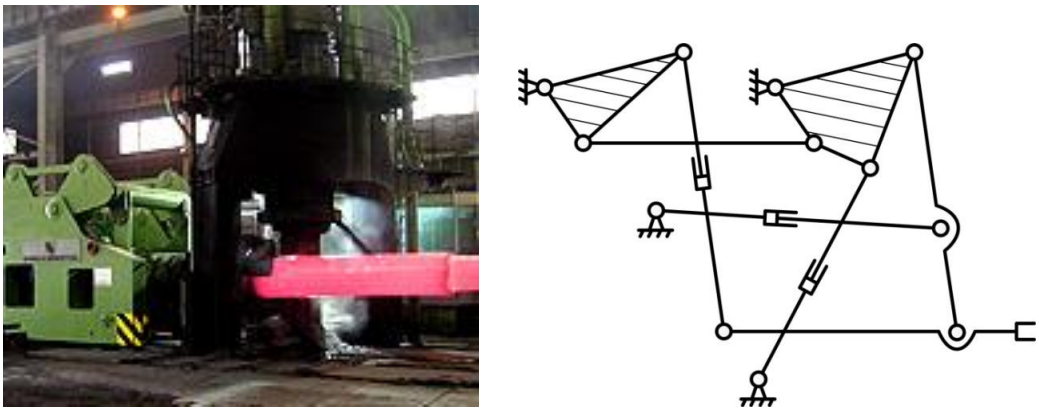

(a) (b)

Fig. 7-10 The forging manipulator built by DDS and its main kinematic mechanism

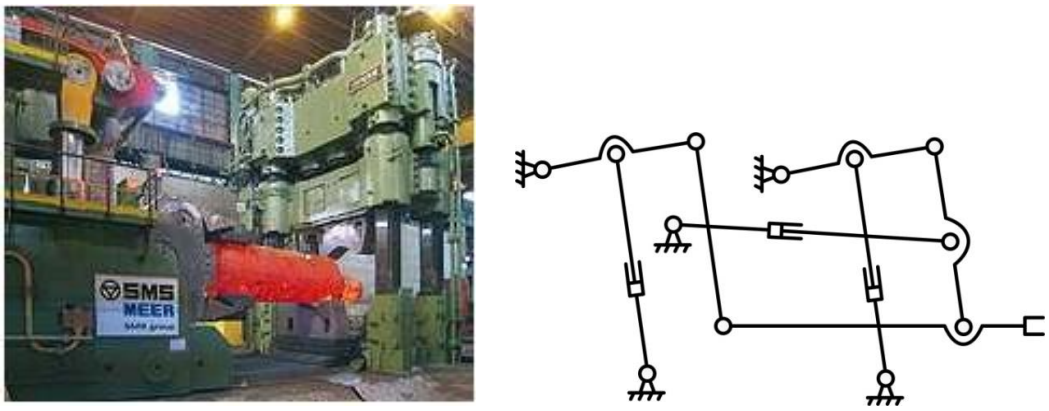

(a) (b)

Fig. 7-11 The forging manipulator built by SMS Meer and its main kinematic mechanism

From the forging manipulators built by DDS and SMS Meer, we can see that the main kinematic mechanism of a forging manipulator is a planar non-fractionated mechanism, which has 12 links and three DOFs. The details of its structural characteristics are shown in Tab.7-10.

Tab. 7-10 The structural characteristics of the main kinematic mechanisms of forging manipulators

No.	Structural characteristics
SC1	The mechanism is non-fractionated.
SC2	The number of links is 12.
SC3	The mechanism has three DOFs.
SC4	The mechanism is confined to planar motion, thus *d* equals three.
SC5	The type of joints is limited to revolute joints and prismatic joints only.
SC6	There are four basic loops.

The functional requirements and other design constraints for the main kinematic mechanisms of forging manipulators are shown in Tab. 7-11 and Tab. 7-12, respectively.

Tab. 7-11 The functional requirements for the main kinematic mechanisms of forging manipulators

No.	Functional requirements
FR 1	The frame link is a multiple-pair link.
FR 2	The gripper support is a binary or ternary link.
FR 3	The connectivity between the gripper support and the frame link is three.

Tab. 7-12 The other design constraints for the main kinematic mechanisms of forging manipulators

No.	Other design constraints
OC 1	There are three *D*-paths.

OC 2	A link cannot be connected directly to two hydraulic cylinder.
OC 3	The gripper support and the frame link cannot be placed at the same loop.
OC 4	There are no useless (redundant) sub-structures.

All of the feasible main kinematic mechanisms of forging manipulators can be obtained from the atlas database of 12-link 3-DOF kinematic chains, including those of DDS, SMS Meer and other patents. Figure 7-11 presents 16 novel main kinematic mechanisms of forging manipulators. These mechanisms are totally new.

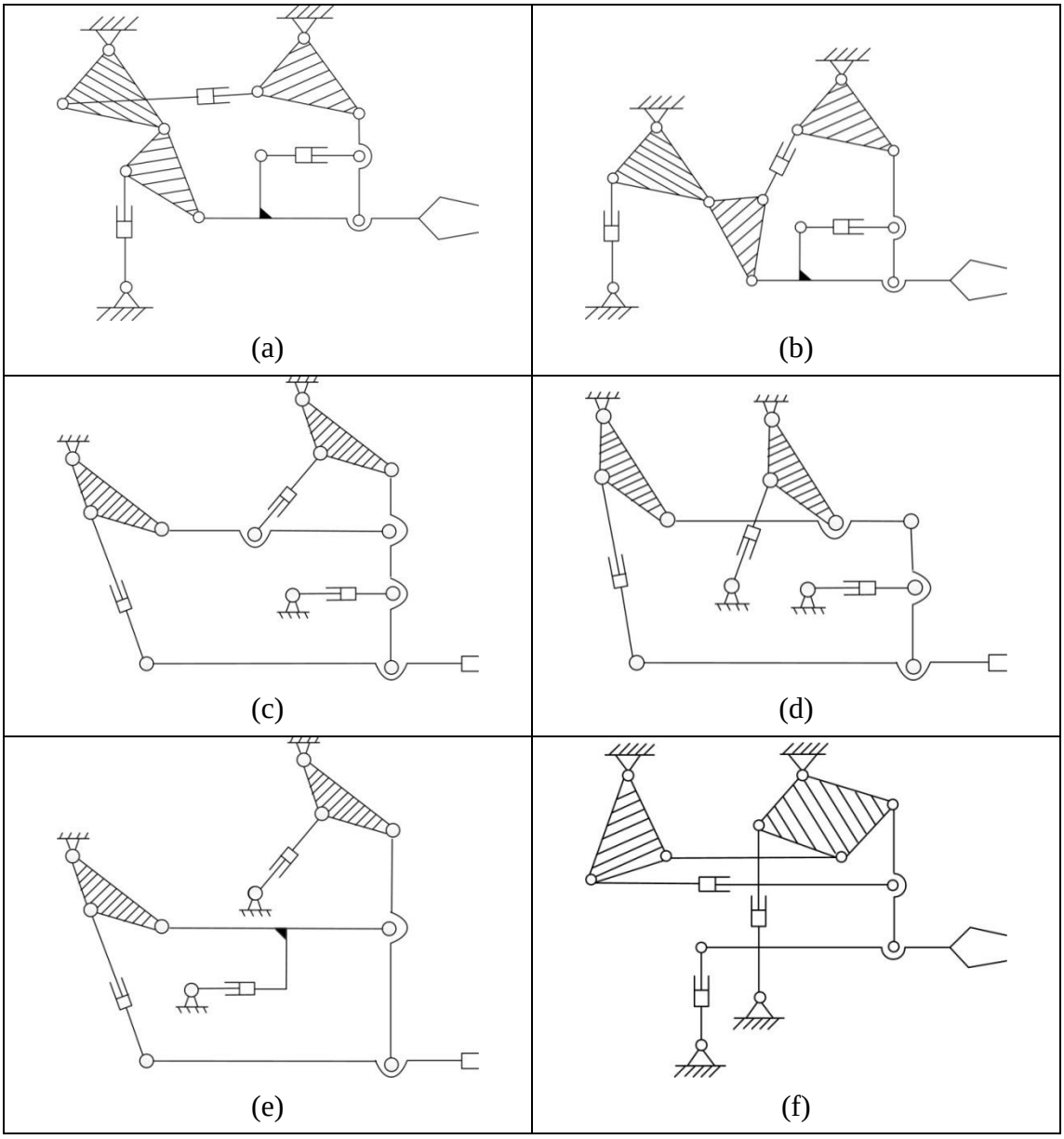

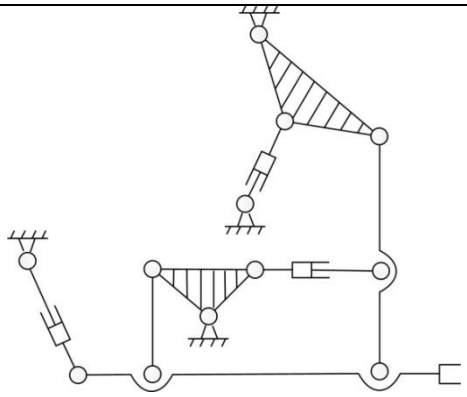

(g)

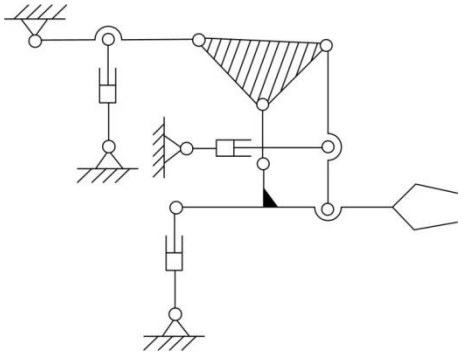

(h)

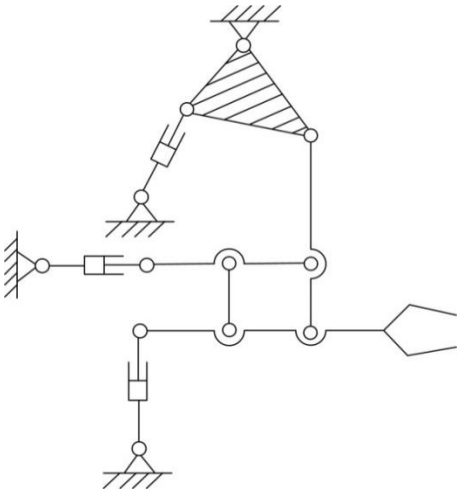

(i)

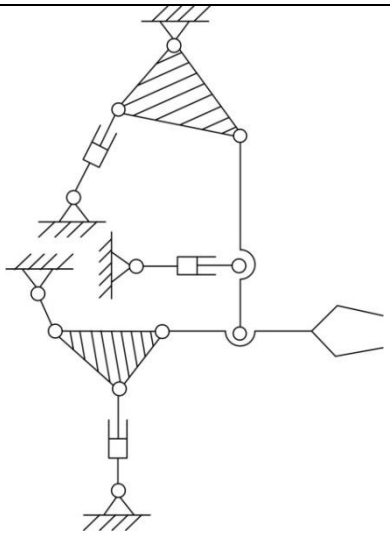

(j)

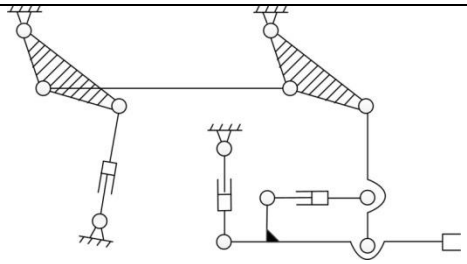

(k)

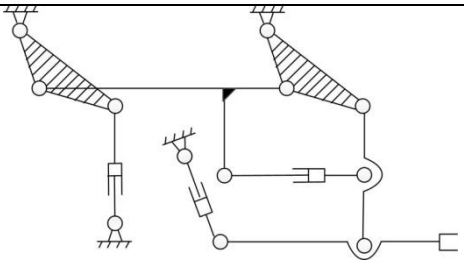

(l)

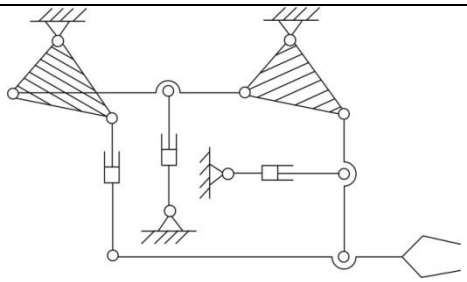

(m)

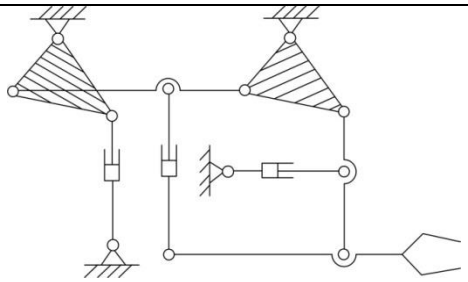

(n)

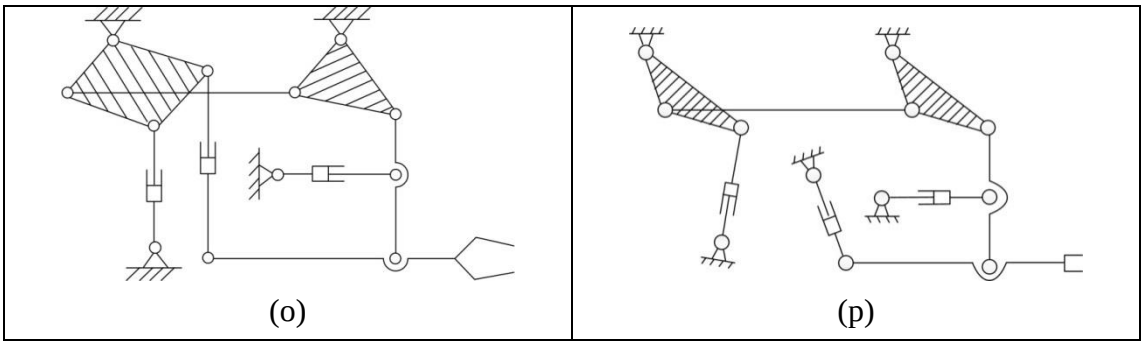

Fig. 7-11 16 novel main kinematic mechanisms of forging manipulators

From the main kinematic mechanisms in Fig. 7-11, new forging manipulators can be obtained, shown in Fig. 7-12. The virtual prototypes of the new forging manipulators can also be achieved, that for the forging manipulator in Fig. 7-12(a) is shown in Fig. 7-13.

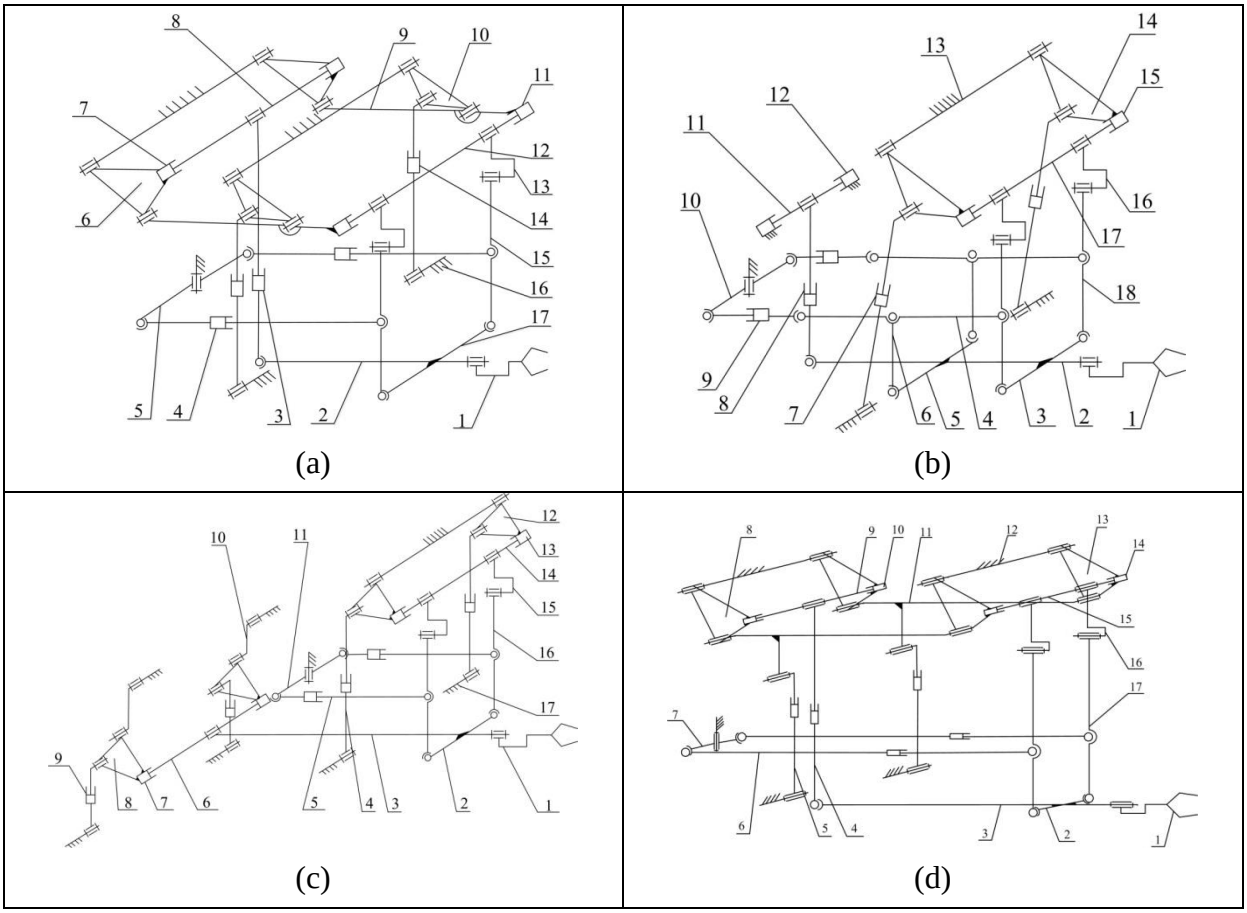

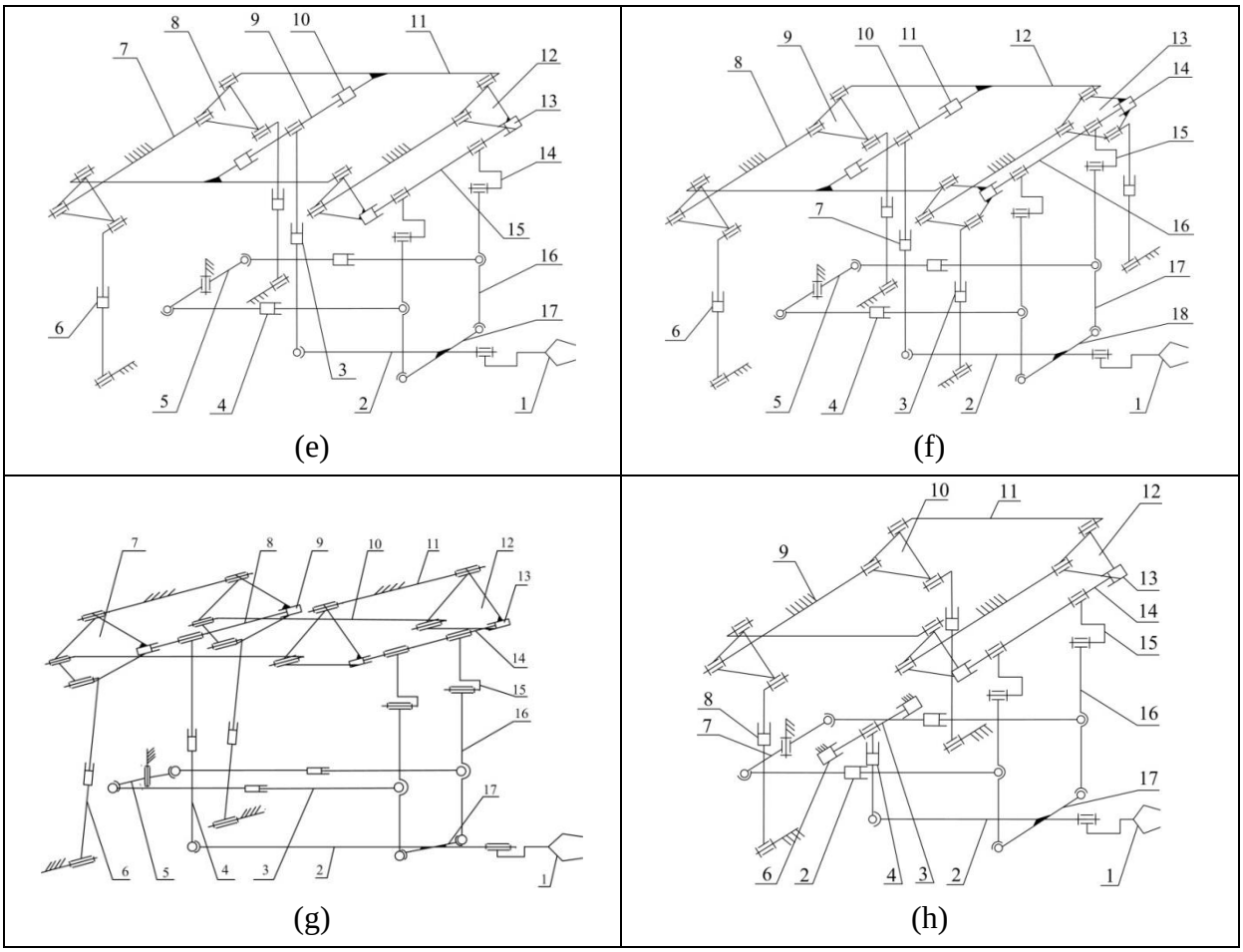

Fig. 7-12 The mechanisms of new forging manipulators

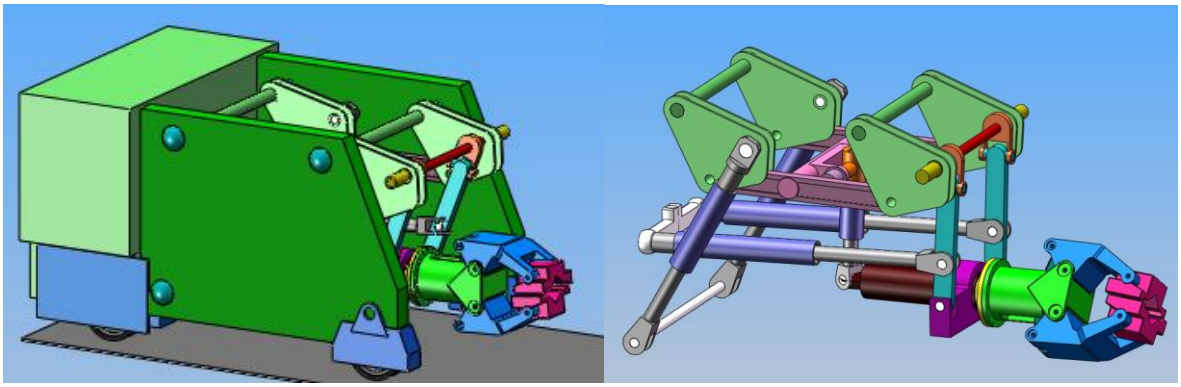

Fig. 7-13 Virtual prototype for the new forging manipulator with the mechanism shown in Fig. 7-12(a)

7.6 Summary

In this chapter, based on the classified atlas databases which can display topological structures of mechanisms in graph forms, a systematic method is proposed for the creative design of mechanisms. The main design processes with the method are computer-aided. For a specified task, all the feasible mechanisms, regardless of simple or complex structures, can be obtained with the method.

The creative design process is illustrated by the generation of all feasible structures for 2-DOF road tractors, 3-DOF hydraulic driven robots and much more complex 6-DOF forging manipulators. With this method, not only can the existing mechanisms already widely used be obtained, but also a number of totally new mechanisms can be derived for the first time, which is more meaningful. These examples verify the effectiveness of the method.

8 Conclusions

This thesis aims to find a systematic approach to aid the creative design of mechanisms. Effective, automatic and human-machine interactive methods are proposed to synthesize planar kinematic chains and mechanisms with simple and multiple joints. The classified atlas databases are also established to classify, store and display the graphs for these mechanisms. Based on the atlas database, the creation design of several kinds of mechanisms is conducted. Some of the originalities of the thesis are as follows.

(1) The relationships of contracted graphs of planar non-fractionated kinematic chains as well as their link assortment arrays are revealed. A fully-automatic method is proposed to synthesize the contracted graphs of planar non-fractionated kinematic chains. The complete families of non-fractionated contracted graphs and of valid contracted graphs with up to 19 links and all possible degrees of freedom are synthesized for the first time. The synthesis results for the contracted graphs of non-fractionated kinematic chains with 2~6 basic loops are the same as some existing results obtained with other methods, while the contracted graphs of non-fractionated kinematic chains with seven and eight basic loops are totally new.

(2) An effective, fully-automatic and designer-friendly method is proposed to synthesize the whole family of planar non-fractionated kinematic chains and mechanisms with specified numbers of links and degrees of freedom. The classified atlas databases of planar non-fractionated kinematic chains and mechanisms are also established. The effectiveness of the method is proved by synthesis of planar non-fractionated kinematic chains and mechanisms with up to 19 links (more i.e. substrantially than the 12 links in literature with graph-based methods) for the first time as well as the establishment of their classified atlas databases.

(3) A fully-automatic approach is proposed to synthesize the whole family of planar fractionated kinematic chains based on the combination of planar non-fractionated kinematic chains and their atlas databases. The synthesis results of planar fractionated kinematic chains with two, three and four basic loops are the same as widely acknowledged results in literature. The whole family of planar fractionated kinematic chains with five, six and seven basic loops are obtained for the first time, showing the effectiveness of the method.

(4) A fully-automatic method is proposed to synthesize the whole family of multiple joint kinematic chains based on the new bicolor topological graph and the classified atlas databases of simple joint kinematic chains. The whole family of multiple joint kinematic chains with up to 16 links is synthesized for the first time, while with other methods only multiple joint kinematic chains with no more than 10 links were synthesized. The classified atlas databases of multiple joint kinematic chains with up to 16 links are also established.

(5) A creative design method is proposed based on the automatic structural synthesis and classified atlas databases of kinematic chains with simple and multiple joints. For a specified task, all the feasible mechanisms can be obtained from the topological graphs in the classified

atlas databases subject to specified design constraints. The creative design of road tractors, hydraulic robots and forging manipulators is conducted as examples, from which a number of novel mechanisms are obtained for the first time apart from the widely used ones, which verifies the usefulness of the classified atlas database and the effectiveness of the creative design method.

While the work has advanced the relevant research, it is likely and feasible to incorporate more work to form a comprehensive theoretical system which would encompass in particular the following two long-term goal

(1) automatic synthesis methods for other types of kinematic chains and mechanisms like geared trains, parallel mechanisms, spatial polycyclic coupling mechanisms, mechanisms with varying topology and metamorphic mechanisms, and others.

(2) automatic and unified methods for the kinematics, dynamics and performance index analysis and optimization of various mechanisms under practical considerations.

References

[1] N.P. Suh, The Principles of Design, Oxford Univesity Press, New York, NY, 1990.

[2] D. Ullman, The Mechanical Design Process, McGraw, New York, NY, 1992.

[3] G. Pahl, W. Beitz, Engineering Design: A Systematic Approach, K.Wallace, Ed., Springer-Verlag, London.

[4] H.S. Yan, Creative Design of Mechanical Devices, Springer-Verlag, Singapore, 1998.

[5] L.W. Tsai, Mechanism Design Enumeration of Kinematic Structures According to Function, CRC Press, 2001.

[6] U. Döring, T. Brix, M. Reeßing, Application of computational kinematics in the digital mechanism and gear library DMG-Lib, Mech. Mach. Theory 41 (8) (2006) 1003-1015.

[7] Z.Huang, Q.C. Li, H.F. Ding, Theory of Parallel Mechanisms, Springer, 2012.

[8] M. Gruebler, Allgemeine Eigenschaften der zwangläufigen ebenen kinematischen Ketten Part I, Civilingenieur 29 (1883) 167–200; Part II, Verh. Ver.Bef. Gew. 64 (1885) 179–223.

[9] E. Pennestrì, N. P. Belfiore, On Crossley's contribution to the development of graph based algorithms for the analysis of mechanisms and gear trains, Mech. Mach. Theory 89 (2015) 1003-1015.

[10] F.R.E. Crossley, A contribution to Gruebler's theory in the number synthesis of planar mechanisms, J. Eng.Indust., ASME Trans., Series B 86 (1964) 1–8.

[11] F.R.E. Crossley, On an unpublished work of Alt, J. Mechanisms 1 (1966) 165–170.

[12] B. Paul, A unified criterion for the degree of constraint of planar kinematic chains, J. Appl. Mech., ASME Trans.,Series E 27 (1960) 196–200.

[13] J. Volmer, Getriebetechnik, VEB Verlag Technik, Berlin,1971.

[14] F. Freudenstein, L.S. Woo, Kinematic structure of mechanisms, in: W.R. Spillers (Ed.), Basic Questions of Design Theory, North Holland/American Elsevier, New York, (1974) 241–264.

[15] T.S. Mruthyunjaya, Kinematic structure of mechanisms revisited, Mech. Mach. Theory 38 (4) (2003) 279-320.

[16] X. Kong, C. Gosselin, Type synthesis of parallel mechanisms, Springer, 2007.

[17] A.F. Al-Dweiri, F.T. Dweiri, O.M. Ashour, A novice-centered decision-support system for type synthesis of function-generation mechanisms, Mech. Mach. Theory 45 (9) (2010) 1252-1268.

[18] F. Gao, Reflection on the current status and development strategy of mechanism research, Chinese Journal of Mechanical Engineering 41(8) (2005) 3-17.

[19] H.J. Zou, F. Gao, Eds. Progress in Modern Mechanism (Vol. 2), Beijing: The High Education Press, 2011.

[20] W. Fang, F. Freudenstein, The stratified representation of mechanisms, ASME J. Mech. Des. 112(3) (1990) 514–519.

[21] J.K. Shin, S. Krishnamurty, On identification and canonical numbering of pin jointed kinematic chains, ASME J. Mech. Des. 116 (1994) 182-188.

[22] J.K. Shin, S. Krishnamurty, Development of a standard code for colored graphs and its application to kinematic chains, ASME J. Mech. Des. 114(1) (1992) 189-196.

[23] T.H.Davies, F.R.E Crossley, Structural analysis of planar linkages by Franke’s condensed notation, Journal of Mechanisms 1 (2) (1966) 171-183.

[24] R. Franke, Von Aufbau Der Getribe, Vol. 1, Beuthvertrieb, Berlin, 1943, Vol. 2, VDI, Düsseldorf, 1951.

[25] S.L.Haas, F.R.E. Crossley, Structural synthesis of a four-bit binary adding mechanism, J. Eng. Indust., ASME Trans, Series B 91 (1969) 240–250.

[26] A.H. Soni, Structural analysis of two general constraint kinematic chains and their practical application, ASME Journal of Engineering for Industry 93B (1) (1971) 231-238.

[27] F. Freudenstein, L. Dobrjanskyj, On a theory of type synthesis of mechanisms, in: Proceedings of 11th International Congress of Applied Mechanics, Springer, Berlin, (1964) 420–428.

[28] F.R.E. Crossley, The permutations of kinematic chains of eight members or less from the graph-theoretic view point, in: Developments in Theoretical and Applied Mechanics, Pergamon Press, Oxford 2 (1965) 467-486.

[29] N.L. Biggs , E.K. Lloyd, R.J. Wilson, Graph Theory, Clarendon Press, Oxford, 1976.

[30] L.S. Woo, Type synthesis of plane linkages, ASME Journal of Engineering for Industry 89B (1967) 158-172.

[31] F. Freudenstein, The basic concepts of Polyas theory of enumeration with applications to structural classification of mechanisms, J. Mechanisms 1 (1967) 275–290.

[32] F. Freudenstein, L.S. Woo, Kinematic structure of mechanisms, in: W.R. Spillers (Ed.), Basic Questions of Design Theory, North Holland/American Elsevier, New York, (1974) 241–264.

[33] L. Dobrjanskyj, F. Freudenstein, Some applications of graph theory to the structural analysis of mechanisms, ASME Journal of Engineering for Industry 89B (1967) 153-158.

[34] M. Huang, A.H. Soni, Application of linear and nonlinear graphs in structural synthesis of kinematic chains, J. Eng. Indust., ASME Trans., Series B 95 (1973) 525–532.

[35] G. Kiper, D. Schian, The twelve-link Gruebler-type kinematic chains, Z. VDI 117 (1975) 283–288.

[36] G. Kiper, D. Schian, Sammlung der Grueblerschen kinematischen ketten mit bis zu zwölf Gliedern, Z. VDI 118 (1976) 1066.

[37] T.S. Liu, C.C. Chou, Type synthesis of vehicle planar suspension mechanisms using graph theory, 115(3) (1993) 652-657.

[38] M.A. Pucheta, A. Cardona, An automated method for type synthesis of planar linkages based on a constrained subgraph isomorphism detection, Multibody Syst. Dyn. 18(2) (2007) 233-258.

[39] M.A. Pucheta, A. Cardona, Synthesis of planar multiloop linkages starting from existing parts or mechanisms: Enumeration and initial sizing, Mech. Based Des. Struct. Mach. 36(4) (2008) 364-391.

[40] B.D. McKay, Practical graph isomorphism, Congressus Numerantium 30(1) (1981) 45–87.

[41] R.P. Sunkari , L.C. Schmidt , Structural synthesis of planar kinematic chains by adapting a Mckay-type algorithm, Mech. Mach. Theory 41(9) (2006) 1021-1030.

[42] Y. Lu, L. Ding, Autoderivation of topological graphs for type synthesis of planar 3DOF parallel mechanisms, ASME Journal of Mechanism and Robotics 2(1) (2010) 0110021.

[43] Y. Lu, B.Y. Mao, et al, Derivation and isomorphism identification of valid topological graphs for 1-, 2-DOF planar closed mechanisms by characteristic strings, J of Mech Sci Technol 25(1) (2011) 255- 263.

[44] Y. Lu, B.Y. Mao, et al, Derivation of valid contracted graphs with pentagonal links plus quaternary links or ternary links for closed mechanisms by arrays. Proc. IMechE Part C, J of Mech Eng Sci 225(4) (2011) 1001-1013.

[45] Y. Lu, L. Ding, et al， Derivation of topological graphs of some planar 4-DOF redundant closed mechanisms by contracted graphs and arrays, ASME Journal of Mechanism and Robotics 2(3) (2010)(031011-1-10).

[46] H.S. Yan, C.H. Kang, Configuration synthesis of mechanisms with variable topologies, Mech.

Mach. Theory 44(5) (2009) 896-911.

[47] E.A. Butcher, C. Hartman, Efficient enumeration and hierarchical classification of planar simple-jointed kinematic chains: Application to 12- and 14-bar single degree-of-freedom chains, Mech. Mach. Theory 40 (9) (2005) 1030-1050.

[48] L.V. Assur, Investigation of plane hinged mechanisms with lower pairs from the point of view of their structure and classification (in Russian): Part I, II, Bull. Petrograd Polytech. Inst. 20 (1913) 329-386; Bull. Petrograd Polytech. Inst. 21 (1914) 187-283 (vols. 21-23, 1914-1916).

[49] N.I. Manolescu, I. Ereceanu. P. Antonescu, The kinematic synthesis of mechanisms, Rev. Roum. Sci. Tech. Ser.Mec. Appl. (1964) 341-363.

[50] N.I. Manolescu, A methodology for creative mechanism, Rev. Roum. Sci. Tech. Ser. Mec. Appl. (1964)1263-1313.

[51] N.I. Manolescu, The synthesis of stable force-close graphs, Rev. Roum. Sci. Tech. Ser. Mec. Appl. (1965) 999-1042.

[52] N.I. Manolescu, I. Tempea, The kinematic and control of a multi-finger, Rev. Roum. Sci. Tech. Ser. Mec. Appl. (1967) 1117-1140.

[53] N.I. Manolescu, I.Tempea, A computerized method for the identification of planar pin-jointed of incident degree, Rev. Roum. Sci. Tech. Ser. Mec. Appl. 12. (1967) 1251-1275.

[54] N.I. Manolescu, For a united point of view in the study of the structural analysis of kinematic chains and mechanisms, Journal of Mechanisms 3 (3) (1968) 149–169.

[55] W.Q. Cao, J.K. Chu, Structural analysis and synthesis of Assur groups with multiple joints, Chinese Journal of Mechanical Engineering 5(1) (1992) 24-27.

[56] J.K. Chu, W.Q. Cao, Systemics of Assur groups with multiple joints, Mech. Mach. Theory 33 (8) (1998) 1127-1133.

[57] W.Q. Cao, The Analysis and Synthesis of Linkage Mechanisms (the 2th Edition), Science Press, 2002.

[58] C.R. Tischler, A.E. Samuel, K.H. Hunt, Kinematic chains for robot hands. I: Orderly number synthesis, Mech. Mach. Theory 30 (1995) 1193–1215.

[59] C.R. Tischler, A.E. Samuel, H.H. Hunt, Kinematic chains for robot hands. II: Kinematic constraints, classification, connectivity and actuation, Mech. Mach. Theory 30 (1995) 1217–1239.

[60] C. Alexandre, B. Christoph, H. Jürgen, A type synthesis method for hybrid robot structures, Mech. Mach. Theory 43(8) (2008) 984-995.

[61] S.J. Li, J.S. Dai, Structural synthesis method of planar mechanisms using the Assur-group based adjacency matrix, Journal of Mechanical Engineering 48(13) (2012) 13-18.

[62] E.R. Tuttle, S.W. Peterson, Symmetry group theory applied to kinematic chain enumeration, in: Proceedings of the 10th Applied Mechanisms Conference, 1987, Vol. 2, Sec IV-B, New Orleans, LA.

[63] E.R. Tuttle, S.W. Peterson, J.E. Titus, Further application of group theory to the enumeration and structural analysis of basis kinematic chains, ASME Journal of Mechanisms, Transmissions and Automation in Design 111 (1989) 494-497.

[64] E.R. Tuttle, S.W. Peterson, J.E. Titus, Enumeration of basis kinematic chains using the theory of finite groups, ASME Journal of Mechanisms, Transmissions and Automation in Design 111 (1989) 498-503.

[65] E.R. Tuttle, Generation of planar kinematic chains, Mech. Mach. Theory 31 (1996) 729–748.

[66] H.S. Yan, Y.W. Hwang, Number synthesis of kinematic chains based on permutation groups, Mathematical and Computer Modelling 13 (8) (1990) 29-42.

[67] H.S. Yan, A methodology for creative mechanism design, Mech. Mach. Theory 27 (3) (1992) 235-242.

[68] H.S. Yan, Y.M. Hwang, The specialization of mechanisms, Mech. Mach. Theory 26(6) (1991) 541–551.

[69] C.C. Hung, H.S. Yan, On the number of specialized mechanisms, 2008 Proceedings of the ASME International Design Engineering Technical Conferences and Computers and Information in Engineering Conference, DETC (2008) 603-609.

[70] H.S. Yan, C.C. Hung, Identifying and counting the number of mechanisms from kinematic chains subject to design constraints, ASME J. Mech. Des. 128(5) (2006) 1177–1182.

[71] C.C. Hung, H.S. Yan, G.R. Pennock, A procedure to count the number of planar mechanisms subject to design constraints from kinematic chains, Mech. Mach. Theory 43(6) (2008) 676–694.

[72] J.M. Hervé, Analyse structurelle des mécanismes par groupe des déplacements, Mech. Mach. Theory 13(4) (1978) 437–450.

[73] Q.C. Li, Z. Huang, J.M. Hervé, Type synthesis of 3r2t 5-DOF parallel mechanisms using the Lie group of displacements, IEEE Trans. Robot. Automat. 20(2) (2004)173–180.

[74] Q.C. Li, J.M. Herve, Parallel mechanisms with bifurcation of schoenflies motion, IEEE Transactions on Robotics 25(1) (2009)158–164.

[75] C.C. Lee, J.M. Hervé, Translational parallel manipulators with doubly planar limbs, Mech. Mach. Theory 24(4) (2006) 433–435.

[76] N.I. Manolescu, A method based on Baranov trusses and using graph theory to find the set of planar jointed kinematic chains and mechanisms, Mech. Mach. Theory 8 (1) (1973) 3-22.

[77] T.S. Mruthyunjaya, Structural synthesis by transformation of binary chains, Mech. Mach. Theory 14 (4) (1979) 221-231.

[78] T.S. Mruthyunjaya, Structural synthesis by transformation of binary chains, Mech. Mach. Theory 14 (1979) 221–231.

[79] T.S. Mruthyunjaya, A computerized methodology for structural synthesis of kinematic chains: Part 1-Formulation, Mech. Mach. Theory 19(6) (1984) 487-495.

[80] T.S. Mruthyunjaya, A computerized methodology for structural synthesis of kinematic chains: Part 2-Application to several fully or partially known cases, Mech. Mach. Theory 19(6) (1984) 497-505.

[81] T.S. Mruthyunjaya, A computerized methodology for structural synthesis of kinematic chains: Part 3-Application to new case of 10-link, three-freedom chains, Mech. Mach. Theory 19(6) (1984) 507-530.

[82] T.S. Mruthyunjaya, H. R. Balasubramanzan, In quest of a reliable and efficient computational test for detection of isomorphism in kinematic chains, Mech. Mach. Theory 22(2) (1987) 131-140.

[83] W.J. Sohn, F. Freudenstein, An application of dual graphs to the automatic generation of the kinematic structure of mechanisms, American Society of Mechanical Engineers (Paper) (1986) 86-DET-1.

[84] T.L. Yang, Topological characteristics and automatic generation of structural analysis and synthesis of plane mechanisms, Part I: Theory, American Society of Mechanical Engineers, Design Engineering Division (Publication) DE 15-1 (1988) 179-184.

[85] T.L. Yang, F.H. Yao, Topological characteristics and automatic generation of structural analysis and synthesis of plane mechanisms, Part II: Application, American Society of Mechanical Engineers, Design Engineering Division (Publication) DE 15-1 (1988) 185-190.

[86] T.L. Yang, Basic Theory of Mechanical Systems—Structures Kinematics Dynamics, Beijing:

Mechanical Press, 1995.

[87] A.C. Rao, Hamming number technique-I: Further applications, Mech. Mach. Theory 32 (4) (1997) 477-488.

[88] A.C. Rao, Hamming number technique-II: Generation of planar kinematic chains, Mech. Mach. Theory 32 (4) (1997) 489-499.

[89] D. Varadaraju, Y. N. Kumar, A.C. Rao, A more direct method for structural synthesis of simple-jointed planar kinematic chains, Mech. Synth. Anal. ASME 70 (1994) 507–516.

[90] K. Vijayananda, Computer-aided structural synthesis of linkages and epicyclic gear transmissions, Ph.D. thesis, IISc, Bangalore, 1994.

[91] W.M. Hwang, Y.W. Hwang, Computer-aided structural synthesis of planar kinematic chains with simple joints, Mech. Mach. Theory 27 (2) (1992) 189-199.

[92] H.S. Yan, C.H. Hsu, Contracted graphs of kinematic chains, Journal of Mathematical and Computer Modelling, 10(9)(1988)681-695.

[93] C.H. Hsu, Simplification of multiple joints, Journal of the Chinese Society of Mechanical Engineers, Transactions of the Chinese Institute of Engineers,12(4)(1991)357-363.

[94] C.H. Hsu, Enumeration of basic kinematic chains with simple and multiple joints, Journal of the Franklin Institute 329(4) (1992) 775-789.

[95] C.H. Hsu, J.J. Hsu, An efficient methodology for the structural synthesis of geared dinematic chains, Mech. Mach. Theory 32(8)(1997) 957-973.

[96] A.C. Rao, P.B. Deshmukh, Computer-aided structural synthesis of planar kinematic chains obviating the test for isomorphism, Mech. Mach. Theory 36 (4) (2001) 489-506.

[97] Z.H. Lan, R. Du, Representation of topological changes in metamorphic mechanisms with matrices of the same dimension, Trans, ASME J. Mech. Des. 130(7)(2008) 074501-1-4.

[98] J.S. Dai , J. R. Jones, Mobility in metamorphic mechanisms of foldable/erectable kinds, Transactions of the ASME: Journal of Mechanical Design 121(3)(1999)375-382.

[99] L. Song, J. Yang, X.M. Zhang , W.Q. Cao, Spanning tree method of identifying isomorphism and topological symmetry to planar kinematic chain with multiple joints, Chinese Journal of Mechanical Engineering (English Edition) 14(1)(2001)27-31.

[100] L. Song, J. Yang, W.Q. Cao, Combination method of type synthesis for planar kinematic chains with multiple joints, Chinese Journal of Mechanical Engineering 40(2)(2004)37-41.

[101] L. Song, Y. Huang, L. Cheng, Adjacent matrix method of identifying isomorphism to planar kinematic chain with multiple joints and higher pairs, Chinese Journal of Mechanical Engineering (English Edition) 19(4)(2006)605-609.

[102] W.H. Li, X.W. Zhang, H.M. Li, A method for structural synthesis of planar kinematic chains, in: Proceedings of the 9th World Congress on the Theory of Machines and Mechanisms (1995)129–133.

[103] P. Mitrouchev, Symbolic structural synthesis and a description method for planar kinematic chains in robotics, Eur. J. Mech. A/Solids 20(2001) 777-794.

[104] J.J. Uicker, A. Raicu, A method for the identification and recognition of equivalence of kinematic chains, Mech. Mach. Theory 10(5)(1975)375-383.

[105] H.S. Yan, A. S. Hall, Linkage characteristic polynomials: definitions, coefficients by inspection, ASME J. Mech. Des. 103(3)(1981)578-584.

[106] T.S. Mruthyunjaya, H. R. Balasubramanzan, In quest of a reliable and efficient computational test for detection of isomorphism in kinematic chains, Mech. Mach. Theory 22(2)(1987)131-140.

[107] P.R. He, W.J. Zhang, Q. Li, etc, A new method for detection of graph isomorphism based on the

quadratic form, ASME J. Mech. Des. 125(3)(2003)640-642.

[108] Z.Y. Chang, C. Zhang, Y.H. Yang, etc, A new method to mechanism kinematic chains isomorphism identification, Mech. Mach. Theory 37(4)(2002)411-417.

[109] P.S. Rajesh, C.S. Linda, Reliability and efficiency of the existing spectral methods for isomorphism detection, ASME J. Mech. Des. 128(6) (2006)1246-1252.

[110] W. Hwang, Y.Hwang, An algorithm for the detection of degenerate kinematic chains, Mathematical and Computer Modelling 15(11)(1991)9-15.

[111] H. Lee, Y. Yoon, Detection of rigid structure in enumerating basic kinematic chains by sequential removal of binary link string, JSME International Journal 35(4) (1992)647-651.

[112] C.H. Hsu , Y.C. Wu, Automatic detection of embedded structure in planetary gear trains, Journal of Mechanical Design, Transactions of the ASME 119(2)(1997)315-318.

[113] H.F. Ding, Z. Huang, The establishment of the canonical perimeter topological graph of kinematic chains and isomorphism identification, ASME J. Mech. Des. 129(9)(2007)915-923.

[114] H.F. Ding, Z. Huang, Isomorphism identification of graphs: Especially for the graphs of kinematic chains, Mech, Mach. Theory 44(1)(2009)122-139.

[115] H.F. Ding, Z. Huang, D.J. Mu, Computer-aided structure decomposition theory of kinematic chains and its applications, Mech. Mach. Theory 43(12)(2008) 1596-1609.

[116] H.F. Ding, Z. Huang, A unique representation of the kinematic chain and the atlas database, Mech. Mach. Theory 42(6) (2007)637-651.

[117] H.F. Ding, Z. Huang, A new theory for the topological structure analysis of kinematic chains and its applications, Mech. Mach. Theory 42(10)(2007)1264-1279.

[118] D.G. Olson, T.R. Thompson, D.R. Riley, et al, An algorithm for automatic sketching of planar kinematic chains, ASME Journal of Mechanisms, Transmissions and Automation in Design 107 (1985) 106-111.

[119] N.P. Belfiore, E. Pennestri, Automatic sketching of planar kinematic chains, Mech. Mach. Theory 29 (1) (1994) 177-193.

[120] S. Mauskar, S. Krishnamurty, A loop configuration approach to automatic sketching of mechanisms, Mech. Mach. Theory 31 (4) (1996) 423-437.

[121] C.F. Hsieh, Y.W. Hwang, H.S. Yan, Generation and sketching of generalized kinematic chains, In: Proceedings of 2008 ASME DETC conference, Chicago, USA.

[122] M.A. Pucheta, N.E. Ulrich, Alberto Cardona, Combined graph layout algorithms for automated sketching of kinematic chains, In: Proceedings of 2012 ASME DETC conference (paper DETC2012-70665), Chicago, USA.

[123] F.G. Flores, A. Kecskeméthy, A. Pöttker, Workspace analysis and maximal force calculation of a face-shovel excavator using kinematical transformers. Proceedings of the 12th World Congress in Mechanism and Machine Science, Besancon, France, June 17-21, 2007.

[124] N.I. Manolescu, A unitary method for construction of the kinematic plane chains and plane mechanisms with different degrees of mobility, Revue Roumaine des Sciences Techniques, Serie de Mecanique Appliquee 9 (1964) 1263–1313.

[125] R. Simoni, A.P. Carboni, H. Simas, D. Martins, Enumeration of kinematic chains and mechanisms review, 13th Word Congress in Mechanism and Machine Science, Guanajuato, México, 19-25, June, 2011.

[126] R. Simoni, A.P. Carboni, D. Martins, Enumeration of kinematic chains and mechanisms, Proceedings of The Institution of Mechanical Engineers, Part C: Journal of Mechanical Engineering Science 223(4) (2009) 1017-1024.

[127] D. Martins, R. Simoni, A.P. Carboni, Fractionation in planar kinematic chains: reconciling enumeration contradictions, Mech. Mach. Theory 45(11)(2010) 1628-1641.

[128] J.K. Chu, Y.H. Zou, P.F. He, A method for structural synthesis of planar simple and multiple joint kinematic chains, International Mechanisms and Machine Science Conference, China, 2012.

[129] F. Freudenstein, E.R. Maki, The creation of mechanisms according to kinematic structure and function, Environ. Plann. B(6) (1979)375–391.

[130] D.Z. Chen, W.M. Pai, A methodology for conceptual design of mechanisms by parsing design specifications, ASME J. Mech. Des. 127(11)(2005)1039-1044.

[131] G. Pahl, W. Beitz, Engineering Design: A Systematic Approach, Springer Verlag, New York, 1999.

[132] Dango & Dienenthal Forging Manipulator, http://www.dds-gmbh.com.

[133] Rail Forging Manipulators, http://www.sms-meer.com/produkte.

List of publication during the doctoral study

[1] **Huafeng Ding**, Fengmao Hou, Andrés Kecskeméthy, Zhen Huang. Synthesis of a complete set of contracted graphs for planar non-fractionated simple-jointed kinematic chains with all possible DOFs. *Mechanism and Machine Theory*, 2011, 46(11):1588-1600.

[2] **Huafeng Ding**, Andrés Kecskeméthy, Zhen Huang (2011): Atlas database of 2-DOF kinematic chains and its application to the creative design of mechanisms. *ASME 2011 International Design Engineering Technical Conference & Computer and Information in Engineering Conference*, August 28-31, 2011, Washington, DC, USA, DETC2011- 47264.

[3] Shuxian Xia, **Huafeng Ding**, Andrés Kecskeméthy (2011): Rigid subchain identification of multi-loop kinematic chains with the method of kinematical transformers. *Kolloquium Getriebetechnik*, September 07-09, 2011, Chemnitz, Germany.

[4] **Huafeng Ding**, Fengmao Hou, Andrés Kecskeméthy, Zhen Huang. Synthesis of the whole family of planar 1-DOF kinematic chains and creation of their atlas databases. *Mechanism and Machine Theory*, 2012, 47(1): 1-15.

[5] **Huafeng Ding**, Wenao Cao, Andrés Kecskeméthy, Zhen Huang, Complete atlas database of 2-DOF kinematic chains and creative design of mechanisms, *ASME Journal of Mechanical Design*, 2012, 134(3): 0310061-03100610.

[6] **Huafeng Ding**, Peng Huang, Bin Zi, Andrés Kecskeméthy, Automatic synthesis of kinematic structures of mechanisms and robots especially for those with complex structures, *Applied Mathematical Modelling*, 2012, 36(12): 6122-6131.

[7] Shuxian Xia, **Huafeng Ding**, Andrés Kecskeméthy. A loop-based approach for rigid subchain identification in general mechanisms. in:Jadran Lenarčič, Manfred Husty (Eds.), *Latest Advances in Robot Kinematics*, 2012, Springer.

[8] **Huafeng Ding**, Weijuan Yang, Peng Huang, Li Ma, Andrés Kecskeméthy, Zhen Huang (2013): Automatic synthesis of planar multiple joint kinematic chains. *ASME 2013 International Design Engineering Technical Conference & Computers and Information in Engineering Conference*, August 4-7, 2013, Portland, OREGON, USA, DETC2013-12915.

[9] **Huafeng Ding**, Bin Zi, Peng Huang, Andrés Kecskeméthy. The whole family of kinematic structures for planar 2- and 3-DOF fractionated kinematic chains. *Mechanism and Machine Theory*, 2013, 70: 74-90.

[10] **Huafeng Ding**, Peng Huang, Jingfang Liu, Andrés Kecskeméthy, Automatic structural synthesis of the whole family of planar 3-DOF closed loop mechanisms. *ASME Journal of Mechanisms and Robotics*, 2013, 5(4): 041006-1-10.

[11] **Huafeng Ding**, Weijuan Yang, Peng Huang, Andrés Kecskeméthy, Automatic structural synthesis of planar multiple joint kinematic chains. *ASME Journal of Mechanical Design*, 2013, 135(9): 091007-1-12.

Acknowledgements

First of all, I would like to deliver my heartfelt gratitude to Prof. Andrés Kecskeméthy, to whom I was indebted for much more than this thesis. I was luckily supervised for my doctoral studies and hosted for my AvH research by him. He has guided me and inspired me with his advanced research work and with his enlightening disussions and conversations with me. Were it not for him, the materialization of the doctorate application would have been impossible in the first place. But I was obliged to him for much more. He supported me for my application for the AvH sholarship with his care, his encouragement, and his valuable suggestions, all of which meant a lot and still means a lot to me. During my stay in Germany, he was always kind and thoughtful, and his help extended beyond my research work there. A busy professor as he is, he went as far as helping me to solve a few personal problems, such as finding a living place, a family doctor and a kindergarten for my daughter. Back in China, that invaluable experience of studying with him has always given me strength in my researches. His appreciation and encouragement have always been an important source of support for me.

My gratitude also goes to Prof. Huang Zhen, my supervisor for the master's and doctor's degree in China, and a life-long teacher to me. He has been supporting me for over 10 years, from when I was an undergraduate till now. To me he is like a light in the dark. Each time I achieved one goal and was about to think about the next, he would show up and suggest another goal. He has been with me, watching me, encouraging me, and reminding me all along the way. Each important step I took in the past was closely associated with him. He was one who truly cares for the progress of mechanical research in China, truly cares for the students, and truly derives joy from the achievements by his students. Though retired he still keeps an eye on the international development of mechanisms and on my work, and offers valuable suggestions when he considers it necessary.

I also thank my friends in Germany for their kindness and help with my research work or with things in life. They are Prof. Müller, Ms. Xia Shuxian, Mr. Zi Bin, Mr.Wang Qiang, Mr. Zhao Xingwei, and Mr. Yu Jie, to name just a few of them. Without them my academic stay in Germany would not have been as pleasant as it was.

I am very grateful for my dear wife Yanqiao Zhao, who has loved me, and helped me in both my life and work. I would also like to thank my charming daughter Xiaoduo Ding, who has brought me much happiness. Last but not least, I would like to express my gratitude to my parents, who have loved me and supported me for all these years.